UNIVERSITY OF MISKOLC
FACULTY OF MECHANICAL ENGINEERING AND INFORMATICS

Enhancing Surface Integrity through Slide Diamond Burnishing: Tool Modification, Novel Process Strategies, and Multi-material Applications

PhD Theses

Prepared by:

Frezgi Tesfom Kebede
Bachelor of Science (BSc) in Mechanical Engineering
Master of Science (MSc) in Mechanical Engineering (Mechatronics)

ISTVÁN SÁLYI DOCTORAL SCHOOL OF MECHANICAL ENGINEERING SCIENCES
TOPIC FIELD OF ENGINEERING MATERIALS SCIENCE, PRODUCTION SYSTEMS AND PROCESSES
TOPIC GROUP OF MANUFACTURING SYSTEMS AND PROCESSES

Head of Doctoral School

Prof. Dr. Gabriella Vadászné Bognár
DSc, Full Professor

Head of Topic Group

Dr. Zsolt Maros

Scientific Supervisor

Dr. Csaba Felho

Miskolc, 2026

SUPERVISOR'S RECOMMENDATION

I first met Frezgi Tesfom Kebede in 2021, upon the start of his PhD studies at the University of Miskolc. As one of my first doctoral students (alongside Ziya Mehdiyev), he holds a special place for me both professionally and personally. From our earliest interactions, it was clear that Frezgi is a highly capable and diligent individual.

After beginning his program, he required an initial period to acclimate to life in Hungary and to the academic environment at the University. This adjustment phase also included the important process of identifying his specific research focus. Once introduced to the diamond burnishing process, however, he was immediately captivated and knew he had found his area of specialization.

I have been consistently impressed by his passion for identifying research gaps and conducting in-depth analysis to develop novel solutions. He immersed himself in the subject, and the fruits of that dedicated work are evident in this dissertation. Supervising his PhD activities was a rewarding experience, as he consistently arrived with new correlations, ideas, and a steadfast commitment to every task, regardless of its complexity.

Throughout his investigations, Frezgi conducted numerous diamond burnishing experiments on both cylindrical and flat surfaces. As a first step of his research, he created a new burnishing tool design for flat surface. This interchangeably burnishing tool was used in lathe and milling machines to conduct cylindrical and flat surface burnishing process experiments. He developed a method for burnishing tool path modification and demonstrated its benefits for improving surface integrity. His scholarly output is commendable, with a total of 10 publications registered in MTMT, including one Q1 and three Q3-ranked articles.

As his scientific supervisor, I can confirm that the results presented in his dissertation are his own original work. While he received valuable assistance from colleagues throughout his research, Frezgi was invariably the primary driver, undertaking the majority of the work himself.

Beyond his research, Frezgi's friendly and collegial nature allowed him to integrate seamlessly into the community at the Institute of Manufacturing Science. He is well-liked by all who work with him. On behalf of my colleagues, I can say we are delighted to see him completing his dissertation and hopefully obtaining his degree after a successful public defense.

It is my sincere hope that we will have the opportunity to collaborate many more times in the future and that we will maintain our productive and personal connection.

Miskolc, December 29, 2025

Dr. Csaba Felhő

scientific supervisor

ACKNOWLEDGMENT

Firstly, I would like to thank you, God. Finishing what I started is a blessing from you when you showered me with health, energy, and hope. Praise to you for blessing me with these and keeping me safe throughout my study time. Praise be to your mother, Saint Virgin Mary, and all saints, too.

I would like to thank the Stipendium Hungaricum scholarship for providing the opportunity to fulfill my dream of pursuing a PhD. I am truly grateful to Dr. Csaba Felho for believing in me and allowing me to study under his supervision. Your wisdom, professional guidance, and friendly approach can convert any student into a full-fledged researcher. Thank you very much.

I am profoundly grateful to the government of Eritrea for providing the opportunity and supporting me financially throughout the duration of my study.

Special thanks go to Prof. Dr. János Kundrák and Dr. Zsolt Maros, the Research field and topic group leaders, for their professional administrative support. I want to say thanks to Dr. Gyula Varga, Dr. István Sztankovics, Prof. Dr. György Kovács, Antal Nagy, Tamás Makkai for their unconditional technical support. A special thanks to István Pásztor, our lab technician, who is always ready to help me conduct my experiments and offer his creative advice. Another important person in the institute is Tamásné Velezdi, our secretary, always ready to help and facilitate administrative duties. All other members of the institute, the faculty of the University of Miskolc community, thank you very much.

I would like to thank my colleagues at the institute, Afraa Adeeb Khattab, Hla Gharib, Ziya Mehdiyev, Tanuj Namboodri, and Inácio Manuel Junqueira, for their help and motivation during every encounter.

To my wife, Soliana Mehari, your love, patience, and unwavering belief in me have been my beacon to guide me to my destination from afar. The sacrifices you made to raise our kids and manage our home during my absence were beyond imagination. It is time now to share the burden and stand beside you. To my beloved children, Eyorusaliem, Naomi, and Abrham, when I start thinking about you, immediate joy fills my body, and a smile appears on my face. You were my motivation to work hard and withstand all kinds of challenges.

Lastly, I would like to thank my father Tesfom, my mother Mulu, my brothers, sisters, uncles, aunts, my wife's family, and generally all family members for your love, support, and prayers. Special thanks to all my friends, the Eritrean community in Hungary, and the Eritrean Scholars' Society (EriSS) who helped me morally, technically, and financially.

LIST OF SYMBOLS AND ABBREVIATIONS

Δh	Reduced roughness by the new feed method.
⌀	Diameter
λc	Cut of length
CNC	Computer Numerical Control
NC	Numerical Control
UAB	Ultrasonic Assisted Burnishing
VABB	Vibration-Assisted Ball Burnishing
UB	Ultrasonic Burnishing
LAB	Laser-Assisted Burnishing
DMM	Differential Morphological Method
LPBF	Laser Powder Bed Fusion
Sa, %ΔSa	Arithmetic means average roughness, Percentage change of Arithmetic means average roughness
Ssk, %ΔSsk	Skewness, Percentage change of Skewness
Sku, %ΔSku	Kurtosis, Percentage change of kurtosis
Sk, %ΔSk	Core roughness depth, Percentage change of core roughness depth
Spk, %ΔSpk	Reduced peak height, Percentage change of reduced peak height
Svk,%ΔSvk	Reduced valley depth, Percentage change of reduced valley depth
f1 – f3	Feed combinations from f1 to f3 in the new burnishing method of C45 burnishing
v1 to v11	Feed combinations from v1 to v11 in the new burnishing method of 42CrMo4 burnishing
N_1 to N_9	Surface number of C45 workpiece from N_1 to N_9 of the new method
O_1 to O_27	Surface number of C45 workpiece from O_1 to O_27 of the conventional method
N1-N44	Surface number of 42CrMo4 workpiece from N1 to N44 of the new method
O1-O48	Surface number of 42CrMo4 workpiece from O1 to O48 of the conventional method
f_1-f_4	Specific selected feeds applied on 42CrMo4 burnishing

$t_{m,n}$	Machining time of the new method
$t_{m,o}$	Machining time of the conventional method
L_w	Length of the burnished surface
n_w	Rotation of the workpiece
σ-Trans	Transverse residual stress
σ-Long	Longitudinal residual stress
Ra	Arithmetic mean roughness (2D)
Rq	Root mean square roughness (2D)
Rp	Maximum profile peak height (2D)
Rv	Maximum valley depth (2D)
Rsk	Skewness (2D)
Rku	Kurtosis (2D)
Rk	Core roughness depth (2D)
Rpk	Reduced peak height (2D)
Rvk	Reduced valley depth (2D)
St	Maximum profile height
Sz	Maximum height
Ssc	Mean summit curvature
Sdr	Developed interfacial area ratio
Sdq	Root mean square value of the slope

TABLE OF CONTENTS

1. INTRODUCTION

Slide burnishing is a non-material-removal machining process that improves the surface integrity of a product by plastically deforming peaks into valleys using a hard tool. Force is applied to the hard tool, which is available in different shapes and material types, to deform the asperities by following a predefined tool path. Appropriate speed and feed and other technological parameters are selected for the required finishing quality. The process can be completed in one round or repeated several times, defined as the number of passes. Surface integrity (Roughness and mechanical and metallurgical properties) of the product is enhanced as a result, making the process a candidate for finishing machining [1], [2]. This research aims to enhance the surface integrity of three different material types using a modified burnishing tool and introduce a novel feed application burnishing method.

With the ever-increasing demand for stringent surface quality and evolving new material types for critical engineering products in aeronautical, automotive, biomedical, marine, and other industries, there is a lack of comprehensive research on the approach of slide diamond burnishing process. Slide diamond burnishing is a sustainable (chip-less, less or no cooling requirement [3]), economical (easy technique and quick) process compared to the other conventional and non-conventional finishing processes. Conventionally, multiple passes were applied with the same setup to enhance the surface integrity, even though the first pass achieves most of the deformation task. Each pass takes equal time and energy unless parameters like feed or force are adjusted, and changing these parameters requires another cycle of passes. This repetitive approach leads to inefficiencies in time and energy, highlighting the need for different approaches to reduce redundancy while improving surface integrity. This experiment aims to enhance the surface integrity of the products by changing these processes by changing the feed after each pass to help the tool follow a different path than the first round. Additionally, the tool adapter was designed to develop the burnishing tool into an interchangeable tool which can be used in a lathe and a milling machine conveniently. By addressing this gap, the present work seeks to contribute to the broader understanding of burnishing finishing techniques and their role in improving the functional performance of critical mechanical components.

Burnishing force, feed, and number of passes were changed to study their effect as they are the most influential technological parameters, including burnishing speed, which was kept constant in these experiments [4].The same tool was applied to burnished 3D metal printed stainless steel (MetcoAdd 17-4PH-A), C45, and 42CrMo4. 3D surface roughness as well as residual stress and microhardness (MetcoAdd 17-4PH-A) surface and subsurface responses are studied.

1.1. Structure of the thesis

The dissertation is arranged as follows:

Chapter 2 presents a literature review of burnishing process tool modifications, the application of the slide burnishing process for different applications and materials. The effect of burnishing parameters on the surface roughness is also explored.

Chapter 3 covers the experimental procedures followed and the workpiece materials applied. Workpiece preparation details, their shape and dimensions, burnishing tool modification, and burnishing process parameters control, as well as the selected roughness responses, are discussed. The newly introduced burnishing feed application method is also part of this chapter.

Chapter 4 contains the results and discussion of measured and analyzed roughness responses of metal 3D printed stainless steel (MetcoAdd 17-4PH-A). Topography measures of roughness, especially height and functional parameters, are discussed to give glimpses of the slide burnishing effect on new printed materials, as post-processing is compulsory due to their poor surface roughness after the printing.

Chapter 5 presents the results of measured surface roughness parameters after burnishing by the new burnishing method and compares them to the old method. Flat C45 steel workpieces burnished by both methods after finishing face milling were studied before and after the slide burnishing, which applied the modified burnishing tool.

Chapter 6 provides slide burnishing of the 42CrMo4 shaft by the newly introduced feed-varying burnishing method. Measured surface roughness before and after the burnishing was compared to show the effectiveness of the new method. The elapsed time of the two methods were also calculated based on the selected burnishing parameters to show their economic comparison, which is important for industries when selecting the methods.

Chapter 7 summarizes the study by highlighting the important cases and presents the further expected studies.

2. LITERATURE REVIEW

The machining process is performed on products to give the desired shape, tolerance, and smoothness based on the designer's specifications. Depending on the capability of the process, the product can pass through different machining processes till the desired property is achieved. For example, grinding and honing could succeed face milling or the turning process to give the final surface property. The attained surface property defines the functionality of the product, such as fatigue life, wear resistance, corrosion resistance, tribological behavior, and others. These functional properties are important when the product acts as a critical component working under dynamic conditions. Cyclic loads, harsh environments such as temperature and acidity, require a specially treated surface that enhances its service quality and life. This is true because most failures start at the surface due to poor roughness and the type of stress induced as a result of the selected finishing machining type. Milling, turning, and grinding produce tensile stress on the surface, which plays a greater role in crack initiation. The initiated crack becomes a stress concentrator and propagates with further application of the load. As a result, the fatigue life of the product decreased [5]. On the contrary, chip-less machining, such as burnishing and shot peening, induces compressive stress that delays crack initiation and propagation. All these machining types affect the properties of the product at the surface and subsurface level, requiring a sound decision on selecting the type of machining process based on the targeted surface quality, cost, time, and other criteria.

Post-machining is essential since the final surface quality can't be achieved by the primary machining types, like milling and turning processes. Traditional post-machining processes, such as grinding, honing, and lapping, remove the unwanted material from the surface after the primary machining process to give the final test. On the other hand, conventional machining processes like burnishing and peening perform the process by pressing the surface without any material removal. There are also costly (compared to the conventional machining process) modern surface treatment processes that apply laser, chemical, and water jets. Due to its cost, coating is usually reserved for high-end products where performance or aesthetics justify the expense. Burnishing is a sustainable (no cooling and chip-less) [3] process, convenient due to its low cost and uncomplicated operation.

Burnishing is a cold work finishing process that smooths the surface by plastically deforming the peaks and moving them to the valley using a hard tool, as shown in Figure 1. In addition to the shape-changing effect, it also induces compressive stress at the surface and subsurface levels. These are realized by applying pressure on the tool beyond the product's yield point. Most of the time, the process is repeated multiple times because the required surface quality is hard to achieve in one pass. By doing so, the surface functional properties are improved in terms of smoothness, mechanical, and microstructure transformations. It has evolved historically, beginning with its application to pottery and wood in ancient times, advancing to mechanical tools like those patented by David A. Wallace for burnishing apparatus in the late 20^{th} century [6], and culminating in modern techniques incorporating laser heat and ultrasonic vibration-assisting techniques. With the introduction of Computer Numerical Control (CNC) in the manufacturing field, its restriction to cylindrical-shaped products was extended to flat surfaces and irregular shapes. Maximov et al. [7] discussed the classification of burnishing

methods based on the contact type with the surface, the shape of the tool, and the desired surface integrity. There is no literature that draws a clear line between different burnishing methods, as they share some attributes with each other. Numerous researchers have used additional auxiliary technologies to enhance the process, which some of them presented to give a general overview. The most common burnishing methods will be discussed to place the applied slide burnishing method.

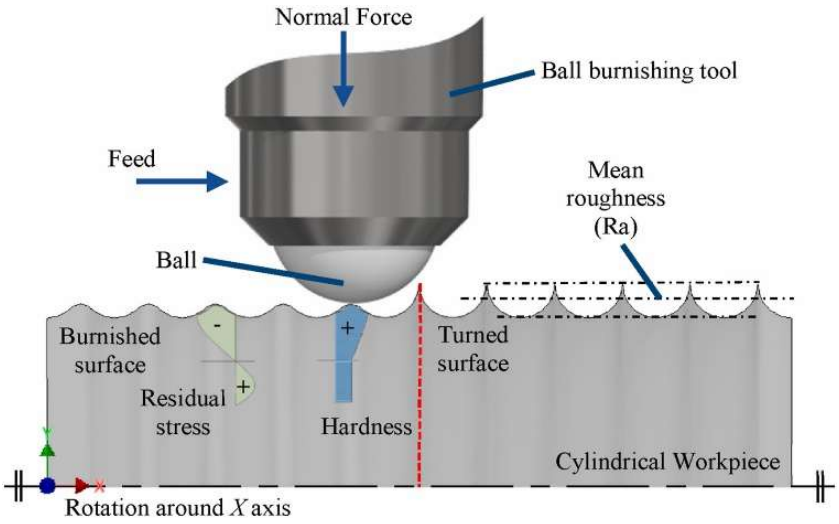

Figure 1. Burnishing process mechanics [8].

2.1. Contact type

The type of contact created between the burnishing tool and product surface is a crucial factor since it affects pressure distribution, surface integrity, and application to different geometries. Rolling and sliding contacts are the common contacts that define the burnishing process. Depending on the advantages and applicability, manufacturers select the appropriate burnishing type.

2.1.1. Roller burnishing

When either a spherical or a cylindrical shaped tool rolls over the workpiece without slipping, it is categorized as roller burnishing. First introduced by General Electric [9], a single or multiple balls supported by hydraulic fluid or spring are also responsible for the pressure control, rotating over the asperities to give the planned surface quality. A single roller is commonly used when the shape is irregular or narrow, like grooves and fillets [10]. Numerous rollers can be arranged like bearings, either when the workpiece is cylindrical or when it is flat, serving the same purpose. In the case of a cylindrical-shaped tool, the same arrangement and approach is used as the spherical-shaped tool. More contact with the workpiece makes it suitable for a wide application area.

2.1.2. Sliding burnishing

A tool fixed to its shank in a spherical or cylindrical shape, as shown in Figure 2, is pressed against a moving surface of the workpiece and slides on it without slipping to produce the anticipated outcome as a result of sliding friction. This process smooths surface irregularities, reduces roughness, increases the hardness, induces compressive residual stress, and improves

wear and corrosion resistance without removing material. During this process, the sliding friction leads to higher heat generation in the contact zone compared to other burnishing processes, responsible for the thermo-mechanical effect, which influences the surface properties and fast tool wear. To deal with the higher heat generation and better durability, a diamond-tipped tool (natural or synthetic, e.g., polycrystalline diamond [11]) that can withstand the friction is used, though other hard materials like carbide are also applied. Like the roller burnishing process, load is transferred to the tool through a spring or hydraulic fluid [12].

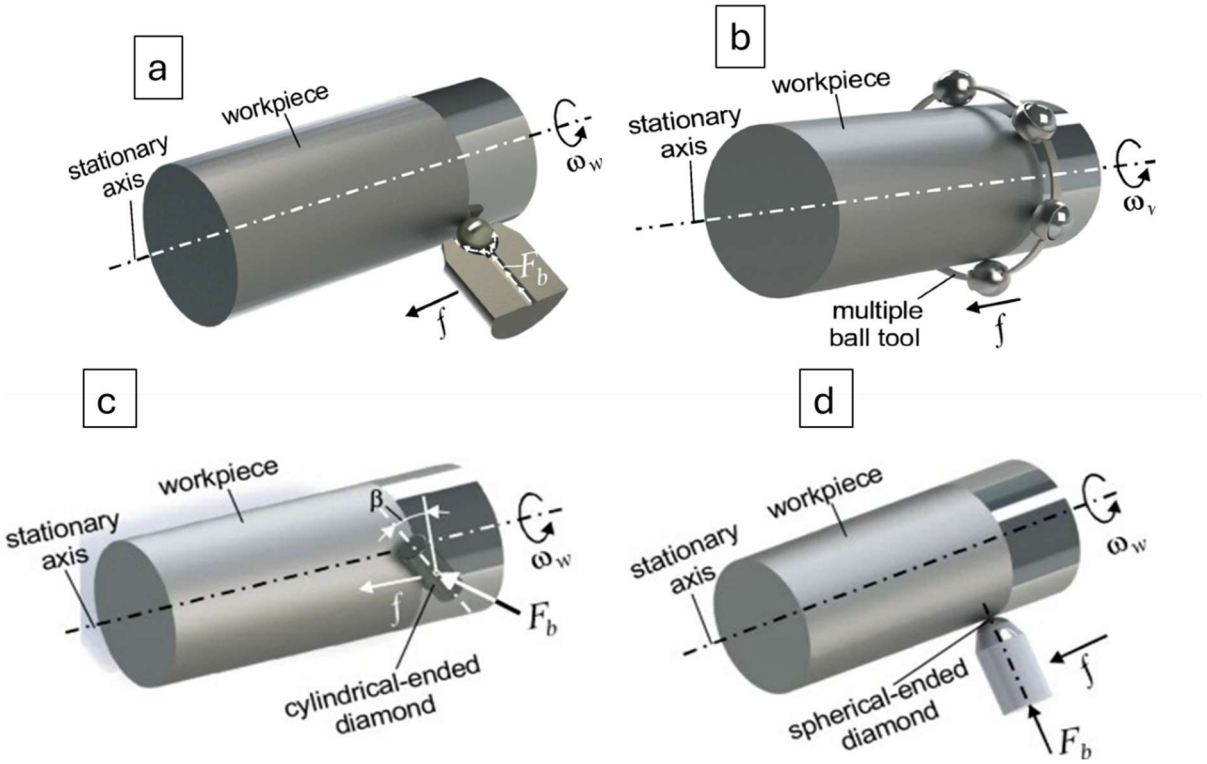

Figure 2. Different burnishing tools schematic, (a) single roller ball, (b) multiple roller ball, (c) cylindrical sliding, and (d) ball sliding [7].

2.2. **Assisting technologies**

With the demand for stringent surface allowance and enhanced surface properties, an additional accessory that can assist the process has been introduced. These technologies induce effective plastic deformation by vibrating the tool (ultrasonic-assisted burnishing), by heating the workpiece for easier deformation (laser-assisted burnishing), or by interfering with the microstructure to change the hardness (magnetic-assisted burnishing).

2.2.1. **Ultrasonic-assisted burnishing**

Ultrasonic Assisted Burnishing (UAB) is an advanced surface finishing technique that combines traditional burnishing with ultrasonic vibrations. The process involves the use of a preloaded ball or tool that applies controlled pressure on the workpiece surface while simultaneously subjecting it to ultrasonic vibrations ranging from 20 kHz to 40 kHz [13]. Additional external vibration has an effect on the deformation process by changing the yield strength [14]. Ultrasonic energy introduces additional dynamic forces to the burnishing action,

leading to enhanced material deformation and surface improvement. It relies on the synergy of mechanical and ultrasonic forces, resulting in more efficient plastic deformation, reduced surface roughness, and improved surface properties [15] .

UAB has achieved significant attention in recent research. Studies, such as those conducted on Ti-6Al-4V surfaces, showcase the mechanical effects and surface integrity modifications achieved through UAB [16]. Furthermore, the development and characterization of tools for Ultrasonic Vibration-Assisted Ball Burnishing (VABB) have been explored, emphasizing its application on materials like Ti-6Al-4V, with a focus on surface integrity properties, such as compressive residual stresses, surface roughness, and surface hardness [13]. The emerging literature underscores the potential of UAB in refining surface integrity and tribological behavior, as seen in techniques like Ultrasonic Burnishing (UB), which not only reduces surface roughness but also enhances material properties [17].

2.2.2. **Laser-assisted burnishing (LAB)**

Laser-assisted burnishing is an innovative manufacturing process that integrates laser technology with traditional burnishing techniques. A laser beam is employed alongside the burnishing tool to enhance the surface properties of materials. This combination allows for precise control over the thermal and mechanical aspects of the process, influencing surface characteristics such as roughness, hardness, and residual stresses. The working principle involves the simultaneous application of mechanical pressure through the burnishing tool and controlled laser irradiation that makes the surface deform easily. This dual-action process results in improved material deformation and surface quality, distinguishing LAB from conventional burnishing methods.

Current research trends in LAB highlight its potential across various materials and application areas. Studies, like the one by Tian Y.G., have explored the effectiveness of LAB in comparison to conventional burnishing, evaluating its impact on materials like MP35N and AISI 4140 [18]. Additionally, recent advancements in the field of laser processing and multi-energy field manufacturing emphasize LAB as a notable technique with applications in improving surface properties and achieving precision in materials processing [19]. These developments underscore the growing interest and potential of LAB in advancing surface engineering and manufacturing technologies.

2.2.3. **Magnetic-assisted burnishing (MAB)**

Magnetic Assisted Burnishing is a contemporary burnishing surface finishing process designed to enhance surface tribological properties by utilizing a magnetic field during the burnishing operation. This technique interferes with the metallic microstructures at a microscopic level by applying a magnetic field to change hardness properties, mainly by aligning and manipulating them.

The application of a magnetic field in conjunction with the pressure applied by the burnishing tool generates burnishing forces, resulting in controlled material deformation and improved surface characteristics. Notably, studies by Kovács Zsolt Ferenc highlight the effectiveness of MAB tools in reducing residual stresses and enhancing the tribological characteristics of

machined surfaces [20], [21]. The MAB approach offers a unique combination of traditional burnishing benefits with the added advantage of magnetic field assistance, making it a promising technique for achieving superior surface integrity. A very limited number of literature is available on this case, indicating the approach is yet to be explored.

2.3. Existing tools and methods for burnishing flat and cylindrical surfaces.

The burnishing tool plays a critical role in the process by receiving the pressure from the source and performing the action. Depending on its shape and strength, it defines the quality of the surface roughness produced, the depth of the burnishing effect, the size of the burnished area, and the type and magnitude of the final retained stresses. These changes occur because deformation mechanics vary with changes in tool attributes, in relation to different workpiece geometries and material properties.

Tool shape is directly related to the deformation efficiency and contact area. Spherical tools provide point contact, making them advantageous for localized burnishing on restricted areas or irregular workpieces for a precise outcome. While cylindrical tools with their line contact are favored for fast burnishing of flat and cylindrical products due to their large coverage. For example, Silva-Alvarez et al. [22] improved the surface roughness of CoCrMo biomaterial up to 77.7% when they applied 450 N and 4 passes, showing ball burnishing applicability for a small-sized product (⌀25.4 mm). Irrespective of the coverage area by the cylindrical tool, El-Tayeb et al. [23] reported that a roller with a larger contact width between 1.5 – 2 mm deteriorates the surface roughness due to excessive plastic deformation. Selecting the optimal burnishing tool shape and size is stated by Saldana-Robles et al. [24] in their study on ball burnishing tool diameter, indicating that a big ball diameter (10 mm) has a lower penetration due to a larger contact area compared to a smaller (⌀3 mm), requiring a higher force.

Selection of tool material is governed by the workpiece hardness, requiring a material 2-3 times harder to manage tear and wear, as well as ensuring an effective deformation process. Tool materials (Tungsten carbide, Chromium-coated steel, and Titanium nitride-coated) as a burnishing parameter were studied by Shiou et al. [25] to burnish plastic injection mold steel PDS5 (HRC33/HS46). They found that a Tungsten Carbide ball with a speed of 200 mm/min, 300 N force, and a feed of 40 μm was the optimum combination to improve the roughness from 1 to 0.07 μm. Varpe et al. [26] in their overview article presented different materials (steel, ceramic, Si_3N_4, Carbon chromium, tin-coated EN31, and Hardened alloy) in addition to what is already mentioned. Natural or synthetic diamond is very popular as a tool material to the extent that it is taken as a type of burnishing process (diamond burnishing process) [27], [28]. These show that variety of materials constitute the tool material selection process based on different phenomena, such as workpiece materials and economic situation.

Tool contact with the workpiece is associated with the type of created friction: higher friction (sliding contact) and lower friction (rolling contact) [29], contact length in relation to tool size and shape with selected burnishing parameters [30]. Even though the heat generation in the process is negligible for coolant usage, lubrication is needed, especially for sliding burnishing

[31]. Ball burnishing is common for deep surface property change, narrow and irregular areas, due to its small contact area [32], [33].

Based on the above-mentioned diversity of burnishing tool attributes and others, researchers designed and modified numerous tools. They focus on tailoring specific features to optimize surface integrity, process efficiency, and applicability to diverse workpiece materials and geometries. Keymanesh et al. and Okada et al. [34], [35] designed a tapered multi-roller tool convenient for chamfered surfaces. Morimoto [36] designed a new tool that can handle the dynamic characteristics of the burnishing tool while applying load. Recently, Okada et al. [37] introduced textured surface formation by applying an intermittent burnishing process realized by a hemispherical tip tool rotating eccentrically from the five-axis machining center. Ball burnishing tools incorporating an advanced helical spring [38], a simple ball held in an adapter by a screwed cover [39], a screw jack type [40], an adjustable type [41], and a bearing [42] type roller burnishing tools are some additional variants of developed tools. As explained by Maximov et al. [7], adding or modifying some features to the tool leads to different morphological signs that can differentiate the process. These designs and modifications are driven by the need to enhance the responses like roughness, hardness, fatigue life, stress distribution, and others. All experiments in this dissertation are conducted using a tool designed for a lathe but adapted for a milling machine with some modifications to its holder.

2.4. **Pre-burnishing machining**

The selected tool shape and material, with the interaction of workpiece and additional accessories that boost the process, play a crucial role in giving the required final output. Another critical input in influencing the efficiency of the burnishing process is the state of the surface prior to its application [43]. Burnishing is a plastic deforming mechanism of surface asperities left by a prior machining, hence topography, integrity, and mechanical properties of this pre-existing surface layer are fundamental parameters that dictate the success of the process. All the advantages of the process, like enhancing surface roughness, hardness, and residual stress, are direct results of the interaction between the burnishing tool and the underlying surface. Understanding this, researchers apply different finishing processes before burnishing that can complement the process [44], [45], [46].

Processes like milling, turning, forging, extruding, and die casting require a finishing process since it is not possible to use the product coming out of these processes as they are, for many reasons. As a result, finishing processes, for example, grinding, honing, polishing, lapping, and superfinishing, are used to give smoothness averagely from Ra = 6.3 μm to 0.0125 μm [47]. These finishing processes are applied as a solo finishing process or supplement each other by starting with the coarse surface producing process and finishing with the fine surface producing process [48]. With the context of the burnishing process, I will proceed with grinding, face milling, and turning as pre-burnishing finishing.

The grinding process is the most practiced machining process that removes surface irregularities. Numerous researchers applied it as a pre-burning process to produce enhanced surface properties. Uddin et al. [49] applied grinding and burnishing to laser-cladded AISI 431 alloys and compared the results with grinding. They found 29 % and 41 % Ra and Rz

improvement, including other properties like surface porosity, microhardness, volume loss, and impact resistance enhancements. Karthick et al. [50] also studied sequential applications of grinding and Low Plasticity Burnishing (LPB) of Ni-based superalloy 718 produced by electron beam additive manufacturing. Their results show that about 0.6 μm lower surface roughness and 17% improved microhardness when compared to grinding only, and higher compressive surface residual stress when compared to LPB. Instead of the sequential application of grinding and burnishing, Charfeddine et al. [51] applied them simultaneously on AISI 4140 workpieces. Stress at the surface was changed from tensile to compressive deep up to 2.7 mm. Turning, grinding, and ball burnishing were the processes applied to AISI 4130 steel by Arsalani et al. [52]. The pre-turned and pre-ground burnished workpieces showed 4.24% and 10.95% improvements in endurance limit compared to the runed samples. Surface roughness and microhardness were also modified. This indicates that grinding the turned, milled, and 3D printed materials before applying the burnishing process can help to optimize the burnishing process. 3D printed stainless steel received grinding machining before slide diamond burnishing to reduce the poor roughness, as the initial roughness affects the performance of the process.

The advantage of grinding before burnishing is not only the reduced roughness but also the absence of deep tool marks compared to milling and turning. The technological advancement of the machining process made the process easy in terms of handling different product sizes, machining flexibility, accuracy, and other advantages. Burnishing of a flat [53] and complicated surfaces [54] is possible using NC machines. EN AW-AlCu4MgSi(A) aluminum alloy, in convex and concave shapes, were ball end milled with a cutting speed of 350 m/min, feed 0.04 mm, stepover 0.53 mm, and depth of cut 0.5 mm [55]. After burnishing it with a 4 mm radius tool, Sa and Sz values were reduced by 4 and 9 folds consecutively, with other properties changing. A multi-roller tool was used to burnish 72 mm long, 22 mm wide, and 12 mm high AISI 5150 hardened steel, after which the average roughness was reduced by 37% and the Brinell hardness was increased by 29.9% [56]. The applied milling conditions were: spindle speed 500 rpm, feed rate 120 mm/min, and depth of cut 0.5 mm. Based on cutting and workpiece material, and other criteria, finishing cutting parameters are selected to give as smooth surface as possible, and they are burnished for further surface enhancement.

Turned surfaces finished by selecting minimum feed and depth of cut with a higher speed served as an initial surface for the burnishing process. 17-4 PH stainless steel was turned using a feed rate of 0.1 mm/rev, depth of cut = 0.25 mm, and cutting velocity = 73 m/min before the diamond burnishing that produced a minimum Ra of 0.199 μm and maximum hardness of 397.48 HV [57]. Another study by Zaghal et al. [58] applied cutting speed = 120 m/min, feed 0.1 mm/rev, and depth of cut 0.2 mm to serve for the same purpose. For AISI 316Ti chromium nickel steel workpiece [59] also applied feed rate = 0.1 mm/rev, speed = 90m/min, and depth of cut = 0.25 mm, which is in a close range to the mentioned researchers, even though the materials are different. This implies that finishing turning is eligible for pre-burnishing surface if the roughness is in an acceptable range; otherwise, the burnishing process produces a poor surface. For example, Kluz et al. [60] Only mentioned 42CrMo4 shafts were turned in such a way that Ra = 2.6 μm average roughness is produced.

Surface asperities are a product of either the production process (drawing, forging, casting, 3D printing, and others) or the used machining process. Since it is not advisable to apply the burnishing process directly to the produced product, the finishing process is compulsory before the burnishing process. In this research work, grinding, finishing face milling, and finishing turning pre-burnishing finishing machining were applied to the workpieces.

2.5. Burnishing parameters' effect on surface roughness

Burnishing performance relies heavily on the selection of technological parameters and their levels of the process, especially on burnishing force, feed, tool radius, speed, and number of passes. Maximov et al. [61] studied these parameters, including the lubricant-cooler, one factor at a time to distinguish the important parameters and their magnitudes. And they found out that burnishing force, feed, tool radius, speed, and number of passes were influential. The most frequently studied slide burnishing parameters, as per Maximov et al. [4] were burnishing force (33%), feed rate (26%), burnishing velocity (18%), and number of passes (8%). The kinetics (cold working) of different workpiece materials and tools depend on these and other parameters to create the targeted surface integrity. But selecting the optimal parameters levels is compulsory, which can be realized using Taguchi design, Response Surface Methodology (RSM), Genetic Algorithm (GA), and other methods [62], [63], [64].

For plastic deformation to occur, the applied force must exceed the yield point. With the help of spring [59] or hydraulic fluid [65], force is transmitted to the workpiece via the tool for this purpose. In some cases, neither spring nor hydraulic fluid is used to apply force to the tool; instead, another mechanism (load cell) is used [66]. Some researchers use a separate force measurement unit that can help to control the applied magnitude [67], [68].

Harder materials require a higher burnishing force, and in the case of slide burnishing, a lubricant, or in some cases, a coolant, is required if the sliding friction produces heat that can affect the performance. Caudill et al. [69] studied 1000 N, 1500 N, 2000 N, and 2500 N burnishing forces under cryogenic, flood-cooled, and dry conditions on Ti-6Al-4V alloy, which delivered a smoother surface when the 2500 N force and dry condition were used. The other responses, like hardness, preferred cryogenic cooling. In the study by El-Axir [70], the optimum force that produced the best surface finish was 245.17 to 343.23 N (25 to 35kgf) for steel-37 of 220 Hv. Due to its interaction with speed, feed, and number of passes, roughness showed an increasing trend when force increased. Roohi et al. [71] used vertical depth of burnishing instead of measured force (0.09, 0.15, and 0.21 mm) to study the slide burnishing effect of AA7075-T651 plate on its surface topography and hardness aspects. 0.15 mm depth, 0.07 mm step-over (equivalent to feed when burnishing flat surfaces), and 3 passes were the optimal parameters. Okada et al. [72] applied admittance force control to the interaction between the tool and the workpiece surface. The developed force sensor system works based on high gains and stable position control. Kistler force sensor applied by [68], [72] to control the burnishing force. These show that numerous researchers use different force sensor types, arrangements, and mechanisms to control the force, in addition to the difficulty of selecting the magnitude with varying material types.

Other important burnishing parameters are feed and number of passes, which define the progress of the tool in each rotation (cylindrical object) or step-over of the tool in each stroke (flat surface), and how many repetitions are needed to finish the process.

Karolczak et al. [73] studied the number of passes limit to produce a smoother surface of aluminum composite materials compared when reinforced with alumina Saffil ceramic fibers (Al2O3) and Silicon carbide (SiC) particles. They found smooth surfaces (Sa = 0.1 μm) when the passes were 7 (Sic particle), and for Al2O3 fiber, they were 4 and 7. Another study by Roohi et al. [74] indicates that the optimal pass was 5, obtained from a multi-objective optimization method, which was applied for the sliding burnishing of AA7075-T651 face-milled plates. Antal and Varga [75] recommended the use of 2 passes in the study of tool pass number effect on surface roughness. They applied 3 pass levels (1, 2, and 3 passes) while slide burnishing X5CrNi18-10 alloyed steel in forward and backward directions. These imply that there is no specific rule that tells how many passes are needed for a material type and burnishing methods. There is no sufficient literature that studies the effect of the number of passes on surface integrity separately.

Feed, in some studies called step-over [71], [76] refers to the linear movement of the burnishing tool after finishing one complete path. In relation to ball diameter, material type, and force, it is compulsory to select an optimal feed for best roughness output [77] From the tested three levels of force, feed, and ball diameter by Bourebia et al. [78], 50 N, 0.22 mm rev−1, and 13.5 mm consecutively gave the best result. Studies by Polanowski et al. and Kumara et al. [79], [80] also indicate that feed significantly affects surface roughness. In addition, Karolczak and his team [73] showed different materials have different optimal feeds for the lowest roughness. It has a direct relation with the production rate of the process. Employing a low feed results in superior finishing at the expense of production rate, while a high feed increases production speed with compromised finishing quality. It affects the quality of the created surface when we observe from the contact duration perspective, which is directly related to the deformation process. Regarding the workpiece material, ball diameter, force, number of passes, and other factors, feed must be optimized to achieve the best finishing output. Amdouni et al. [81], for example, suggested a 500 mm/min burnishing speed, 40 μm depth of penetration, and 0.2 mm feed were the optimum parameters to burnish a flat aluminum alloy. These all indicate that careful feed selection for a balanced production rate and required surface finish is compulsory. With all these in place, the approach of applying the feed to flat and cylindrical surfaces remains unchanged. The author has introduced a novel method that changes the feed in every pass to give a chance to the tool in order to deform unattempted area or leftover peaks.

2.6. Convenient materials for the burnishing process

The burnishing process is considered a superior finishing technology for enhancing the surface integrity of different material types. A study by Maximov et al. [7] shows that steel constitutes 65% share of the slide burnishing treated materials. A recent study by Varpe and Tajane [26] indicates that the Al family accounts for 36% of the materials that received a burnishing process, including Cu (6%), Brass (6%), Steel (47%), Ti-alloy (11%), Polymers (3%), and Wc (3%). Due to its capability to induce severe plastic deformation resulting in a mirror-like finish, a work-hardened surface layer, and its effect on affecting the stress, burnishing poses a challenge

to study over the mentioned and newly evolving material families. Additive manufacturing (AM) technology is a continuously growing metal-producing system [82], [83] that needs a study about the effectiveness of the burnishing process. Their unique microstructure is characterized by heterogeneity, porosity, and residual stress from rapid solidification [84], [85], which requires post-machining, making the burnishing process one of the candidates due to its surface integrity enhancement advantages. In addition, the available AM technology is known for its poor surface roughness [86]. Despite the available extensive studies on the burnishing process of 3D printed metals, stainless steel (MetcoAdd 17-4PH-A) has received negligible attention. The other two workpiece materials used in this research are C45 medium carbon steel and 42CrMo4 low alloy steel, which are very popular in structural, automotive, aeronautical, and heavy-duty machine applications. Slide burnishing with a modified tool post-machining was applied to these three materials to study its effectiveness. Burnishing force, feed, and number of passes were the studied parameters due to their dominant effect compared to the other burnishing technological parameters.

2.7. Effect of burnishing on surface roughness

A hard tool pressed against the workpiece surface with controlled pressure based on the material type causes the peaks to plastically flow to the valley and, as a result, a smooth surface and other advantages are created. The responses of the burnishing process are characterized by the created surface roughness, fatigue life, developed stress type, hardness, corrosion resistance, wear resistance, and microstructure changes. Surface roughness changes are measured and discussed in this research. Cracks are initiated and propagated from the surface, which determines the fatigue life of the product. Tribological, clearance, fit, and corrosion characteristics of the product are also directly related to the roughness. Several roughness parameters are utilized by researchers that measure amplitude, spatial, hybrid, functional features, and other parameter characteristics of 2D and 3D roughness [87], [88]. In the case of 2D roughness parameters, only vertical values of the roughness are measured.

The most applied roughness parameter in surface characterization is the arithmetic mean roughness (Ra). This parameter is widely utilized due to its simplicity and historical significance in manufacturing processes [89]. However, recent studies indicate that while Ra is prevalent, it may not fully capture the complexities of surface morphology, leading to a growing interest in alternative parameters.

2D surface roughness measurement (Ra, Rq, Rp, Rv, Rsk, Rku, Rk, Rpk, and Rvk) were used by Maximov et al. [90] while studying the effect of roller burnishing and slide roller burnishing on the surface integrity of AISI 361. Roohi et al. [71] also studied Ra along the x and y directions with the best improvement of 90.4% and 88.5% respectively. Compared to the 3D roughness measure, the 2D measure is simple and can be applied when a quick measurement is required. But it lacks information about the third axis, that tells about other important features of the surface. 3D parameters were used by Skoczylas et al. [91] (Sa, Sz, Sp, Sv, Ssk, and Sku) and Korzynski et al. [92] (Sa, St, Sz, Ssc, Sdr, Spk, and Sdq), which include height, hybrid, and functional measures. These 3D parameters help to measure the roughness, which can be interpreted in terms of the functional property of the generated surface. Core roughness depth (Sk, Spk, and Svk), which can tell tribological behaviour of the surface, is, for example, one of

the most important 3D measures, but not extensively applied. Height and functional parameters (Sa, Sq, Ssk, Sku, Sk, Spk, and Svk) are applied in this research to measure roughness that can help to discuss the transformation of the surface.

2.8. Research gaps and motivation

The existing literature on slide burnishing demonstrates its efficacy in enhancing surface roughness, hardness, and fatigue life across various metallic materials, particularly through modifications in tool design, such as shape, material, and contact type. However, critical gaps remain in the advanced manufacturing contexts with the advantage of creating new materials. First, there is a notable absence of studies on slide burnishing applied to 3D printed stainless steel (MetcoAdd 17-4PH-A), a material increasingly used in additive manufacturing for complex components. While burnishing has been explored for traditional stainless steels, no research addresses the effect of slide burnishing on the unique microstructural characteristics of 3D printed variants, such as porosity and anisotropy, which may alter deformation responses. Additionally, conventional burnishing tools are primarily designed for cylindrical workpieces on lathes, with limited adaptations for flat surfaces by milling machines. An interchangeable tool capable of handling both flat and cylindrical geometries without compromising process efficiency is crucial for tool management costs.

Further gaps emerge in the application of technological parameters of the process, specifically the feed. The literature predominantly focuses on standard feed strategies by only changing their magnitude. No such approaches exist that could optimize surface enhancement while affecting processing time. Similarly, when extending these methods to cylindrical 42CrMo4 steel, a higher-hardness alloy used in high-stress applications, the response of the burnishing process may vary significantly due to changes in material hardness and workpiece shape. Existing studies rarely account for these interactions, leading to an incomplete understanding of how parameters like feed rate, force, and geometry influence outcomes across diverse materials and forms. These gaps highlight the need for empirical investigations into modified tools and processes to bridge theoretical insights with practical implementation in CNC environments.

Addressing these research gaps is motivated by the growing demand for efficient, versatile surface finishing techniques in modern manufacturing, where additive and subtractive processes must integrate seamlessly to produce high-performance components. For slide burnishing of 3D printed stainless steel, the motivation lies in developing an interchangeable tool designed initially for lathe applications but modified for milling to enable burnishing of both flat and cylindrical surfaces. This adaptability not only reduces tooling costs and setup times but also facilitates the study of burnishing's effects on the material's surface roughness, which is crucial for improving the durability of 3D printed parts in industries like aerospace and biomedical engineering.

In the case of flat C45 steel, the introduction of a novel feed application method aims to enhance surface roughness while significantly reducing burnishing time, offering a more efficient alternative to traditional methods. This innovation is driven by the potential to achieve superior surface quality with minimized time, which leads to less energy consumption, aligning with

sustainable manufacturing goals. Extending this approach to cylindrical 42CrMo4 steel shares the same motivation, as variations in material hardness and shape provide an opportunity to validate the method's robustness, ensuring broader applicability across alloys with differing mechanical properties. Overall, this research is motivated by the need to advance slide burnishing as a chip-less, cost-effective process that enhances component performance and fills voids in the literature.

2.9. Objectives and scope of the study

Maximov et al. [7] mentioned in their review article about slide burnishing, that there is no universal classification of burnishing methods. They advised the usage of the Differential Morphological Method (DMM), which has the advantage of expanding morphological signs with new features based on the researcher's preferences. Elements of the structure, such as workpiece, deforming element, and force control mechanism (spring and viscous), and morphological signs for example, geometrical form and motion, constitute the feature of the burnishing method. The burnishing parameters' magnitude range also varies depending on these phenomena. These parameters follow a specific order when applied to the burnishing process architecture to produce the desired output. By focusing on tool adaptation, workpiece material, and the process parameters application approach, the objectives listed below are the targets of the study.

- To modify a tool for flat surfaces burnishing, design an optimized path of the tool in terms of surface quality, time, and analyze its performance.
- To study and analyze the effect of burnishing parameters on surface roughness of 3D metal printed stainless steel (MetcoAdd 17-4PH-A).
- Develop a novel burnishing process feed application method and analyze its performance (surface roughness) on flat C45 medium carbon steel.
- To study the performance of the newly developed feed application on a cylindrical workpiece (42CrMo4) by analyzing its effect on surface roughness change.
- Comparing the old and the newly introduced burnishing methods’ elapsed time to give their economic picture.

3. MATERIALS AND METHODS

Surface integrity of the selected materials (MetcoAdd 17-4PH-A, C45, and 42CrMo4) were measured and evaluated during the research to study the effect of slide burnishing. Roughness, residual stress, and microhardness were measured before and after the slide burnishing process for that purpose. The experimental setups of machining and measurements of the required responses are discussed in this chapter.

3.1. Burnishing tool and its adapter for clamping

The technological advancement of machine tools boosted the capability of the machines to incorporate processes that were not previously possible. Numerically controlled movements of the machine to handle the cutting process made machining irregularly shaped products easy. CNC milling machine usage to perform planner and free-form shaped burnishing is reported by numerous researchers [93], [94] that indicate its importance. However, the diversity of available tool shapes and their mechanisms necessitates careful integration to perform the process. I designed an adapter shown in Figure 3 for the tool that was initially designed for a lathe machine to be applied to a milling machine.

Traditionally, specialized burnishing tools are designed for specific machine tools such as a lathe or milling machine. This modification addressed the significant limitation, which is the inability to utilize the existing lathe-specific burnishing tool on the CNC milling center. Therefore, the objective was to design, fabricate, and validate a cost-effective adapter that would enable the seamless and precise integration of a standard lathe burnishing tool into a milling machine spindle, thereby extending its functionality without compromising performance.

3.1.1. Adapter design and fabrication

The core of this innovation is a custom-designed two-section stepped shaft adapter. Its geometry was strategically determined to fulfill two primary interface requirements:

Milling machine interface

The smaller diameter end of the adapter is designed to be securely gripped by the milling machine tool holder, ensuring concentricity and robust torque transmission. The dimensions of this section were precisely machined to match the specific tool holder dimensions. Based on the tool holder dimensions and features, it can be redesigned to fit with them.

Burnishing tool interface

The larger diameter end features a precisely machined hole to provide a snug, non-torating fit for the shank of the existing lathe burnishing tool. The geometry of this hole was reverse-engineered from the tool’s shank to prevent any slippage during the burnishing process which is critical for achieving a uniform surface finish.

The critical design consideration was the preservation of the burnishing tool's original functionality. The adapter engages only with the tool's shank, allowing all its native components such as the burnishing head and the integral spring mechanism that provides the

required burnishing force to operate as intended by the manufacturer. This approach ensures that the process mechanics of the burnishing operation remain unchanged.

Operational principle

In operation, the adapter acts as a mechanical intermediary. First the lathe burnishing tool is inserted into the square hole of the adapter. Then it is mounted into the milling standard tool holder. During a burnishing operation, the CNC CAD program guides the assembled tool and adapter. The movements in the directions parallel and perpendicular to the machined surface are made by the table and thus the workpiece, while the axial movement is carried out by the spindle and thus the tool. The spring-loaded mechanism of the burnishing tool maintains consistent pressure against the workpiece surface, producing a plastic deformation and creating a smooth, hardened surface, identical to its function on a lathe but now applied to planar geometry achievable on a milling machine.

3.1.2. Contribution and significance

The development of this adapter provides a novel and pragmatic engineering solution with several key contributions:

- **Significant Cost Reduction:** This modification eliminates the need to purchase a dedicated, burnishing tool for the milling machine. It leverages existing capital equipment (the lathe tool), leading to direct and substantial cost savings for the laboratory or production facility.
- **Enhanced Process Flexibility:** It significantly increases the flexibility of the manufacturing process. A single burnishing tool can now be used for finishing operations on both rotational parts (on the lathe) and prismatic parts (on the milling machine), streamlining tooling inventory and setup procedures.
- **Resource Efficiency and Sustainability:** By extending the utility of an existing tool, this approach aligns with principles of resource efficiency and sustainable manufacturing, reducing waste associated with redundant tooling.

This simple yet effective adapter design successfully bridges a functional gap between two distinct machining platforms. It represents a low-cost, high-impact innovation that enhances our manufacturing capabilities and demonstrates a practical application of design for versatility principles.

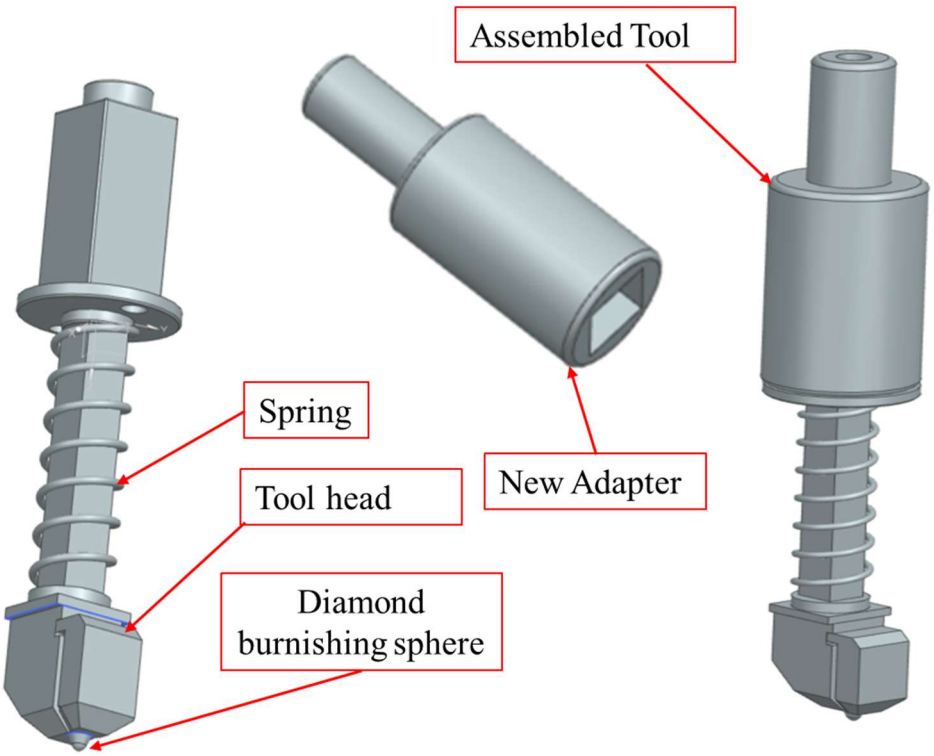

Figure 3. CAD model of the adopted burnishing tool.

3.2. Description of Materials Used (MetcoAdd 17-4PH-A , C45, and 42CrMo4)

The slide burnishing process was applied independently to three materials: MetcoAdd 17-4PH-A, C45, and 42CrMo4. The response (roughness) of each material to the machining was analyzed to evaluate the process's effectiveness across different conditions and initial conditions. Details about all three materials are provided below.

3.2.1. Stainless Steel

The regular flat burnishing experiment utilized workpieces fabricated from MetcoAdd 17-4PH-A powder, an iron-based alloy (FeCrNiCu) with similar properties to 17-4PH, EN 1.4542, and UNS S17400 [95]. Produced via gas atomization, the powder exhibits a spheroidal morphology, enhancing its suitability for a variety of 3D printing methods, but more for powder-bed additive manufacturing processes. This martensitic precipitation-hardening stainless steel offers high versatility, making it applicable in aerospace, nuclear technology, chemical processing, and oil refining industries [96]. A 60 mm ×26 mm × 10 mm size workpieces shown in Figure 4 were printed to contain three burnishing surfaces in each piece.

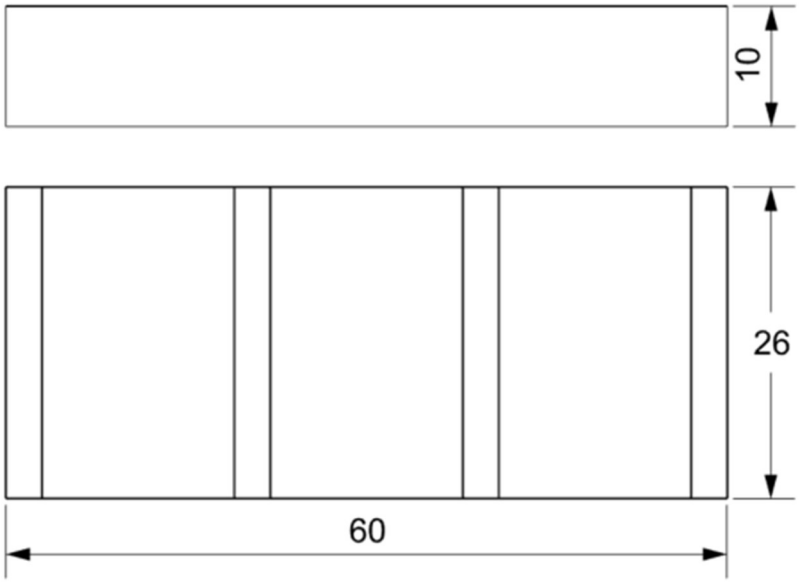

Figure 4. CAD model geometry and dimensions (mm) of 3D-printed workpiece, 1, 2, and 3, indicating burnishing area.

3.2.2. **Medium carbon steel C45**

Medium carbon C45 steel, popular in automotive, construction, and other industries, and known for its good machinability [97], is one of the materials used in this research. It is shaped as depicted in Figure 5 to accommodate three burnishing surfaces (10 mm×10 mm each) and holes to fix it with the force sensor. The two holes were lowered from the top surface by 20 mm to avoid collision with the tool. With the chemical and mechanical properties presented in Table 1, it is one of the most popular materials that undergoes a burnishing process due to its wide application range, serving as a critical component.

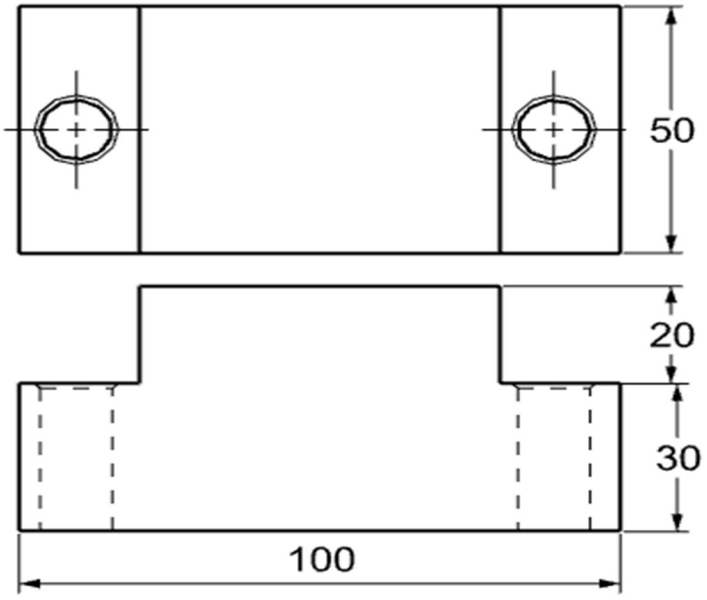

Figure 5. C45 steel workpiece CAD model.

Table 1. Percentage of chemical composition and mechanical properties of C45 steel [98].

Chemical Composition (Average), (%)								
C	Mn	Si	P	S	Cr	Ni	Mo	Fe
0.48	0.74	0.36	0.011	0.01	0.09	0.02	0.002	rest
Mechanical properties								
Yield Strength (min.)				Re = 430 MPa				
Tensile strength (min.)				Rm = 740 MPa				
Hardness (min.)				250 HB				

3.2.3. **Low alloy steel 42CrMo4**

The third tested workpiece was 42CrMo4, a chromium-molybdenum steel known for its excellent tensile strength, toughness, and hardenability. Its specific chemical composition and mechanical properties are shown in Table 2 and Table 3, and it was studied to evaluate changes after the burnishing process. Hardened to 410 HV10 before the machining process, making it suitable for the proposed burnishing process performance with higher hardness materials. The mentioned mechanical properties are the main reasons for its popularity in the automotive, aerospace, machinery, heavy equipment, and other industries [99], [100]. A 65 mm diameter, shown on Figure 6 was prepared to handle two burnishing surfaces.

Table 2. 42CrMo4 alloy steel chemical composition [101].

Chemical Composition						
C	Mn	Si	P	S	Cr	Mo
0.38-0.45	0.60-0.90	0.40 max	0.035 max	0.035 max	0.90-1.20	0.15-0.30

Table 3. 42CrMo4 alloy steel mechanical properties [101].

Mechanical Property				
Size Ø mm	Yield stress Rp0.2,N/nn2, min.	Ultimate tensile Stress, Rm, N/nn2	Elongation A5,%, min.	Hardness HB
<40	750	1000-1200	11	295-355
40-95	650	900-1100	12	265-325
>95	550	800-950	13	235-295

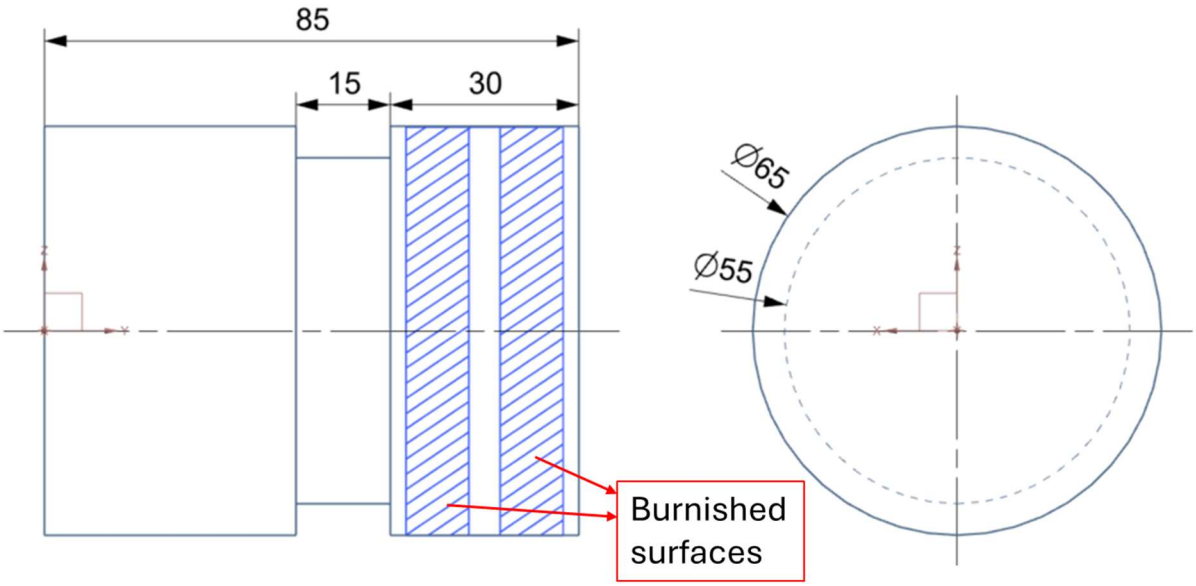

Figure 6, CAD model of 42CrMo4 workpiece for cylindrical burnishing.

3.3. Machining experimental setup of flat and cylindrical workpieces

As the first task for each experiment is to prepare the workpieces, the steps followed to prepare them are presented in this subsection. Machining cost depends on the selected machining technological parameters. For example, using higher feed reduces machining time, but the surface quality is compromised. To address poor surface quality after machining, post-machining finishing processes like grinding and burnishing are performed. Roughing and finishing are steps followed by familiar machining like milling and turning. The initial machining process has a nontrivial effect on the finished surface. It decides the amount of material to be plastically deformed or moved by the burnishing process. A relatively smoother initial surface requires less effort than a rough surface to achieve a desired final finish. Three machining processes, namely grinding, face milling, and turning, were applied to prepare the initial surface for the proposed burnishing process. To increase the effectiveness of the burnishing process, finishing technological parameters are selected to face mill and turn the workpieces as an initial surface preparation step. This was planned to study the effect of the modified tool and applied novel burnishing methods on the generated final surface. Stainless steel 3D printing and grinding

The additive manufacturing process was carried out using the ORLAS CREATOR 3D Metal Printer (manufactured by OR LASER, Dieburg, Germany), which employs a laser powder bed fusion (L-PBF) techniques. To optimize the printing process a two-stage scanning strategy was implemented, with each stage featuring distinct laser parameters tailored to specific functional requirements.

In the first stage, the laser operated at 50% of its maximum power (corresponding to 107 W) to ensure controlled energy input, minimizing thermal stress and porosity formation. The scan speed was set to 1200 mm/s, and the laser passed over each layer only once. This stage prioritized efficient material consolidation while maintaining dimensional accuracy.

The second stage utilized 85% laser power (182 W) at a reduced speed of 600 mm/s, also with a single repetition. The higher energy density in this phase promoted improved layer adhesion and densification, critical for achieving enhanced mechanical properties. Both stages shared consistent parameters, including a focused beam diameter of 40 μm, a layer thickness of 50 μm, and a hatch spacing of 40 μm, resulting in an 80% overlap between adjacent scan tracks.

To mitigate directional anisotropy and distribute residual stresses evenly, a 120° rotation angle was applied between successive layers, combined with a continuous zig-zag scanning pattern. This approach reduces preferential grain orientation and minimizes defects such as balling or keyholing.

The selected parameters reflect a deliberate trade-off between production speed, surface quality, and mechanical performance, ensuring repeatability and structural integrity. The two-stage strategy enhances process control by separating the initial consolidation phase (for stability) from the high-energy finishing phase (for strength), ultimately optimizing material usage and part performance.

Even though 3D printing's main objective is to avoid or reduce machining by producing exact dimensions and shapes from a 3D model, its rough surface still exposes it to further finishing machining. Preliminary tests revealed that burnishing the as-built surface directly resulted in a poor surface finish, necessitating an intermediate grinding step prior to burnishing. The grinding process was performed using a Metallkraft FSM 4080 series surface grinding machine (Stürmer Maschinen, Hallstadt, Germany) equipped with a 6A60M8V 38 Granit wheel operating at 1450 RPM. It was conducted in two steps, which are roughing and finishing operations.

3.3.1. **C45 Steel finishing face milling**

Finishing face milling cutting parameters were selected while preparing the initial surface for the succeeding burnishing process, as a rougher surface affects the burnishing efficiency. Cutting speed of 250 m/min, feed rate of 0.25 mm/rev, and depth of cut of 1 mm were used. To perform this process, Perfect Jet MCV-M8 CNC milling machine depicted in Figure 7 a with milling head R252.44-0800271SM produced by Ping Jeng Machinery Industry, located in Taiwan was applied. A SANDVIK cutter with an 80 mm diameter and ATORN OCKX0606AD-TR HC4640 octagonal inserts, without changing the cutting parameters, to make sure a similar initial surface was applied to face mill the workpieces. 5% emulsion of Rhenus TS 25 coolant and lubricant was also applied during the cutting process to avoid the temperature effect on cutting performance and its effect on the created surface.

3.3.2. **42CrMo4 alloy finishing turning**

The idea of using finishing cutting parameters during face milling of the workpiece for the face surface was kept for the turning process during initial surface preparation. A cutting speed of 120 m/min with 0.1 mm/rev feed and 0.1 mm depth of cut were utilized. Lower feed and shallow depth of cut combined with higher speed assures a smoother surface. Optimum OPTiturn S600 CNC lathe, produced by a German company called Optimum Maschinen Germany GmbH was used to turn the workpieces. Its heavy cast iron bed feature makes it

suitable for high-speed cutting. SANDIV DCLNL 2525M tool with 4NC-CNGA120412 (PCBN Tipped Carbide coated by TiN) finishing insert was selected for the mentioned purpose. The four cutting edges insert geometry includes an included angle of 80°, an inscribed circle of 12.7 mm (½ inches), a thickness of 4.76 mm (3/16 inches), a corner radius of 1.19 mm (3/64 inches), and a clearance angle of 0°.

3.4. Burnishing process setup

To use the same tool for flat and cylindrical surfaces, a modification is needed that has already been discussed for the flat surface. The same CNC milling center and CNC lathe (which are used to face mill and turn the surfaces) were also applied to conduct the burnishing process. The burnishing parameters were coded in terms of G and M code for both machines but an additional path generating care was taken in the milling machine case. From the controllable technological parameters, force, feed, number of passes, and speed are the most influential [4], [26], [102]. Even though it is advisable to study all the parameters, it is not feasible due to resource and time constraints. I studied the effect of force, feed, and number of passes in all experiments, keeping the other parameters constant.

Controlling burnishing force is crucial when conducting burnishing experiment. Kistler 9257A force sensor, a Kistler 5011A signal processing charge amplifier (both from Kistler Instrumente AG, Winterthur, Switzerland) were applied in all experiments. NI Compact DAQ 9171 four-channel signal acquisition unit (NI Hungary Kft. Debrecen, Hungary) was integrated with LabView for real-time data display and control.

3.4.1. Flat surface burnishing

When using the same burnishing tool for cylindrical and flat surfaces was raised as an idea, tool modification, parameter control, and its path selection were the tasks that need to be addressed.

The tool adopter shown in Figure 3 was designed and manufactured in the workshop of the Institute of Manufacturing Science (University of Miskolc) to fit a tool made for a lathe machine and to be used in a milling machine as well. The milling head supported the tool and was only responsible for force control movement along the Z axis. Figure 7 c shows the burnishing tool in action. Table was moving along the X and Y axes against the tool to generate the planned burnishing path. The parallel tool path was selected because of its easy-to-apply procedure. Controlled pressure was applied by the milling head holding the tool. Feed action along the Y axis and parallel linear movement along the X axis were controlled by the table at a specified constant burnishing speed for all surfaces. Force, feed, and number of passes were varied to study the effect of the process. Table 4 and Table 5 shows the applied parameters to flat C45 with their levels and the experimental plan. Feed combinations (f1, f2, and f3) are used as a new approach which is discussed in section 3.5. The applied parameters and their levels to the 3D printed stainless steel (MetcoAdd 17-4PH-A) are depicted on

Table 6 and Table 7. The remaining parameters, such as speed, were kept constant to manage experimental costs. Due to the material and printing cost, I applied L16 orthogonal array Taguchi design to reduce the experimental runs without compromising the amount of data.

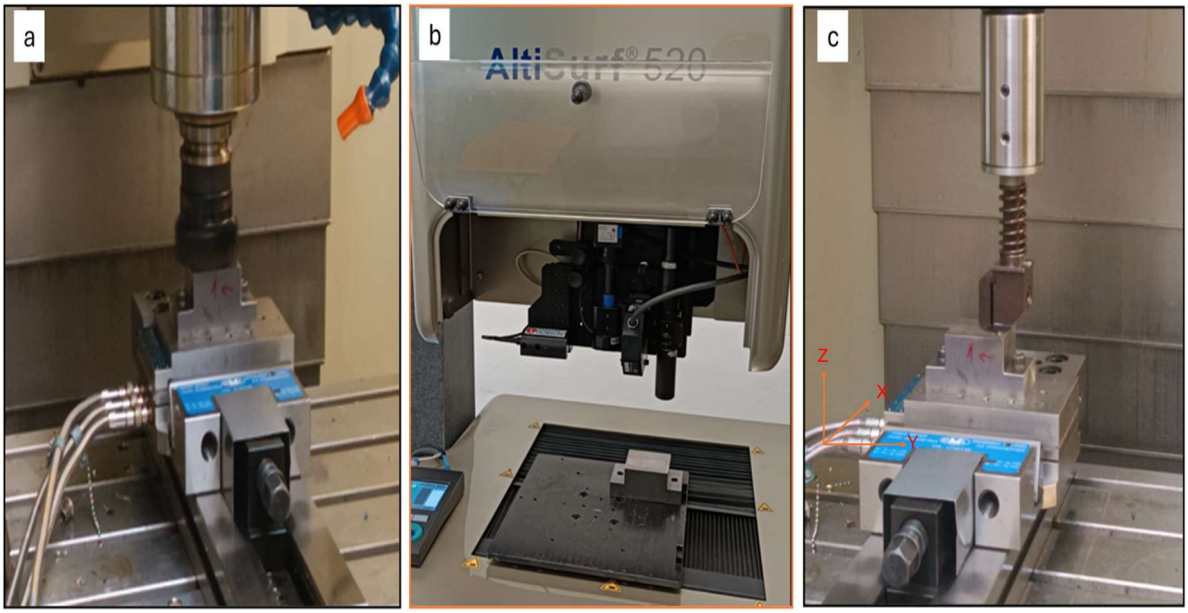

Figure 7. Experimental equipment: (a) face milling, (b) roughness measurement, and (c) burnishing process.

Levels of the burnishing force were selected based on preliminary trial experiments. A fixed force level is not universally applicable as the optimal value depends on the specific mechanical properties of each material. Pathade et al. [103] report that 84% of feed rate used in literature are between 0.01 and 0.27 mm/rev, and the suggested number of passes are between 1 and 4, with a maximum of 7 passes reported. All selected feed/feed rate and number of passes in this dissertation adhere to these ranges.

Table 4. Burnishing parameters and their levels of flat C45 workpiece.

Burnishing parameters	**New Method**			**Old Method**			
	Level 1	**Level 2**	**Level 3**	**Level 1**	**Level 2**	**Level 3**	**Level 4**
Force [N]	70	90	110	70	90	110	-
Feed [mm]	f1	f2	f3	0.02	0.08	0.14	0.2
Pass	2	3	4	2	3	4	-

Table 5. Experimental runs flat C45 slide burnishing process.

New Method				Old Method			
Surface	**Force [N]**	**Feed [mm]**	**Pass**	**Surface**	**Force [N]**	**Feed [mm]**	**Pass**
N_1	70	f1	2	**O_1**	70	0.02	2
				O_2	70	0.08	2
N_2	70	f2	3	**O_3**	70	0.02	3
				O_4	70	0.08	3
				O_5	70	0.14	3
N_3	70	f3	4	**O_6**	70	0.02	4
				O_7	70	0.08	4
				O_8	70	0.14	4
				O_9	70	0.2	4
N_4	90	f1	2	**O_10**	90	0.02	2
				O_11	90	0.08	2
N_5	90	f2	3	**O_12**	90	0.02	3
				O_13	90	0.08	3
				O_14	90	0.14	3
N_6	90	f3	4	**O_15**	90	0.02	4
				O_16	90	0.08	4
				O_17	90	0.14	4
				O_18	90	0.2	4
N_7	110	f1	2	**O_19**	110	0.02	2
				O_20	110	0.08	2
N_8	110	f2	3	**O_21**	110	0.02	3
				O_22	110	0.08	3
				O_23	110	0.14	3
N_9	110	f3	4	**O_24**	110	0.02	4
				O_25	110	0.08	4
				O_26	110	0.14	4
				O_27	110	0.2	4

Table 6. Parameters and their levels of metal 3D printed stainless steel

Levels	**Force (N)**	**Feed (mm)**	**Pass**
1	40	0.02	1
2	60	0.07	2
3	80	0.12	3
4	100	0.17	4

Table 7. Uncoded L16 orthogonal array Taguchi experimental design metal 3D printed stainless steel.

Run	Force (N)	Feed (mm)	Pass
1	40	0.02	1
2	40	0.07	2
3	40	0.12	3
4	40	0.17	4
5	60	0.02	2
6	60	0.07	1
7	60	0.12	4
8	60	0.17	3
9	80	0.02	3
10	80	0.07	4
11	80	0.12	1
12	80	0.17	2
13	100	0.02	4
14	100	0.07	3
15	100	0.12	2
16	100	0.17	1

3.4.2. **Cylindrical surface burnishing**

The same tool shown in Figure 8 was used to burnish cylindrical 42CrMo4 workpieces by CNC lathe (Optimum OPTiturn S600). The same parameter selection (presented in Table 8) and control method as flat surface burnishing (C45) was used. The tool was held with controlled pressure against the rotating workpiece and progressing linearly based on the specified feed rate. The process is repeated based on the number of passes, as it is a multi-pass process. Unlike the burnishing process of a flat surface using a milling machine, which can give a chance to decide the direction of the feed (for example, perpendicular or at an angle to the cutting direction), the burnishing of a cylindrical shape using a lathe and cutting direction are parallel. Hence, the performance of the process can be affected. The proposed feed varying approach (section 3.5) changes the feed after each pass repetition, which is only applicable in the multi-pass case. For this reason, 2, 3, and 4 passes, 60 N, 90 N, 120 N, and 150 N forces, as well as 0.02 mm/rev, 0.08 mm/rev, 0.14 mm/rev, and 0.2 mm/rev feeds, were applied for both burnishing methods. Burnishing force levels were selected based on a study by Jawad et al. [58] on similar material and burnishing tool. While feed and number of passes levels are selected based on the suggested range by researchers like [103]. For each force and pass category, all possible feed combinations were tried, and their equivalent old burnishing method feeds were tested for comparison. Since it is difficult to represent feed combinations (new feed application approach) with their exact value during graphical presentation of measured values, v1 to v11 (hence after represents the feed combination of the feed varying burnishing method) symbols are used as presented in Table 8**Error! Reference source not found.**. In addition, a systematic naming convention was used for the workpieces: samples N1 through N44 correspond to the feed-varying method, while samples O1 through O48 correspond to the conventional method.

The table presents an experimental plan for one force (F) only (N1-N11 and O1-O12), since the same feed combination and number of passes apply for all forces used. A larger-to-smaller feed application procedure was followed to smooth tool marks created by the higher feeds and remove leftover asperities through the smaller feed overlapping tool path. For example, if v1 is selected, 0.08 mm/rev is applied first, then 0.02 mm/rev

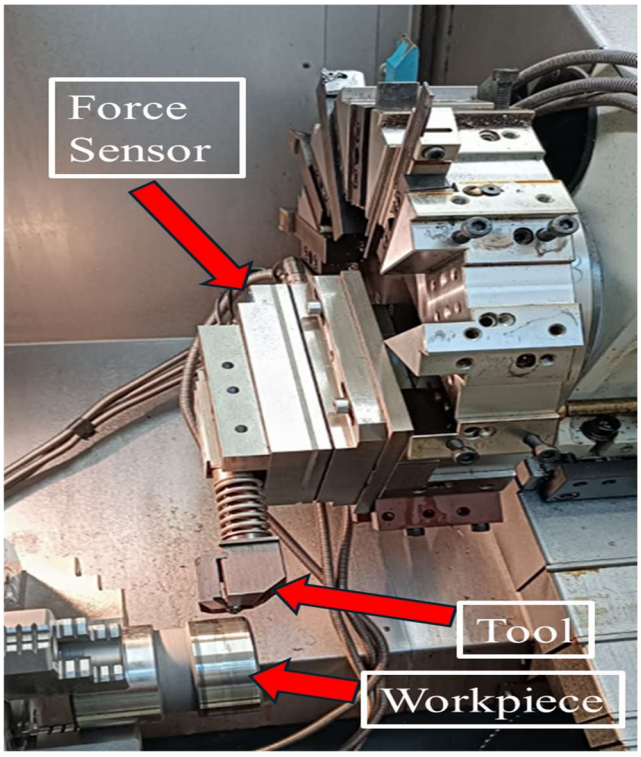

Figure 8. Slide burnishing process of 42CrMo4 setup.

Table 8. Burnishing plan for the burnishing of a cylindrical 42CrMo4 shaft.

New Burnishing Method				Old Burnishing Method			
Surface number	Force [N]	Pass	Feed Combination [mm/rev]	Surface number	Force [N]	Pass	Feed [mm/rev]
N1	F	2	v1 (0.02, 0.08)	O1	F	2	0.02
N2			v2 (0.02, 0.14)	O2			0.08
N3			v3 (0.02, 0.2)	O3			0.14
N4			v4 (0.08, 0.14)	O4			0.2
N5			v5 (0.08, 0.2)	O5		3	0.02
N6			v6 (0.14, 0.2)	O6			0.08
N7		3	v7 (0.02, 0.08, 0.14)	O7			0.14
N8			v8 (0.02, 0.08, 0.2)	O8			0.2
N9			v9 (0.02, 0.14, 0.2)	O9		4	0.02
N10			v10 (0.08, 0.14, 0.2)	O10			0.08
N11		4	v11 (0.02, 0.08, 0.14, 0.2)	O11			0.14
				O12			0.2

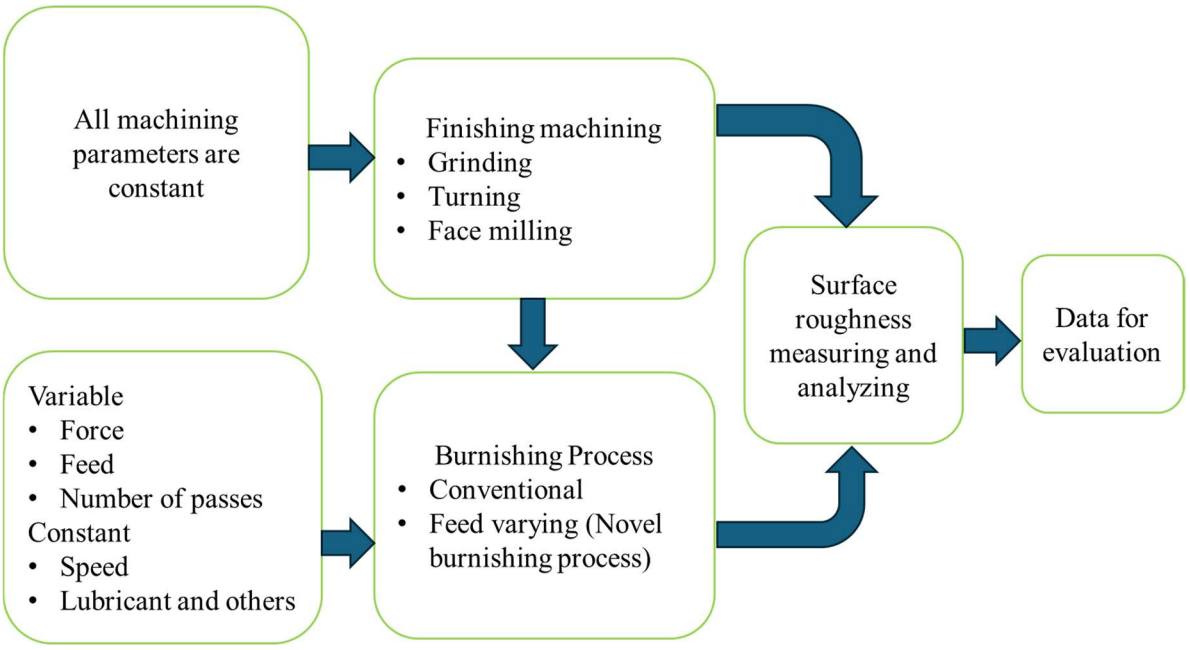

Figure 9. Flowchart of steps applied to conduct the experiment.

3.5. Novel burnishing feed application method

A smoother surface, in addition to other mechanical properties enhancements, is achieved after a hard and smooth tool burnishes the surface based on the specified parameters. It is evident that the selected parameters greatly affect the surface finish. Researchers tend to find the optimal burnishing parameters for different environments, tool properties, and material types. But they fail to apply the feed in different ways for response optimization than by changing its magnitude. I introduced new burnishing approaches that change how the feed is applied so that it follows a different path.

Burnishing force pushes the tool against the surface, and the milling table moves the workpiece along a CAM program-generated path at a specified speed to finish a complete the loop. The table progresses by the feeding amount along the feed direction and keeps doing it till the targeted surface is covered. The whole process is repeated numerous times to achieve enhanced surface integrity and are called number of passes. This new proposed method works when the number of passes are more than two. This method is referred to here as the new method or the feed-varying method. And the conventional method is also referred to as the old method.

The mechanism of plastically deforming the peaks of the surface toward the valley also deforms the plane part of the surface. Due to this cold-working process, the surface integrity of the product changes. The initial peaks and those grown after the plastic deformation can be left unaddressed by the succeeding passes, which gives a low smoothness modification. This problem is much pronounced when the feed is high because the path overlap percentage is low. This happens because the selected burnishing parameters are the same while repeating the process based on the number of passes, which causes the tool to pass through the same path.

To address the discussed problem, I changed the feed values after each complete pass to give the tool a deviated path. By doing so, the tool follows a new path in each loop and in each repetition or number of passes. This helps it to deform the leftover peaks and newly created

peaks by the first repetition. Either increasing or decreasing the feed based on the tool ball diameter can achieve the required task by the tool. Figure 10 shows the old and the proposed method CAD model in a and b. In Figure 10 a, tool marks increased by the succeeding passes and unfilled valleys are shown. In Figure 10 b, the change in feed made the tool to shift its center of path and as a result the red hatched section is deformed which gave Δh reduction of the peak. When the combined feeds were applied, the larger feed was applied first, then the smaller one, to achieve an overlapping feed path due to the low feed, to avoid tool marks.

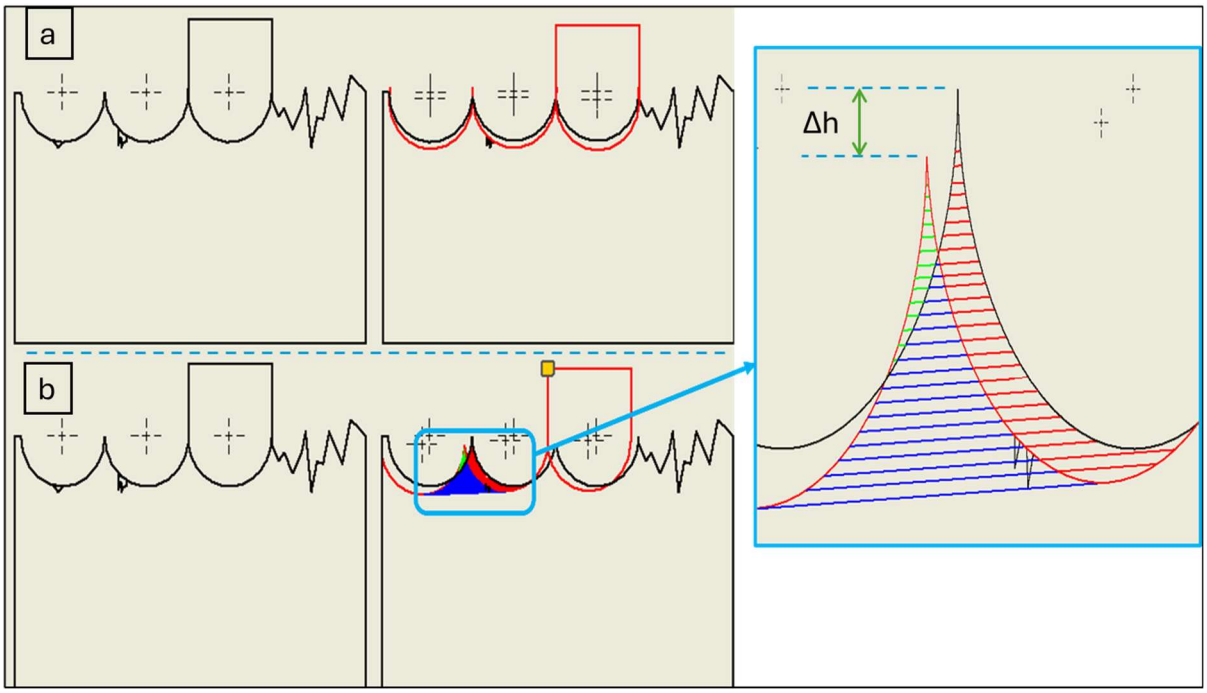

Figure 10. New burnishing methodology mechanism model: (a) old method and (b) new method.

What distinguishes the new method is that it requires no additional physical accessories and can be applied to both milling and lathe machines. Selecting optimal burnishing parameters in addition to the proposed method can enhance the surface finish.

3.6. Surface Roughness Measurement

To compare the physical change (micro-change) on the workpieces induced by the machining process, in our case, grinding, milling, turning, and burnishing, measuring surface roughness is the selected method. Flat printed stainless steel and C45 medium carbon steel as well as cylindrical 42CrMo4 with an initial machining status of ground, face milling finishing, and turning finishing were measured before and after the machining. AltiSurf 520 (Altimet SAS, Thonan-Les-Bains, France), shown in Figure 11, was used to measure the 3D roughness parameters. CL2 confocal chromatic sensor and MG140 magnification were selected to scan an area of 4mm×4mm. To catch the perpendicular profile, perpendicular scanning direction of the sensor to the machining direction was used. Workpieces were cleaned of debris and lubricants with alcohol and compressed air to maintain the accuracy and reliability of the measurements.

The device is equipped with Altimap 6.2 software of Digital Surf to analyze and process surface topography data obtained from measurement instruments. A Gaussian filter on a 4mm×4mm area, based on ISO 25178-2:2021 [104], was applied to evaluate the data.

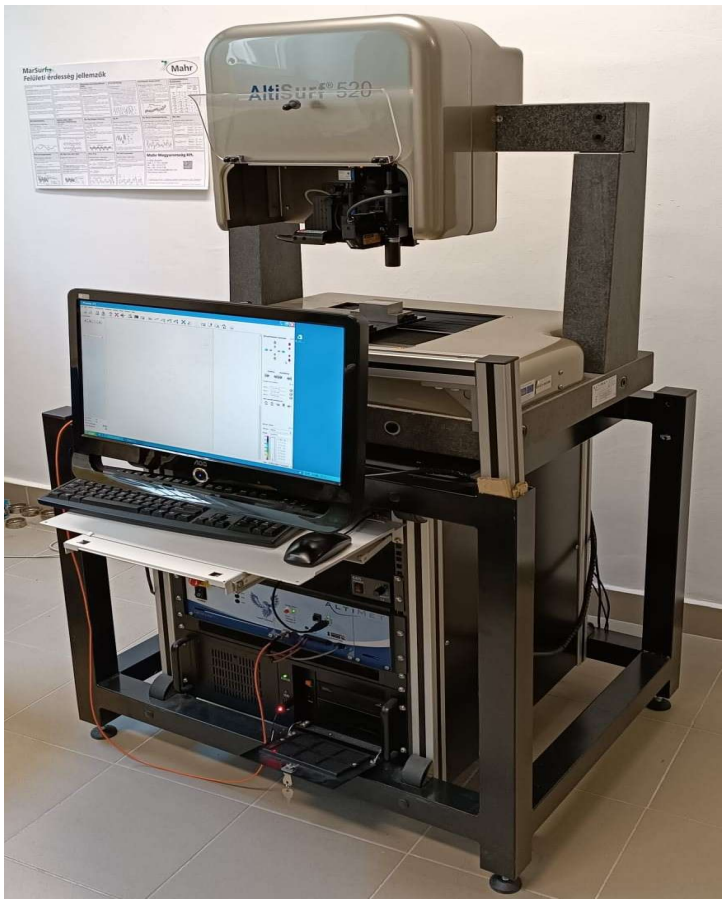

Figure 11. AltiSurf 520 surface roughness measuring device.

When selecting the evaluation parameters, height, spatial, and functional characteristics of the surface were considered. 3D roughness parameters arithmetic mean height (Sa), root mean square height (Sq), skewness (Ssk), kurtosis (Sku), core roughness depth (Sk), reduced peak height (Spk), and reduced valley depth (Svk) selection was based on their ability to comprehensively characterize the surface topography and capture the variations induced by the machining processes. Sa and Sq provide general information on surface amplitude, while Ssk and Sku offer insights into the asymmetry and sharpness of the height distribution, helping to identify irregularities such as peaks or valleys generated during machining. The core roughness parameters (Sk, Spk, and Svk) indicate the material plastic flow by measuring the vertical characteristics of the surface texture. They are a powerful way to analyze a surface's functionality especially for parts that involve ear, lubrication, or bearing. Since 2D profile-based roughness parameters can be biased by measurement location selection, while 3D parameters were chosen to ensure a more representative analysis by averaging over a defined area, minimizing measurement variability, and providing a robust evaluation of surface modifications post-machining.

Initial roughness measurements for the burnishing process are averaged in all experiments as the same machining parameters were applied. Sample workpieces were selected and measured to give the starting roughness level for the succeeding process. Specifically, roughness values were averaged after 3D printing, grinding, face milling, and turning. For all burnishing processes, each surface was measured separately since the burnishing parameters are different.

3.7. Residual stress and microhardness measurement of MetcoAdd 17-4PH

The analysis of residual stress, using the Xstress G3 diffractometer (Stresstech GmbH, Rennerod, Germany), was crucial for comprehending the stress distribution within the workpiece after all three processes (printing, grinding, and burnishing). For the purpose of measuring stress distribution at depth, the QETCH 100 M electrolytic etcher from QATM (ATM Qness GmbH, Mammelzen, Germany) was utilized for the removal of steel layers, with the thickness of these etched layers being precisely measured by the Mitutoyo ABSOLUTE depth gauge (Mitutoyo Europe GmbH, Neuss, Germany).

Concerning the microhardness analysis, a Tukon 2100B device, by Wilson Instruments, Norwood, MA (USA) was used to assess the variations in hardness across the burnished surfaces. Surfaces were prepared for the indentation process by cleaning them to avoid any possible errors. An indenter with a 1.96 N (0.2 kg) of load was applied for 10 s. Three measurements were achieved in three different places on each surface, and an average value was then taken for the purpose of the analysis.

3.8. Percentage change calculation

Percentage changes realized due to the introduced surface enhancement machining methods are calculated using Equation (1) [58], [105] to help in understanding the increased or decreased degree of the surfaces' responses. The terms initial and final in the equation represent the starting measured value and the value after a specified machining process is applied.

$$\%\, change = \left(\frac{final - initial}{initial}\right) * 100 \qquad (1)$$

4. RESULTS AND DISCUSSION

Measured and evaluated results of three different workpiece materials burnished using the same tool but different burnishing environments are discussed and presented in this chapter.

4.1. Surface Roughness Analysis of flat 3D Printed MetcoAdd 17-4PH-A

The experiment began by analyzing the surface roughness of 3D-printed stainless steel in its as-printed form. It exhibited high roughness with average Sa a values of 11.3 μm (Table 12). These high value indicates the finishing process requirement after the metal 3D printing. The Kurtosis value of 3.19 gives a Gaussian height distribution information that requires careful evaluation, as it is sensitive to outliers. Skewness, core roughness depth, reduced peak height, and reduced valley depth are evaluated to give a good understanding of the created surface after the grinding and burnishing process. Residual stress and microhardness are also other studied responses of the surface after the performed machining process. The burnishing process enhanced them as shown in Table 9.

The grinding process is one of the popular finishing processes of 3D printed materials due to its low roughness, as I discussed in the literature review section. All ground surfaces' roughness, residual stress, and hardness were measured, and their average was applied to compare the improvement with the as-built and burnished status. After the grinding process, the roughness of the surface improved dramatically, with Sa reduced to 1.08 μm, which is around 90%. Table 9 presents the percentage change of the studied responses to compare the achieved smoothness. The negative sign indicates a reduction of the measured parameter after the specified machining process, and the positive sign indicates an increase.

Table 9. Percentage changes after 3D printing, grinding, and burnishing.

Responses	3D printed	Grounded	Burnished (Average)	Percentage changes		
				3D printed to grounded	Grounded to Burnishing	3D printed to Burnishing
Sa	11.3	1.08	0.46	-90.4	-57.1	-95.9
Ssk	-0.449	-0.208	-1.00	-53.7	380.0	122.4
Sku	3.19	3.82	7.83	19.7	105.0	145.5
Sk	35.7	3.29	1.06	-90.8	-67.9	-97.0
Spk	8.91	1.37	0.56	-84.6	-58.8	-93.7
Svk	16.9	1.64	0.90	-90.3	-45.3	-94.7
σ (MPa), S.R.S Trans	129.9	-189.9	-847.7	-246.2	346.4	-752.6
σ (MPa) S.R.S Long	43.5	98.5	-540.3	126.4	-648.5	-1342.1
HV 0.2 Average, Burnished	241	350.6	430.5	45.5	22.8	78.6

By taking the ground surface as a starting surface, slide diamond burnishing further refined all surfaces to a great extent. From Figure 12, it can be observed how the surfaces are transformed by the two machining processes. The red and green colors represent the peak and valley of the scanned surface. Each measured response, compared with the initial surface and with respect to the burnishing variables, will be presented in this section.

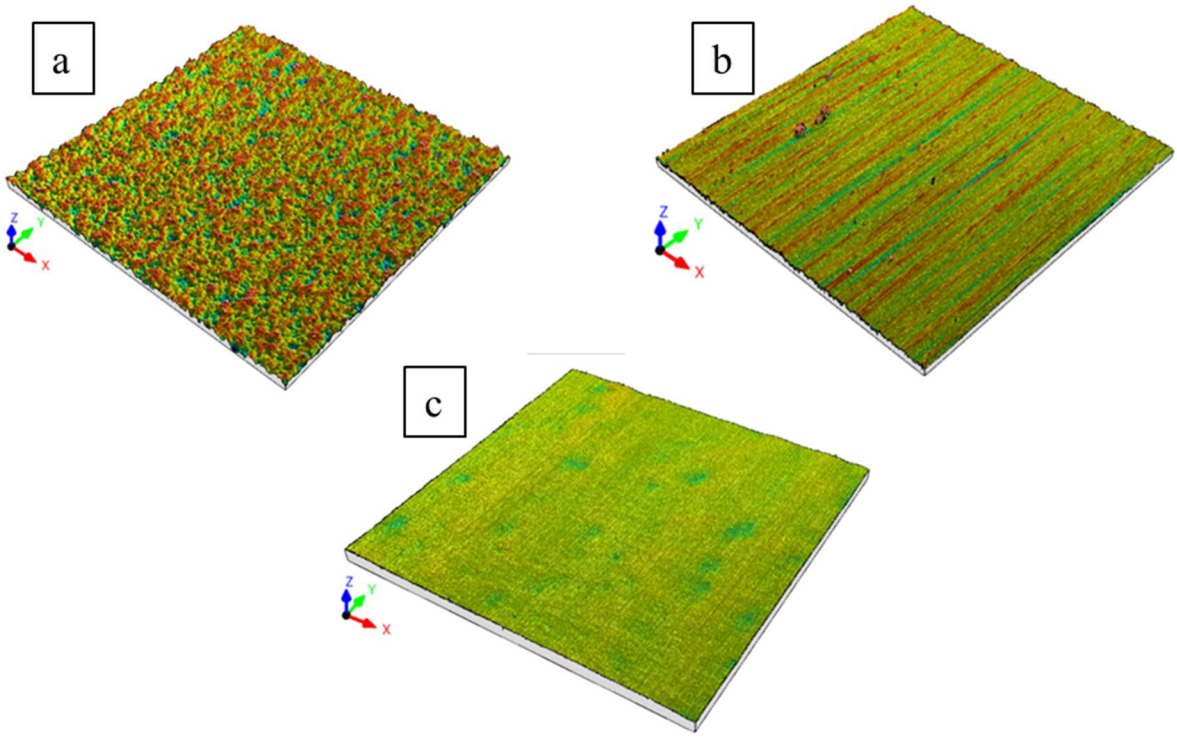

Figure 12. Scanned (a) 3D printed MetcoAdd 17-4PH-A as-built, (b) ground, and (c) slide burnished (surface number 6).

4.1.1. **Height parameter changes**

The height parameter answers the question of what the overall shape and character of the surface texture is by describing the statistical nature of the surface's topography. Average height difference (Sa), the symmetry of the surface height distribution around the mean plane (Ssk), and sharpness of the surface height distribution relative to a normal distribution (Sku) are discussed. Measured values of the surfaces are given in Table 12.

4.1.1.1. **Arithmetic means roughness (Sa)**

Arithmetic means average roughness dropped to as low as 0.20 µm (surface 9) by 446% compared to the ground surface. Figure 13 shows a bar graph for the comparison of the three machining stages, which shows the roughness level decreasing generally but with different trends (Figure 13b) in the burnishing process due to the systematic changes of parameters to study their effect. The Taguchi design of experiment Table 7 assigned increasing burnishing force from 40 N to 100 N while feed and number of passes change systematically automatically by Minitab 18 software. A decreasing roughness trend from surface 1 to 9 and an increasing roughness on the remaining surfaces are observed. This shows how force affects the roughness

combined with the other parameters. Given that grinding and burnishing are finishing processes, it is obvious that they will reduce the roughness. The roughness reduction due to the slide burnishing process, with reference to before and after grinding process, and the effects of its parameters will be presented and discussed.

Following the burnishing force held constant for each group of four surfaces and increased by 20 N for the next group of four surfaces, it is manageable to analyze the effect of feed and pass. Feed increased from 0.02 mm to 0.17 mm while the number of passes changed systematically by the Taguchi design. Surface one with minimum feed but the smallest pass shows the highest roughness compared to the other three surfaces, which shared the same force (40 N). Surface four also experienced the second-highest roughness from the group, which reflects the highest feed. From these, we can understand that higher feed and fewer passes contributed to higher roughness in this group. The second group of burnished surfaces (5-8) with 60 N force showed decreased roughness compared to the first group, except in surface six. Surface five with minimum feed (0.02 mm) is smoother within its group, and surface six with maximum Sa due to its low pass (1). In both the first and the second groups, the surfaces with 0.07 mm and 0.12 mm feeds, as well as 2 and 3 passes, showed minimum differences without taking force into consideration. A general decreasing pattern of roughness was witnessed when the force increased from 40 N to 60 N which can be observed in Figure 13b.

The surfaces burnished by 80 N and 100 N are rougher than the surfaces burnished by 40 N and 60 N, except surface 9. A sudden shift of roughness with three patterns, namely, surface nine, which is the lowest of all surfaces, surfaces 10, 13, 14, and 15, which are moderate, and the last pattern of surfaces 11, 12, and 16, which are the highest. If we check the parameters of the highest roughness surfaces, they share higher feed (0.12 mm and 0.17 mm) and the fewest passes (1 and 2). The medium roughness surfaces in these two groups contain almost all feed and pass values except the extreme values, 0.17 mm feed and one pass. Surface nine, having burnishing parameters of 80N force, 0.02mm feed, and three passes, experiences the lowest roughness among all burnished surfaces.

In addition to the patterns, exceptions and the influence of burnishing parameters, it is helpful to consider percentage improvements for better understanding. Taking the ground surface as an average initial surface, burnishing process gave a minimum roughness decrease of 63% to surfaces 16 and 446% to surface 9. These two surfaces belong to 80 N and 100 N burnishing force groups. From the 40 N and 60 N forces group, surface five with 294% and surface six with 139% are the maximum and minimum increase, respectively. These show how the burnishing process improved the roughness to a great extent.

The results show that the burnishing process successfully reduced the roughness more when optimal parameters are used. The force needs to be strong enough to plastically deform and flatten the peaks but limited from destroying the surface by producing microcracks and material pile-up. These two effects are shown in Figure 13b 40 N and 60 N with a decreasing and 80 N and 100 N with an increasing impact. Feed affects the roughness property positively when a smaller value (surface 9, 0.02 mm) is selected and negatively when a larger value (surface 17, 0.17 mm) is selected. It decides the distance covered by the burnishing tool between two successive tool paths. If a small distance is selected, it gives the tool a chance to deform the

peaks in some cases with an overlapping path, or to avoid undeformed peaks if high feed is selected. The other very important parameter is the number of passes, which helps in smoothing the surface by repeating the process. Optimal value selection is essential for this parameter, too. Otherwise, residual peaks if fewer passes are used and work hardening as well as cracking of the surface can be realized if an excessive number of passes are applied. Surfaces 1, 6,11, and 16 were burnished with one pass only and its effect is shown with a higher roughness value. While four passes were applied, no exaggerated roughness increase was observed compared to fewer passes. So, optimal burnishing force and number of passes with a smaller feed gave a smoother surface. It is evident that their contributions to the final output differ, as reported by several researchers [106], [107].

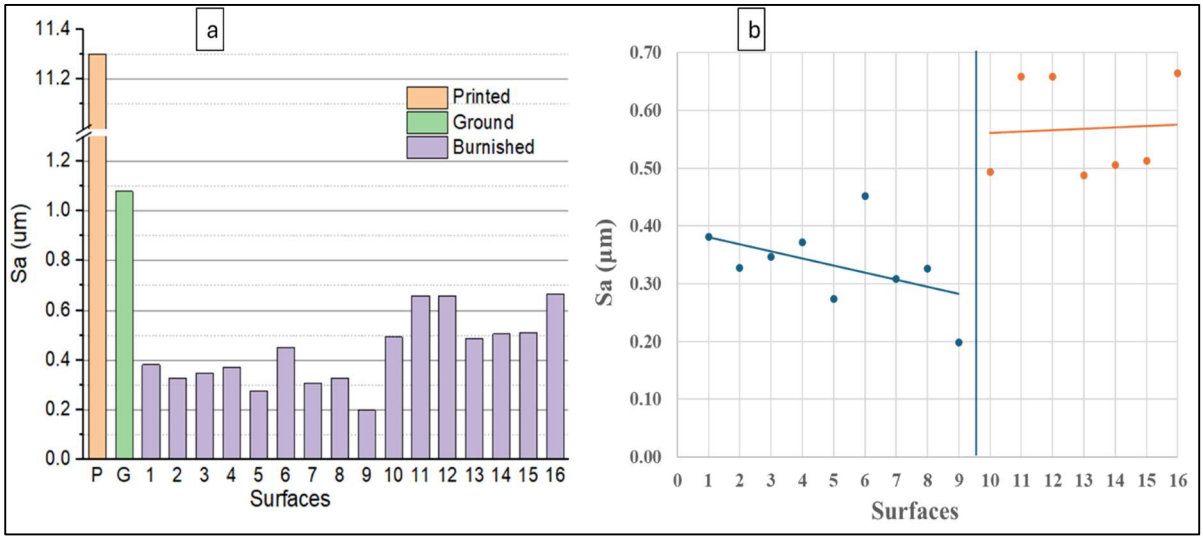

Figure 13. Arithmetic means average roughness (Sa) of (a) printed, ground, and burnished, (b) burnished surfaces.

The combined effects on the Sa response of the surface are also an important aspect to present and discuss. If three-level category (low, medium, and high) of the burnishing parameters are taken into consideration, there are 27 possible combinations. For some of these combinations, roughness responses can be predicted. Surfaces 11, 12, and 16 have a combination of higher force, higher feed, and fewer passes that resulted in a rough surface. On the other hand, surfaces 5 and 9 share medium force, lower feed, and medium pass number, resulting in a smoother surface. But due to dominance, these predictions can favor one or two parameter values despite the level category of the other. For example, surface 6 variables favor low Sa compared to other surfaces that share similar level categories, but due to its lower number of passes, Sa value is higher.

4.1.1.2. **Skewness and Kurtosis (Ssk, and Sku)**

Other important amplitude roughness measure that tells about peaks and valleys of the surfaces are skewness (Ssk) and kurtosis (Sku). Their average values were initially measured as -0.449 and 3.19, respectively, indicating a slightly valley-dominated surface with a near-Gaussian height distribution. After grinding, these values shifted to -0.208 (Ssk) and 3.83 (Sku), suggesting that grinding reduced valley depth while slightly increasing peak sharpness compared to the as-printed condition.

Significant surface texture changes were observed as showed in (Figure 14) following the diamond Sliding diamond process. The burnished surfaces exhibited an increase toward negative skewness except surface 5 and 7. Most samples (11 out of 16) showed Ssk values between -0.93 and -2.00, indicating deeper valleys compared to the ground state. All surfaces burnished by a 40 N force showed a higher increase compared to the other applied forces. Sudden high decreases (surfaces 6, 11, and 16) were observed for 60 N, 80 N, and 100 N when the number of passes is one. Otherwise, a stepped increases were shown for an increasing feed. Surfaces 5 and 7 were the only surfaces that showed a decrease burnished by 60 N, 0.02 mm, and 2 as well as 60 N, 0.12 mm, and 4 passes consistently. Minimum feed for surface 5 and highest passes for surface 7 could be the reason for this distinct behaviour. These indicate a strong enough force for the plastic deformation, and an optimal feed and pass number must be selected for the required peak and valley heights. This suggests that deep valley dominated surfaces created by burnishing enhance lubricant retention capabilities, which is beneficial for tribological applications. However, a few samples (5, 7, 9, 13, 14, and 15) displayed less negative skewness, likely due to the selected burnishing parameters that affect the localized material flow.

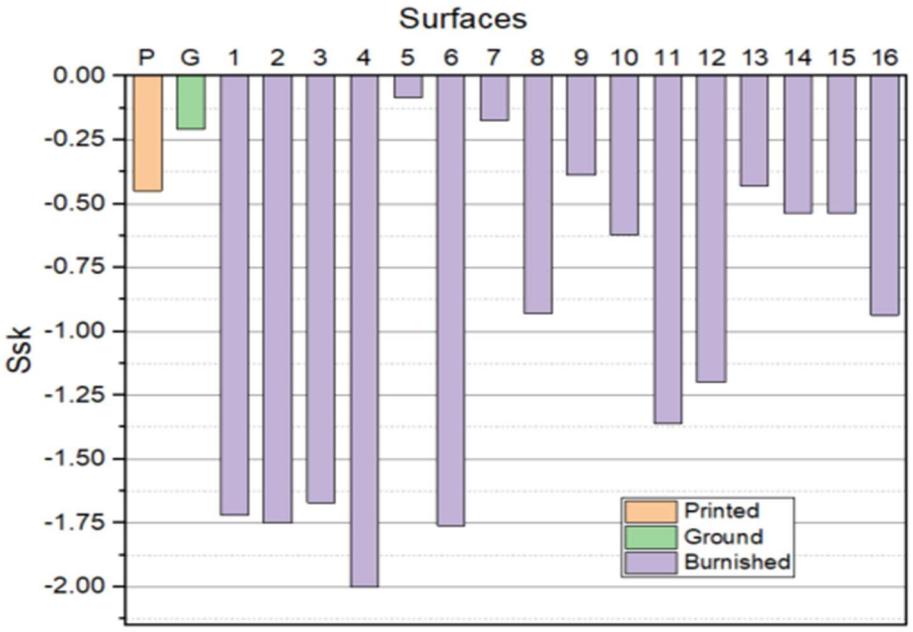

Figure 14. Measured skewness values of printed, ground, and burnished surfaces.

In addition to the information by skewness about the dominance of peaks or valleys, it is crucial to know their features with the help of kurtosis. Kurtosis values after burnishing, as depicted in Figure 15, increased substantially, ranging from 5.04 to 12.6, compared to the ground condition (3.83). A similar trend to skewness decrease was observed for kurtosis increase also. But, unlike the skewness exceptional surfaces of 5 and 7, all surfaces showed increased values compared to the as-printed and ground after the burnishing process. This indicates a spikier surface texture with sharper peaks and deeper valleys, confirmed by skewness, which could influence contact mechanics and wear behavior. The highest kurtosis (12.6, surface 4) suggests

extreme peaks and valleys, possibly due to aggressive burnishing conditions, whereas lower values (e.g., 5.04, Sample 14) imply a smoother but still non-Gaussian distribution.

When comparing burnishing to grinding:

- An average skewness decrease is by 380% confirms that burnishing enhances valley formation.
- Kurtosis increased by 105%**,** indicating a shift toward a more peaked surface topography.
- Sample 5 and 7 showed anomalous behavior**,** with skewness moving toward positive values, possibly due to insufficient burnishing force or uneven material displacement.

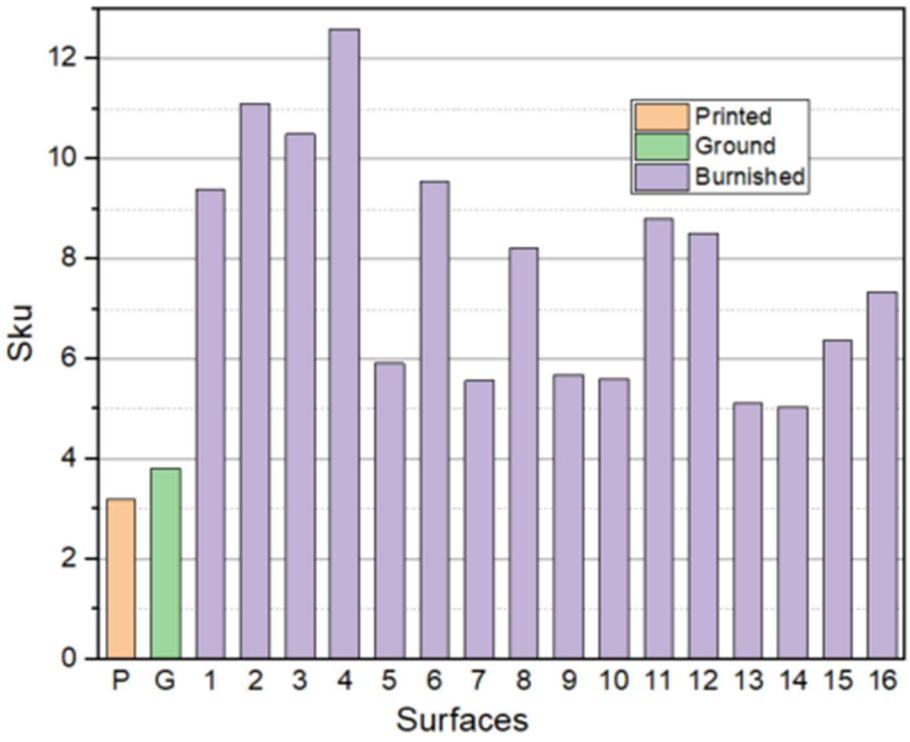

Figure 15. Measured kurtosis values of printed, ground, and burnished surfaces.

The results demonstrate that Sliding diamond burnishing significantly alters surface texture without transforming, making it more favorable for applications requiring improved lubrication retention (due to deeper valleys) but potentially increasing initial wear due to higher kurtosis. The variability among samples highlights the importance of optimizing burnishing parameters (force, feed, passes) to achieve consistent surface characteristics. Compared to grinding, burnishing offers superior control over skewness, making it suitable for functional surfaces in bearings, seals, and biomedical implants, where controlled valley depth is critical.

Varga et al. [105] decreased the Sa value of Ti6Al4V Titanium alloy printed by the SLM method after burnishing up to 3.86 µm from 13.91 µm without applying a grinding process before the burnishing process. They studied other 2D and 3D roughness parameters, but their Sa values show how successive grinding and burnishing can reduce the roughness compared to the result I found, which is much lower. There is a workpiece shape difference (cylindrical shape), which also contributed to the achieved value difference. Velazquez et al. [108] also observed a perfect

Gaussian distribution of skewness and kurtosis for all specimens (LPBF printed AISI 316L steel) analyzed after being burnished by VABB, which is similar to the Ssk and Sku results of this experiment. Generally there are almost no literature that studies 3D roughness parameters after successive grinding and burnishing of stainless steel which makes this study very important.

4.1.2. **Functional Parameters (Stratified surfaces)**

Height parameters like Sa are a general indicator of roughness without distinguishing the height and depth of peaks and valleys. The functional parameters analyze the surface's bearing area ratio curve by breaking the roughness into three zones as shown in Figure 16, which is very important to understand the functional characteristics of the roughness. Grinding and burnishing reduced the roughness of the 3D printed surfaces as shown in the same figure. This subsection discusses how the technological parameters of the burnishing process change these properties. All measured functional parameters are presented in Table 12.

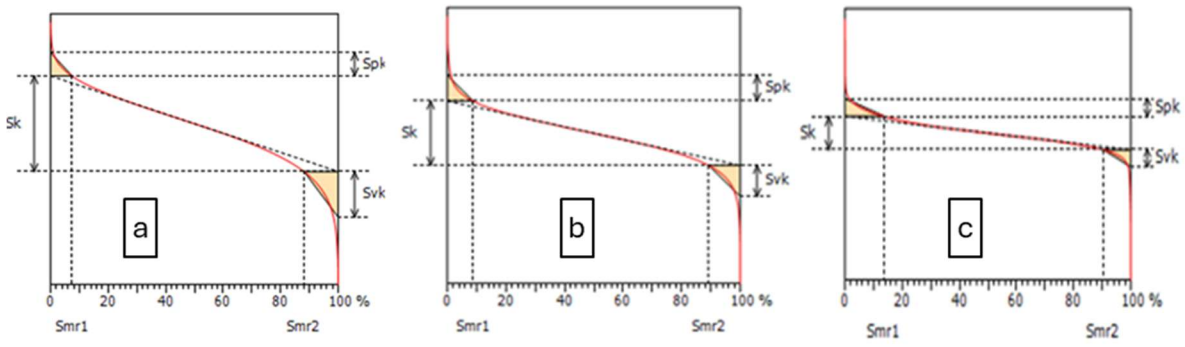

Figure 16. Functional parameter of (a) printed, (b) ground, and (c) burnished (Surface 7).

4.1.2.1. **Core roughness depth (Sk) analysis**

The height of the core material volume represents the part of the surface that will bear the load under normal running conditions after a short run-in period of two contacting surfaces. Properties, for example, friction, wear resistance, and loading carrying capacity of the surface, depend on this parameter. Core roughness depth of the printed surface was measured after grinding and the slide burnishing process to understand their effect. The technological parameters of burnishing showed variation on the produced surface since it changes the plastic deformation mechanism of the process.

Sk was decreased from 35.7 µm by the grinding to 3.29 µm and up to 0.34 µm by the burnishing when a 60 N force, 0.17 mm feed, and 3 passes were applied. The grinding removes the asperities of the printed surface to give a smooth surface reflected in Sk value, with a reduction by 90.8% (Table 9). Since grinding is not enough to give the final smoothness, burnishing further reduced the Sk value by 67.9%. Figure 17 presents the Sk values of the printed, ground, and burnished surface machined based on the design of experiment on Table 7.

The core roughness depth did not significantly change with the change of feed and number of passes when 40 N and 60 N forces were applied. The lowest Sk was achieved with the application of 0.17 mm feed, 60 N force, and 3 passes. With in these two force range, the

highest Sk was surface 6 burnished with 60 N force, 0.07 mm feed, and 1 pass. In these two surfaces, effect of pass was substantial in which higher passes (3) produced lower Sk and the lowest (1) pass produced higher Sk. In terms of feed and force, there is not much theoretical relation, as both surfaces were burnished with the same force and lower (expected to produce lower Sk) and higher feed (expected to produce higher Sk). A higher force is expected to produce enough pressing magnitude to plastically deform the peaks, or if it is much higher, the tool can plow the surface. On the other hand, lower feed generates a smoother surface directly related to Sk by giving the tool to follow near to each other or overlapping paths that can deform all the surface asperities.

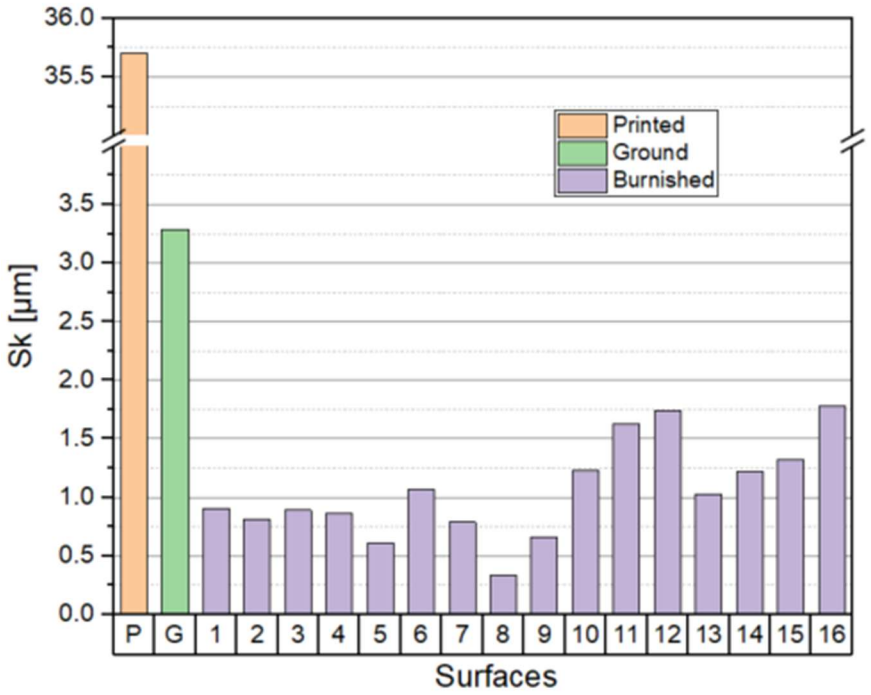

Figure 17. Core roughness depth of printed, ground, and burnished surfaces.

Higher forces (80 N and 100 N) clearly demonstrated their association with feed by increasing the Sk when the feed was increased from 0.02 mm to 0.17 mm (surfaces 9 to 12 and 13 to 16). Both forces generated lower Sk when applied with lower feed and higher Sk with higher feed. In these two force categories, the number of passes showed no significant effect, dominated by the force and feed. These all indicate that the core roughness depth was reduced by the grinding and burnishing, which was further affected by the technological parameter change of the burnishing process. Lower Sk means shorter vertical height of the core roughness part of the roughness zone, interpreted as lower load-carrying capacity of the surface. Based on the application of the product surface, the machining processes can be selected to produce the required smoothness.

4.1.2.2. **Reduced peak height (Spk) analysis**

Another important roughness zone located above the core roughness depth is the reduced peak height, which measures the vertical peak height. The grinding process decreased the Spk value of the printed surface by 84.6% when further attempted by slide burnishing decreased up to

58.8%. Figure 18 depicts the Spk values after the successive grinding and slide burnishing of the 3D printed surfaces.

Compared to the core roughness depth, the achieved reduced peak height constituted a shorter zone with a different initial height. Except for surface 3, 40 N force (surface 1 to 4) produced decreasing Spk on a low slope when increasing the feed. Increasing the force to 60 N for the next four surfaces showed no much change after the abrupt increase when the feed changed from 0.02 mm to 0.07 mm. Without the exceptions (surface 3 and 5), the two forces produced similar Spk with negligible effect of changing the feed and number of passes.

Increasing the force to 80 N and 100N also generated a surface with a similar Spk value, a little higher than the first two forces. Like in the case of 40 and 60 N forces, the feed has no significant effect on the process. Surfaces 11, 12, and 16 showed increased values compared to the other surfaces or lower Spk reduction compared to the ground surface. A common technological parameter for these three surfaces is a lower number of passes (1 and 2). When higher force and fewer passes are combined, their effect produces a higher Spk value, indicating a peaky surface compared to the other forces and number of passes combined effect. Generally, a decreased reduced peak height means shorter peaks that flatten after the run-in. A lower Spk is preferred for most applications since it reduces the friction and wear of the surface.

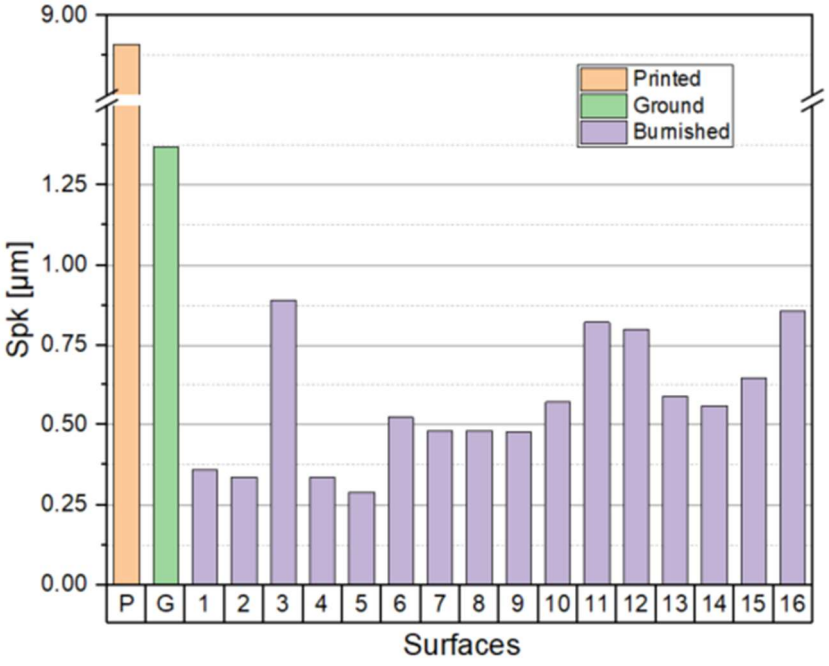

Figure 18. Reduced peak height of printed, ground, and burnished surfaces.

4.1.2.3. **Reduced valley depth (Svk) analysis**

The printed material has a deeper valley (Svk = 16.9 µm) presented by Figure 19 compared to the peak height (Spk = 8.9 µm), which decreased by the grinding process to an average value Svk = 1.64 µm. When burnished, Skv was shallowed as the process displaced the peak material to the valley. Across the various parameter settings, the burnishing process achieved a significant reduction in the measured value of Svk by 45.3%.

The lowest burnishing force, 40 N, was not strong enough to send the peaks to the valley compared to the other forces, especially 60 N. Increasing the pass and the feed sharing the same force, first decreased the Svk of surfaces 2 and 3 but increased again for surface 4. This happened due to the applied maximum feed (0.17 mm). Increasing the force to 60 N applied to surfaces 5, 6, 7, and 8, achieved the lower Svk compared to 40 N force except surface 6 which was burnished with 1 pass. Comparatively higher feed effect on producing higher Svk value was also reflected on surface 8. 80 N and 100 N forces were applied to burnished surfaces from 9 to 16 four surfaces each. After achieving the lowest Svk value on surface 9 with 80 N force, 0.02 mm feed, and 3 passes, a gradual increase was observed except for surfaces 11, 12, and 16. This indicates further increasing the force can roughen the surface with deeper valley, especially when it is combined with less number of pass (1 and 2) and higher feeds (0.12 mm and 0.17 mm).

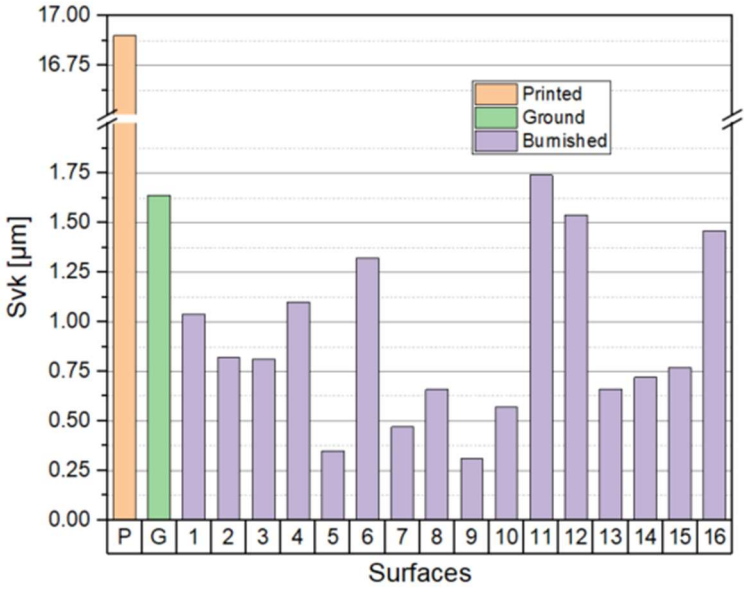

Figure 19. Reduced valley depth of printed, ground, and burnished surfaces.

All three tested burnishing technological parameters showed different characteristics in affecting the functional parameters, from an insignificant effect of 80 and 100 N force on Sk to a dominant effect of the number of passes on Svk.

Swirad [109] studied functional parameters of X37CrMoV5-1 steel after milling, grinding, and burnishing. He achieved 1.1 µm of Sk, 0.34 µm of Spk, and 0.53 µm of Svk after the grinding, as well as 0.28 µm of Sk, 0.108 µm of Spk, and 0.11 µm of Svk after ball burnishing. When compared to my results, all parameters are less than what I achieved. This could be due to the type of workpiece material production (not 3D printed and different material) and the burnishing environment, like application of different ball diameters, supply of burnishing force, and others. Lesyk et al. [110] also studied functional parameters of LPBF printed Inconel 718 alloy, but another postprocessing mechanism was applied to treat the surface. Due to the unavailability of literature related to the material printing method, the type of applied burnishing process, and the studied surface roughness parameters, I am not able to thoroughly compare the results I found in the experiment.

4.1.3. **Effect of grinding and burnishing process on residual stress**

The burnishing process is essential for enhancing the performance and longevity of mechanical components by inducing compressive residual stress at the surface. This shift from tensile to compressive stress significantly improves fatigue resistance, as compressive residual stresses counteract tensile stresses during operational loads, thereby inhibiting crack initiation and propagation. This improvement in surface integrity and smoothness contributes to the overall strength and durability of materials, making burnishing critical for producing high-performance engineering components.

The type of residual stress, either tensile or compressive, induced in a material depends on the machining process and the applied force. For example, pressure applied by burnishing tools causes the plastic deformation of surface layers, compressing the underlying layers and creating compressive residual stress as the deformed surface tries to revert to its original shape. In stainless steel, the initial tensile residual stress in the transverse and longitudinal directions (as observed in Figure 20 and Figure 21) becomes compressive after grinding and is maintained through burnishing. Residual stresses were measured longitudinally, along the machining direction, and transversely, at 90 degrees to the machining direction. For as-built materials, the longitudinal direction corresponds to the printing direction, and the transverse direction is perpendicular to it; for ground and burnished materials, the measurement directions align similarly.

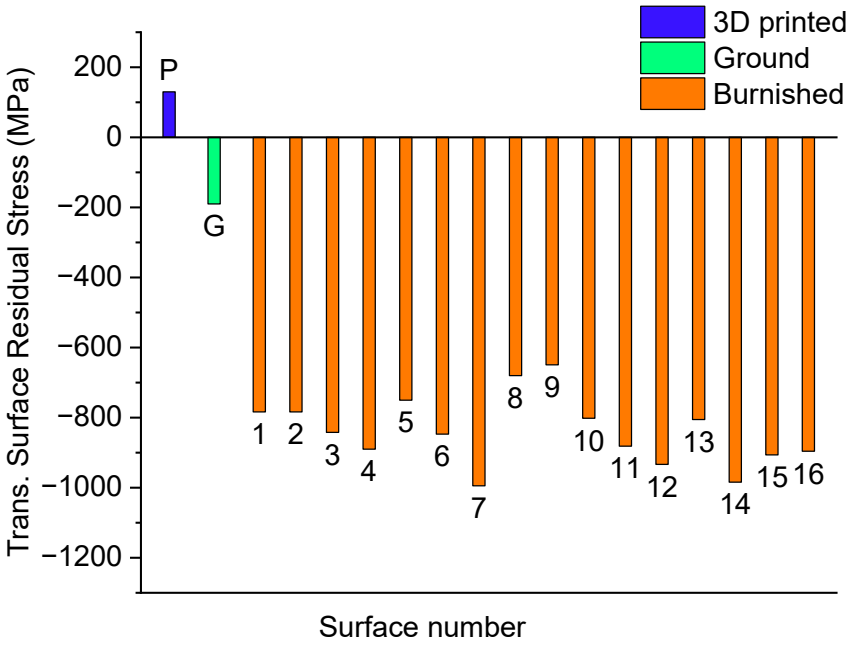

Figure 20. Transverse stress of printed, ground, and burnished surfaces.

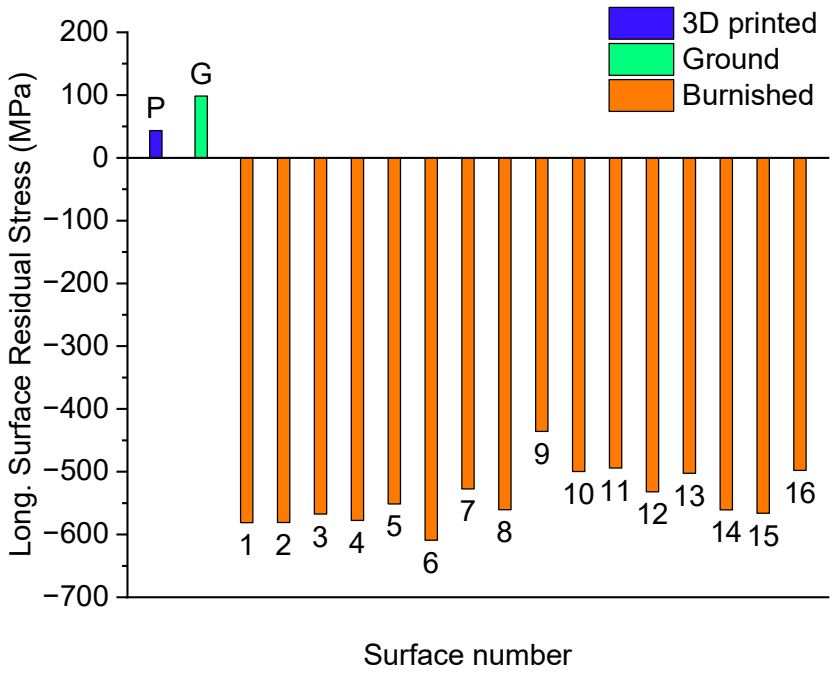

Figure 21. Longitudinal stress of printed, ground, and burnished surfaces.

4.1.3.1. **Transverse residual stress**

The as-built stainless steel workpieces had a tensile residual stress of 130 MPa, which then changed to a compressive residual stress of −190 MPa, as shown in Figure 8. The same figure shows the increase in compressive residual stress of the burnished surfaces. When compared in percentage form, the average burnishing process showed a 346% increase over the ground surface. This indicates a huge amount of enhancement by the burnishing process.

Like the other surface integrity properties, the burnishing parameters have different effects on residual stress. Surfaces 8, 7, and 4, with minimum increases, share low burnishing forces of 60 N, 60 N, and 40 N, high numbers of passes, of three, four, and four, and high feeds, of 0.17 m/min, 0.12 m/min, and 0.17 m/min, respectively. This indicates that the applied forces are not strong enough to induce maximum compressive residual stress. Even though the number of passes is not small, their effect is reduced as the applied force is low. A high feed also has a negative effect, as it indicates higher spacing between two parallel tool paths. In the maximum increase category, surfaces 6, 13, 11, and 16 have similarities in terms of the applied force and number of passes, as shown in Table 1. Higher force and a smaller number of passes, for except surface 13, with four passes, imply favorable parameters for maximum increase. This illustrates that a high burnishing force is dominant in inducing maximum compressive residual stress and causes the material to be compressed.

4.1.3.2. **Longitudinal residual stress**

The longitudinal compressive residual stress, like the transverse, showed tendencies of increase and decrease, depending on the burnishing parameters depicted in Figure 9. Since all the surfaces showed an increasing trend, the 16 surfaces were categorized into two halves, named minimum and maximum increase, based on the degree of increase. A clear relationship between the longitudinal residual stress and the burnishing parameters is shown only with the burnishing force when the surfaces experience minimum increase. Surface 9, burnished with 80 N of force,

a 0.02 m/min feed, and three passes, possesses the lowest value, of −436 MPa. To have a better understanding, we can check the additional force parameters of surfaces 11, 16, and 10, which have higher values than surface 9, but still have a low value. Unlike the transverse residual stress, the longitudinal residual stress experienced a lesser increase when higher burnishing force values were used. From these observations, we can say that the longitudinal residual stress has an inverse relation to the burnishing force, but an unclear or weak relation with the feed and the number of passes with low increase. Surfaces 6, 1, and 2 experienced the highest increases, with values −609 MPa, −581 MPa, and −5801 MPa. For all these surfaces, the common parameter behavior of minimum forces of 60 N, 40 N, and 40 N, feeds 0.07 m/min, 0.02 m/min, and 0.07 m/min, and numbers of passes of one, one, and two, respectively, were observed. These indicate that lower forces, feeds, and numbers of passes give better longitudinal residual stress. Generally, the burnishing force is the dominant factor, showing a good relationship to the longitudinal residual stress. This is due to the ability of force to affect the plastic deformation phenomenon.

Tensile residual stresses introduced by the prior 3D printing and grinding (along the longitudinal direction) process are concentrated at the sharp peaks and valleys of the surface. Deforming these stress concentrators, increased dislocation density and grain refinement as a result of work hardening due to the burnishing process change the stress type to compressive residual stress. Along the longitudinal direction, the tool pushes the material in front of it, leaving behind elastically unloaded material with locked-in plastic deformation. The shear stress is also different compared to the transverse direction. In the transverse direction, the material is plowed to the sideways facing higher resistance from the undeformed material. These residual stress phenomena are reflected in this experiment, with transverse residual stress having a higher magnitude than the longitudinal residual stress.

4.1.4. **In-depth residual stress**

The surface and subsurface study of a material gives an immense perspective on the influence of different machining processes on properties like fatigue, strength, and wear resistance. Depth residual stress measurements of some selected surfaces were taken into account to study the grinding and burnishing processes' effects on the subsurface. The measurements taken before and after grinding, as well as after the burnishing of surfaces 3, 8, 9, and 14 in both directions (longitudinal and transverse), are shown in Figure 22 and Figure 23. The four burnished surfaces were selected based on the same number of passes (three) and representative forces 40 N, 60 N, 80 N, and 100 N, with varying feeds, as they were directly selected from the orthogonal experimental array. The study of the effect of the burnishing force was the aim when investigating the depth residual stress, as its dominance is reported in many studies of regular materials processes.

Due to the reason discussed in the surface residual stress section, different machining methods induce different stress types. At the surface, the as-built workpiece in each direction has tensile stress. However, when the depth increases, first it increases in the positive stress direction abruptly, in the case of the transverse direction, and gradually in the longitudinal direction, and then it decreases gradually until it attains a stable condition. This indicates the stress variation at different depths of the as-built material due to the printing process [111]. The grinding

process did not have much of an effect on the initial state of the stress, except in the transverse direction up to a depth of 4 µm, which changed the stress polarity to a magnitude of −232 MPa. In the transverse direction, the as-built and ground surfaces show the same trend of sharp increase and then gradual stabilization. In both directions, the burnished surfaces show a similar effect of burnishing force on surfaces 3, with 8, and 9, with 14. The changing effect with the increase in depth could have been due to the varying feed, otherwise, a clear increasing effect of burnishing with an increase in force magnitude is demonstrated. Another important observation is the distinct group-like similarity shown in both longitudinal and transverse directions. If we compare the feed of the 40 N and 60 N forces (0.12 m/min and 0.17 m/min) with those of the 80 N and 100 N forces (0.02 m/min and 0.07 m/min feeds), the former are in the higher group if we categorize the feed into two groups of higher and lower. In both directions, the printing, grinding, and burnishing processes induced stress apart from their magnitude and direction. The burnishing process effect is clearly shown in both pictures, with higher depth and stress magnitude and burnishing force increases inducing higher compressive residual stress. Generally, the burnishing process shows significant compressive residual stress enhancement at the subsurface level of the as-built material. Even though it is in small amounts, the grinding process also shows a pronounced increase.

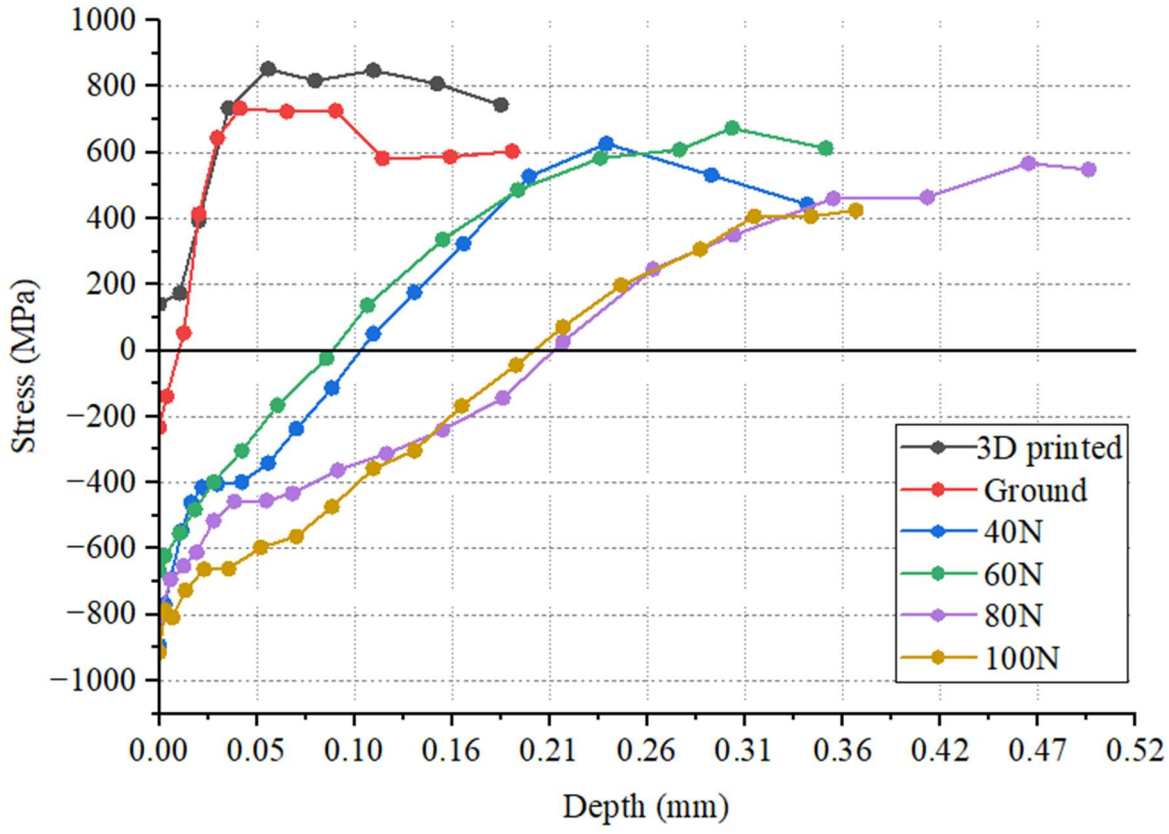

Figure 22. Transverse in-depth residual stress of printed, ground, and burnished surfaces.

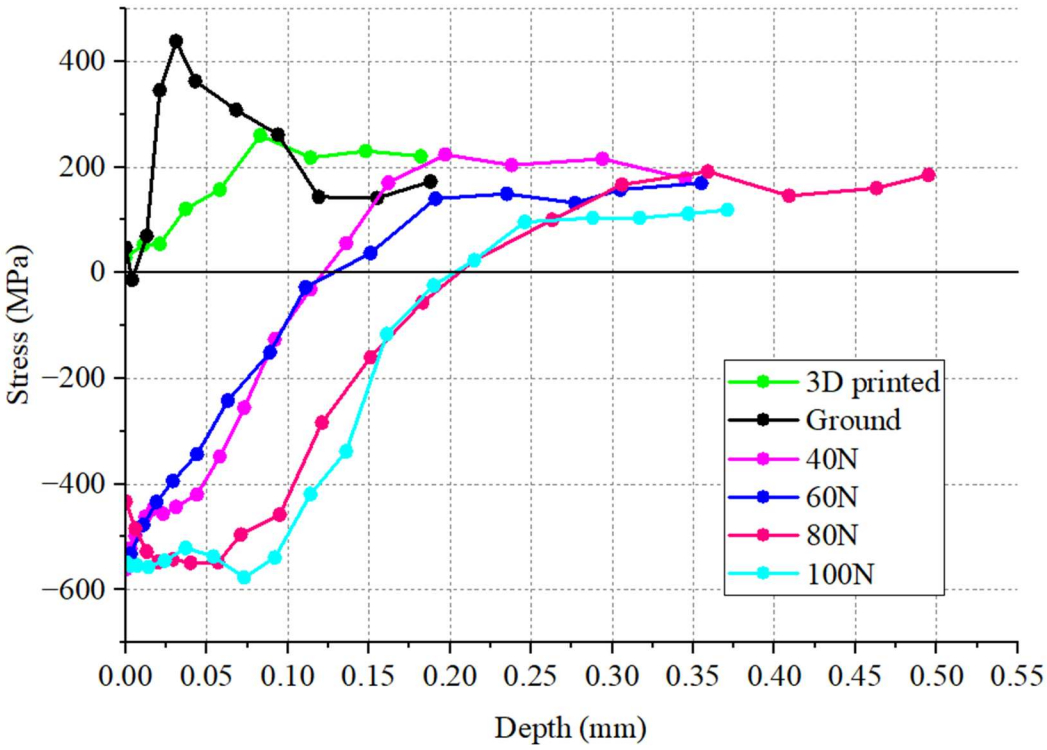

Figure 23. Longitudinal in-depth residual stress of printed, ground, and burnished surfaces.

4.1.5. **Microhardness evaluation**

Understanding the microhardness provides insights into the material's resistance to plastic deformation and wear, which is essential for evaluating the durability and performance of a workpiece in practical applications. The HV 0.2 microhardness results measured for the as-built, ground, and burnished surfaces with different burnishing parameters are depicted in Figure 24. From the measured microhardness results, different material properties, like mechanical properties, the performance of the material, and its behavior at different conditions, can be inferred. As shown on the bar graph, the microhardness values were found to have increased after the grinding process and burnishing process. The as-built material's initial hardness was 241 HV, and it was increased to 35 HV after grinding, and to 371 HV and 457 HV if we take surfaces 3 and 8 as representative minimum and maximum values of the burnished surfaces. As presented in Table 4, a 45.5% increase in grinding effect, an average increase of 22.8% after burnishing compared to grinding, and a general 78.6% increase with reference to the printed surface hardness were measured. This shows that both post-processes of the 3D-printed stainless steel have a positive effect on increasing the microhardness of the material. Heat generation due to the abrasive nature and the induction of different stress types are the main characteristics of the grinding process, which can lead to work hardening of the material. This work hardening process, either by grinding or burnishing, is the main reason for dislocation movement, which affects the hardness of the material. Teimouri et al. [112] discussed this issue with uniform microstructure refinement due to severe plastic deformation, and because of this microstructure refinement, the hardness increases.

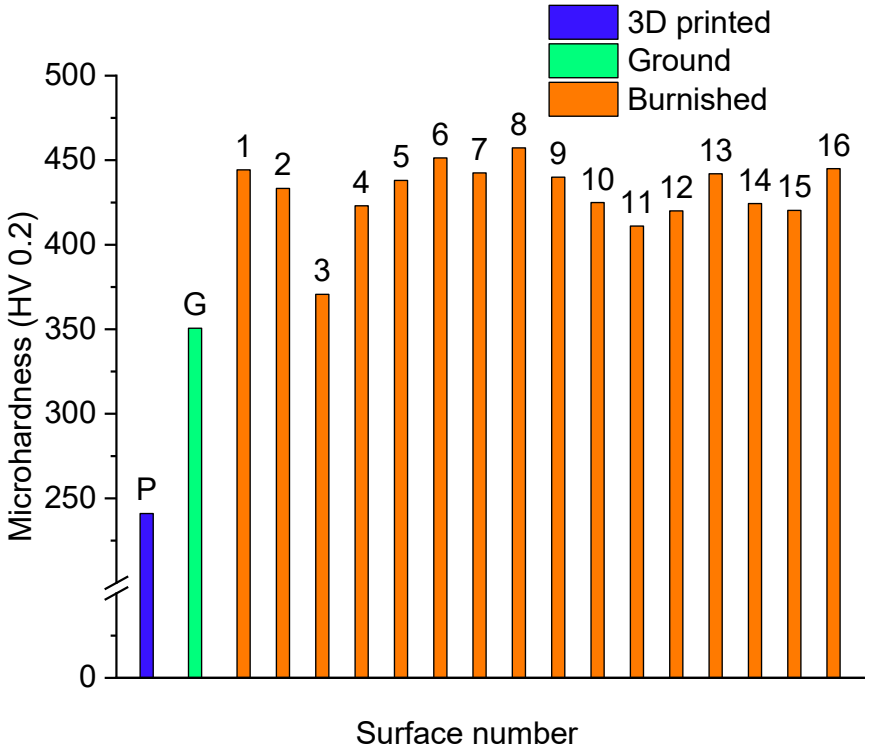

Figure 24. Microhardness of printed, ground, and burnished surfaces.

Diving into the burnishing results of each surface to study the effects of the parameters changes, I found a weakly associated general trend in the increasing or decreasing direction of the parameters in terms of hardness change, despite the increased hardness results, as discussed previously. Surface number 3, with 371 HV, and number 11, with 411 HV, are surfaces with a minimum increase. If we check their burnishing parameters, surface 3 is burnished with 40 N of force, a 0.12 m/min feed, and three passes, while surface 11 is burnished with 80 N of force, a 0.12 m/min feed, and one pass. For both surfaces, the second highest feed is the only common parameter, which is also shared by surfaces 12, 15, and 4, with feeds of 0.17 m/min, 0.12 m/min, and 0.17 m/min, respectively. In this case, we can say that high feed has a minimum hardness increase. On the other end, surfaces 8 and 6 have the maximum hardness increase, with values of 457 HV and 451 HV, respectively. Their parameters are 60 N of force, a 0.17 m/min feed, and three passes for surface 8, 60 N of force, a 0.07 m/min feed, and one pass for surface 6. Here, 60 N of force was used in both experiments, but the other parameters were different. If we check surfaces 16, 1, and 7, which have an increased hardness on the maximum side, to obtain general information, low forces of 40 and 60 N were used, except in surface 16, and few passes were shown, except in surface 7. From these, I can say that low force, few passes, and slow feed are the characteristics of the maximum increase in microhardness.

4.2. A novel burnishing feed application method on the surface roughness of C45 steel

An approach different from the conventional burnishing process that changed the application of the tool feed was used in these experiments. Results of the newly applied method and its counterpart, the old approach (conventional), of C45 steel are presented and discussed in this section. Flat surfaces were burnished with the same burnishing tool used for the 3D printed stainless steel after milling, and significant improvements in surface roughness were observed. Amplitude roughness parameters are considered to study roughness height characteristics, as well as additional topography parameters that can help to understand the functional properties.

An investigation of the novel feed mechanism of the slide burnishing process's effect on surface roughness characteristics is presented. The initial face milled surface shows a cutting insert mark on the surface with a periodic pattern depicted in Figure 25a. These marks were attempted by both the new and old burnishing methods, as shown in Figure 25 b and Figure 25c, and they were smoothed to a certain degree. For the same number of passes (3), the new method with 0.02 mm, 0.08 mm, and 0.14 mm, and the old method with 0.14 mm feed, the picture shows significant modification by the new method. Surfaces burnished by both burnishing methods are studied by analyzing different roughness parameters. The percentage change of all measured burnishing parameters by both methods are presented in Table 10 to give a general overview of their effect. The maximum and minimum values achieved, as well as the average value, are evaluated in addition to the discussion based on the burnishing technological parameters. All mentioned measured values of amplitude and functional parameters are given in

Table 13.

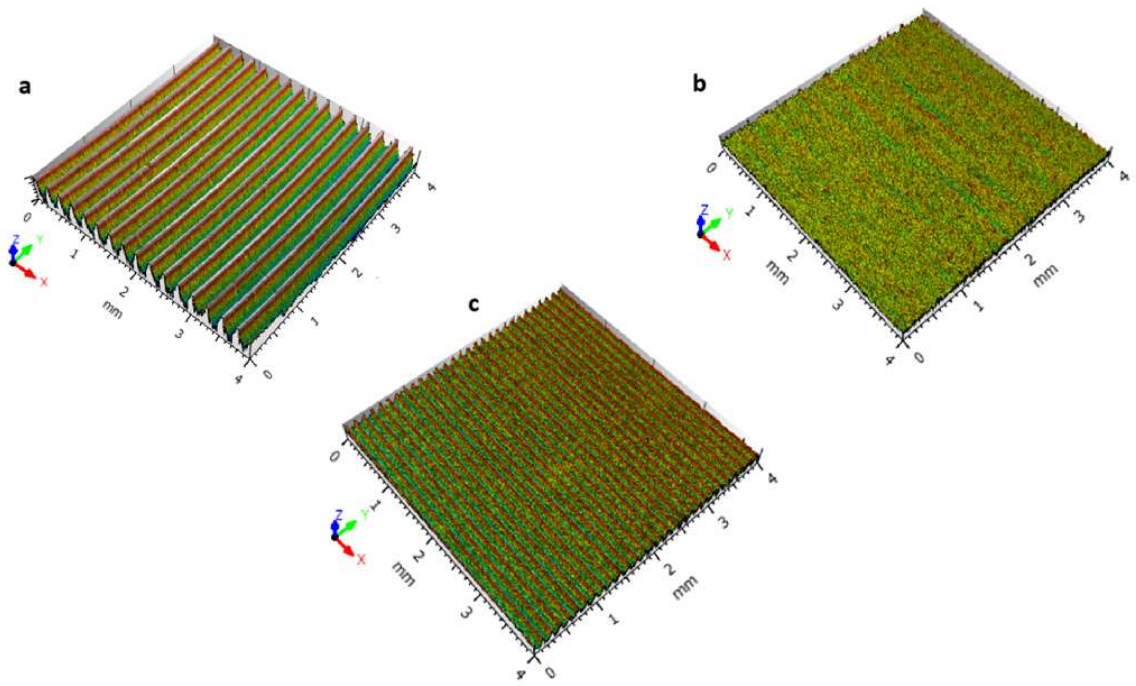

Figure 25. 3D view of scanned (a) face milled, (b) burnished by the new method (surface 6), and (c) burnished by the old method (workpiece 17) surfaces.

Table 10. Maximum and minimum percentage change of measured responses after the two burnishing methods with respect to the milled reference.

Conventional Method						
	% Δ Sa	**% Δ Ssk**	**% Δ Sku**	**% Δ Sk**	**% Δ Spk**	**% Δ Svk**
Maximum	-6.3	224.5	196.1	-5.7	-7.0	27.8
Minimum	-66.3	-79.4	-10.9	-68.0	-57.6	-5.2
Average	-46.9	25.8	66.1	-46.9	-32.1	10.4
New Method						
Maximum	-65.6	7.1	198.3	-65.8	-41.9	20.1
Minimum	-70.2	-69.3	100.0	-72.2	-52.7	7.1
Average	-67.4	-28.7	133.3	-67.9	-47.4	14.8

4.2.1. **Study of amplitude parameters of the milled and burnished surfaces**

The quickest and easiest to understand surface roughness parameters are amplitude parameters. Peaks and valleys are measured with reference to the mean plane and evaluated to study the effect of the burnishing process.

4.2.1.1. **Arithmetic mean roughness (Sa) of successive milling and burnishing**

Roughness level of a 4 mm×4 mm area of face milled, burnished by the new and old method, are presented using a bar graph in Figure 26. They are grouped with a number of passes for the three force categories, and the initial surface is included in each graph for comparison purposes. Two X axes, one for the workpiece/surface number and the second axis for the applied feed. Since the new method applies a group of feeds, they are represented by f2, f3, and f4, as explained in the methodology section. In each force and number of pass categories, the new method showed reduced roughness compared with the face milled and old burnishing process methods.

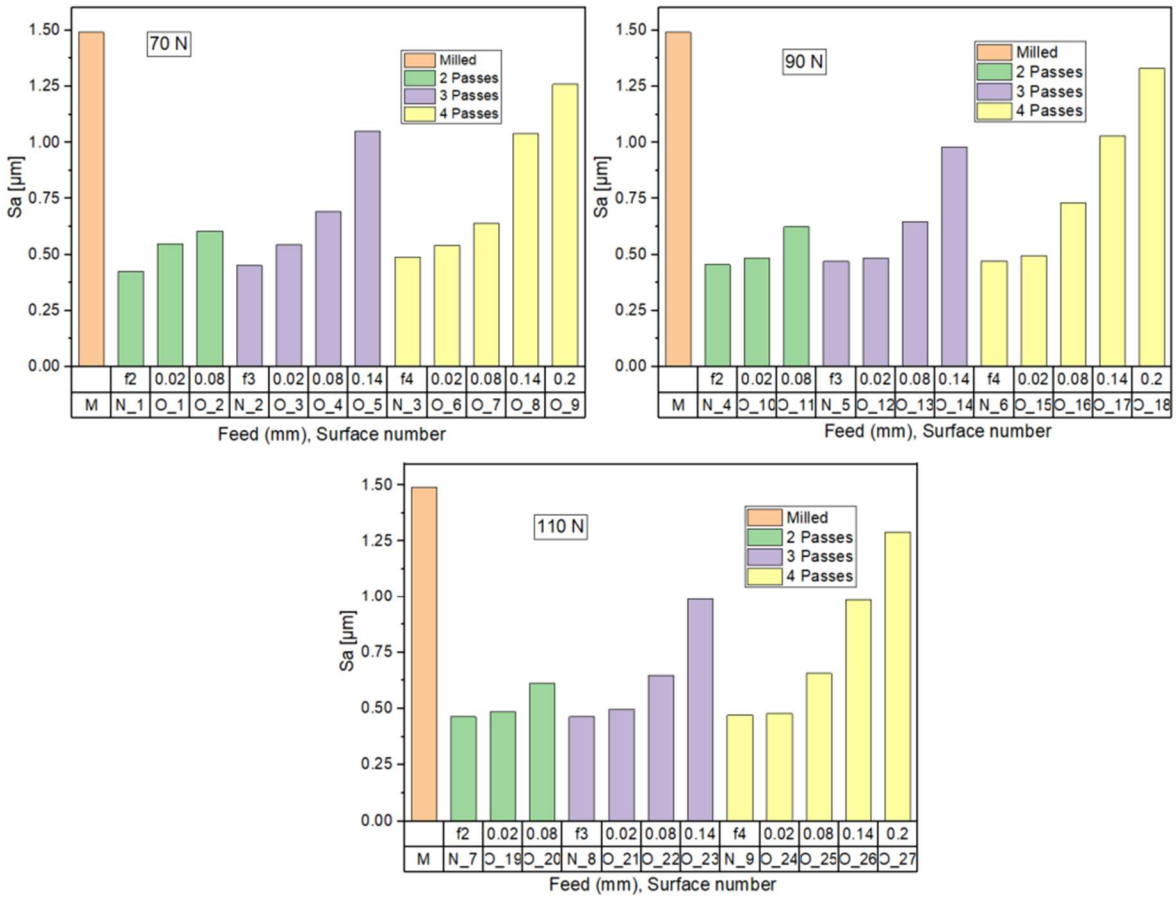

Figure 26. Arithmetic mean roughness: 70 N, 90 N, and 110 N

The periodic initial surface with 1.49 µm roughness was reduced to a great extent by the new method and by the old method when a lower feed was applied. From the same figure of Sa, a similar trend of increasing roughness with an increase in feed and roughness values close to each other of the new method are observed. This trend comes from a lower roughness by the new method and an increasing roughness due to an increasing feed by the old method. This is true for all pass and force groups except very close values of surfaces N_9 and O_24 in the 110 N force with 4 passes group. This indicates how the feed affected the old method, irrespective of the pass number and applied force, even though a combined effect of all burnishing parameters is inevitable. From all applied feeds, 0.14 mm and 0.2 mm showed minimum roughness decrease. During the burnishing movement of the tool, the material flows plastically into the valley and both sides of the tool. The successive passes of the tool address the materials that flowed to the sides if the feeds are small enough to close the gap; otherwise, a rough surface is produced due to material pileup.

Roughness reduced from 1.49 µm to 0.49 µm and 0.42 µm (surface 3 and 1), which are the minimum and maximum reductions when burnished with the new method. This indicates that all tried combinations of the new method reduced the roughness to almost the same level. Varying the feed after each pass worked as intended to move leftover peaks or material pileups by shifting the tool path. To achieve this, bigger feed is applied first, then the others with a reducing order to avoid higher feed tool marks on the surface, like in the old method. With

these results as a starting point, different burnishing parameter levels and combinations can be researched to study their impact.

It is essential to examine the new burnishing method parameter levels to understand how the surface responds upon receiving them. Figure 27 will serve this purpose, taking into consideration the burnishing force and the number of passes. Two and three passes showed a similar increasing roughness trend for 70 N force, while four passes showed a decreasing roughness. The remaining force levels (90 N and 110 N) and all pass combinations settled to a close roughness value, indicating deformation saturation. With two passes and 70 N force giving lower roughness and increased force producing less changes, further study on both ends can give a better understanding.

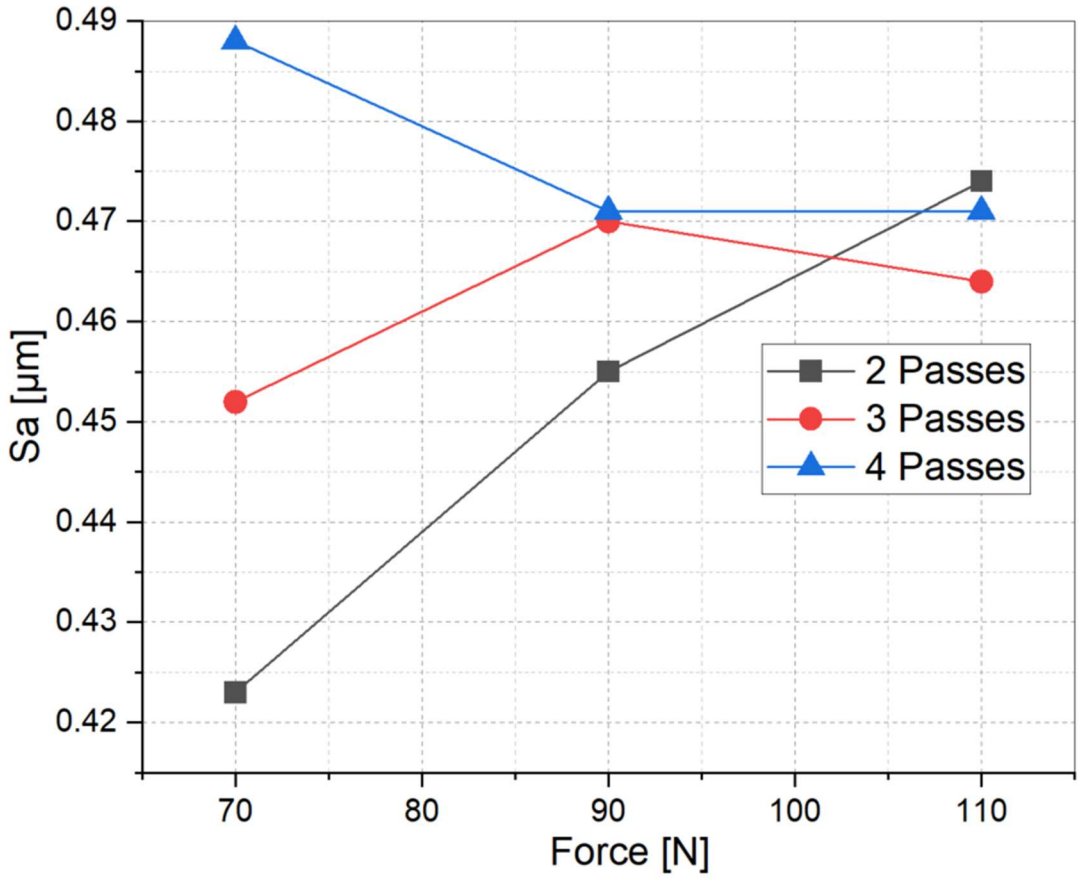

Figure 27. Burnishing parameter effect on the new method.

In all pass and force categories, surfaces burnished by the old method with 0.02 mm feed produced the smoothest surfaces close to the new method values. The value ranges from 0.47 µm to 0.55 µm while the new method values range from 0.42 µm to 0.49 µm. Compared to the tool tip diameter (4.4 mm), this feed produced overlapped paths. As a result, surface asperities existing before the burnishing process and created as a result of burnishing due to material pileup, tool marks, leftover, and other sources are addressed. Other machining processes, like milling and turning, produce a smooth surface when low feeds are used. From this, we can conclude that both burnishing methods produce a close smoothness level when low feeds are used.

4.2.1.2. **Skewness (Ssk) study of milled and burnished surfaces**

The primary task of the burnishing process in surface roughness improvement is to smooth the surface by displacing the irregular bumps or peaks caused by machining or other surface treatments into the valleys. As a result, the surface's topography characteristics changed to serve the required application. Skewness is a response measure that reveals the distribution of peaks and valleys. A zero skewness value represents a symmetrical profile, while positive and negative skewness values represent dominant peaks and valleys, respectively.

With a milled initial surface of 0.339 skewness, the new and old burnishing, as exhibited in Figure 28, did not change the surface's profile symmetry. The new burnishing method reduced the skewness compared to the milling process except when 70 N force was used, which increased it by a negligible value. But compared to the old burnishing method, we can generalize that it performed better in reducing it when a higher number of passes were used. During 70 N burnishing force usage by the old method, skewness was reduced for more passes. While 90 N and 110 N forces were used, increasing and decreasing trends were observed. This shows an unstable skewness level when a higher force and number of passes are used compared to the new method.

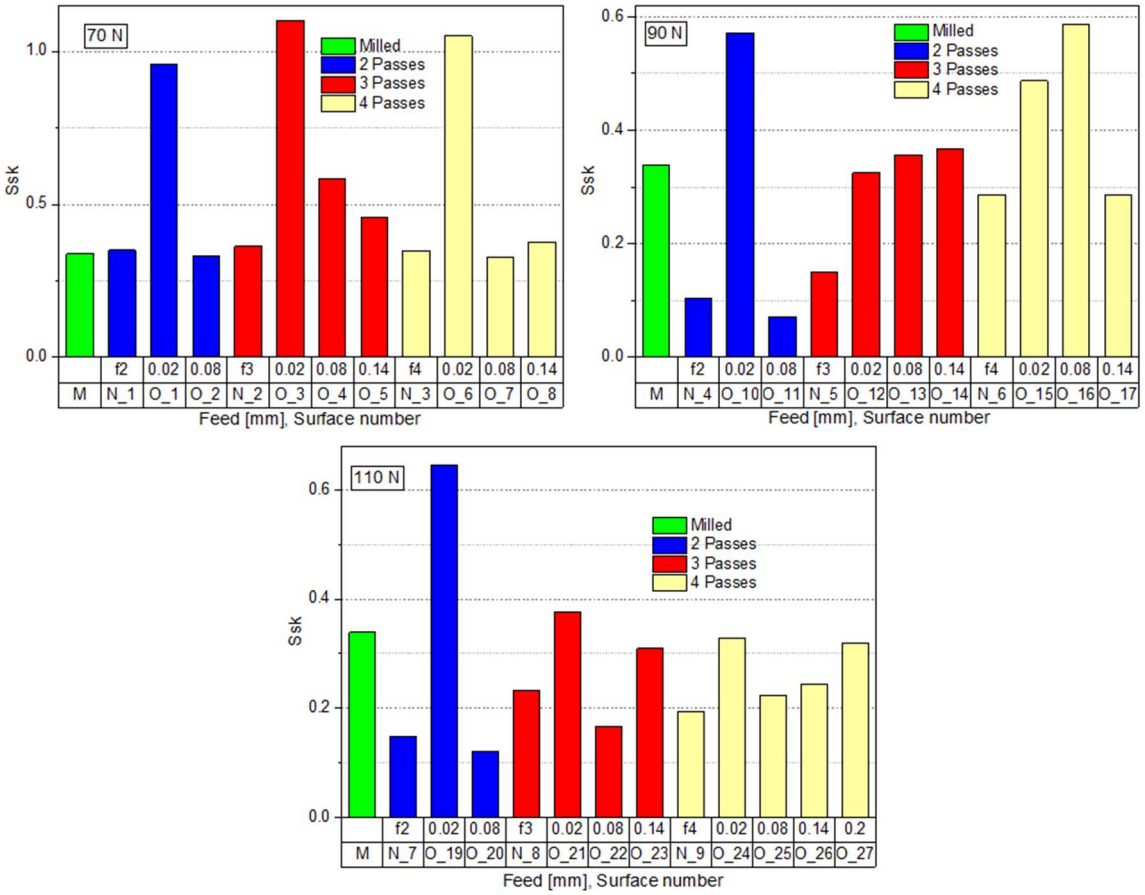

Figure 28. Skewness (Ssk) values of surfaces: 70 N, 90 N, and 110 N.

Surfaces burnished by the old method with two passes and 0.02 mm feed gave higher skewness than surfaces burnished by the new method. Additionally, the 0.02 mm feed gave the same result when three and four passes were used, except for the 90 N burnishing force. Of the nine

surfaces burnished with this feed, only two experienced lower roughness than their counterpart feeds. This indicates that more passes are required to produce a symmetrical surface profile by repetitively attempting to deform the peaks plastically. From these skewness results, our new method outperformed the old method in changing topographic peaks and valleys distribution.

Surfaces number N_4 and N_2 burnished by the new method presented in Figure 29 are those that experienced the lowest and highest skewness. For all tried passes and feed combinations, all forces played a reducing role when compared to the initial values. Further increase in burnishing force reduced towards symmetrical peaks and valley distribution except for the combination of 110 N force with three and four passes. Increasing the burnishing force tends to transform the topography texture until it achieves a similar level when the maximum force is used. This graph shows a promising feature of reducing the skewness by optimizing the technological parameters. The right force magnitude with optimal feed and pass can help the tool to displace the peaks to the valleys to produce the required smoothness. Reducing the initial skewness value from 0.339 to the symmetry level indicates deforming the peaks and valleys towards the mean plane.

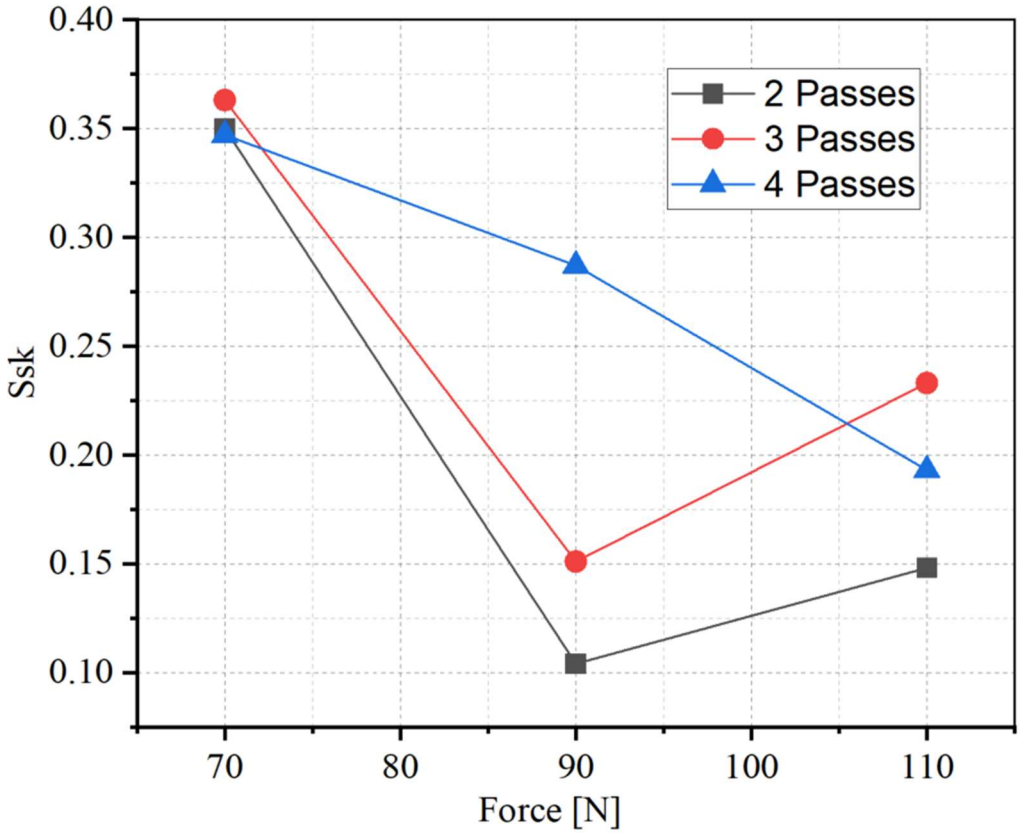

Figure 29. The skewness value of surfaces burnished by the new method.

4.2.1.3. **Kurtosis (Sku) analysis of milled and burnished surfaces**

Another important parameter to measure the effect of the machining process is kurtosis (Sku), which quantifies the distribution of surface roughness height, taking three as a reference value (mesokurtic). The milled surface, a starting surface for the old and new methods, had a flat and uniform texture with a value of 2.29, less than the reference.

The surfaces were burnished by varying the feed in each burnishing round, which increased the kurtosis value and changed the characteristics of the peaks and valleys distribution to more frequent extremes, as visualized in Figure 9. This is because the face milled surface has periodic marks by the tool marks located near the mean plane, disturbed later by the burnishing. It minimally doubled it, 6.83 and 4.58, as maximum and minimum values belonging to surface numbers N_1 and N_5, respectively. Three passes scored lower values than two and four passes in each burnishing force category. From the burnishing force perspective, 110 N gave close values to each other (4.95, 4.90, and 5.09), lower than burnishing by 70 N and 90 N, except in three passes, while the 70 N force produced higher kurtosis (6.83, 5.68, and 5.75).

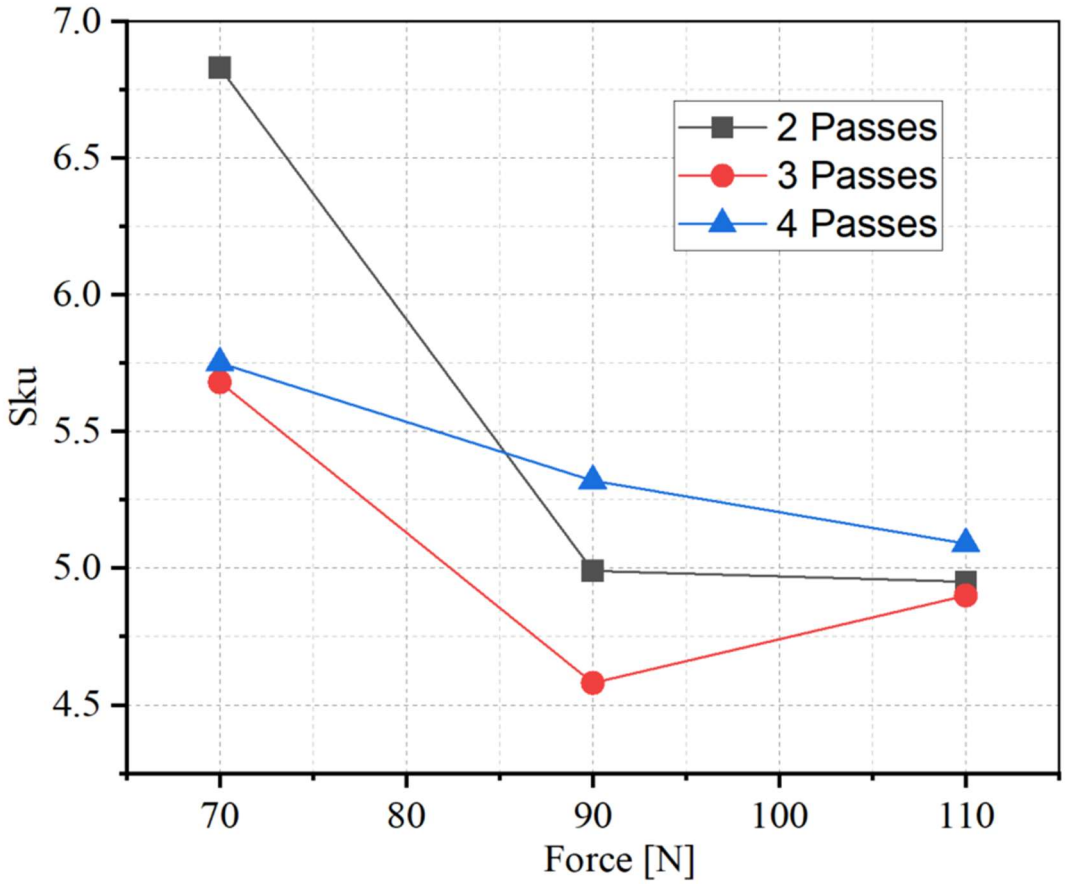

Figure 30. Effect of force and passes on the kurtosis of the surfaces burnished by the new method.

The burnishing process destroys the initial milling insert imprints on the surface, and the new tool path is blurred or undistinguishable unless the feed is high. If the feed is less than the tool diameter, an overlap section of the path makes the material displacement unpredictable.

As our main aim is to compare the old and new feed mechanisms, it is important to compare the kurtosis of the face milled with the old feed mechanism too, as presented in Figure 10. Unlike Sq, the kurtosis of surfaces burnished by the old method decreased during an increase in feed and the number of passes for all force categories. Another important observation is a higher gradient decrease when two passes were used. The modification of the kurtosis level after each pass aligns with the aim of the burnishing process to address undeformed material after the first pass by repeating the process. The second case is when the pass and feed

combination affects the performance. This happens in two extremes of feed, either high or low. If a higher feed is used, an unburnished area can be left, which can be a source of higher kurtosis and other roughness parameters like Sa. On the contrary, low feed leads to material overflow to the sides of the tool. A 0.02 mm feed is used with all of the passes but gives worse results with two passes.

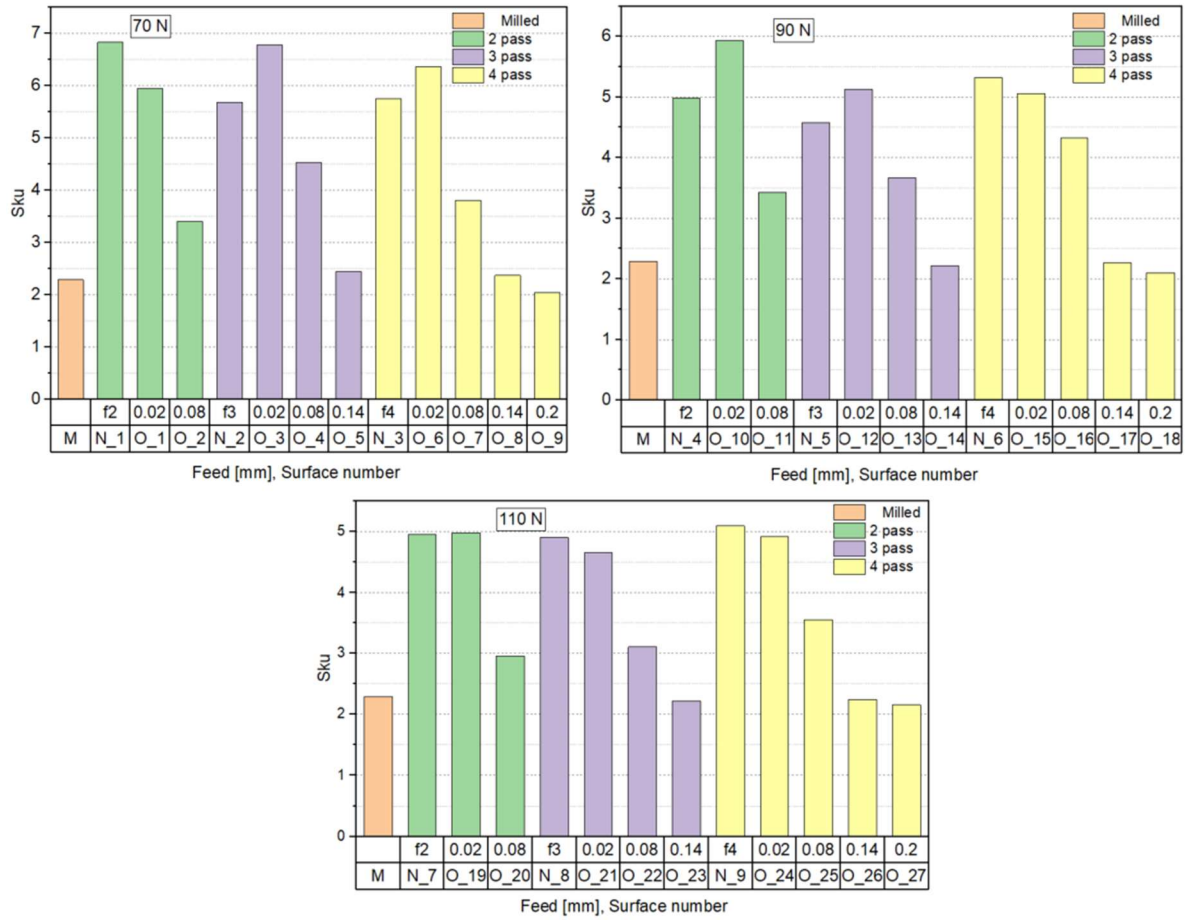

Figure 31. Kurtosis of face-milled surface, burnished with the new and old method: 70 N, 90 N, and 110 N.

The first surface in each force and pass category, burnished by the lowest feed (0.02 mm), led to increased kurtosis compared to the milled surface and surfaces burnished by the same force and passes. As presented by the bar charts, there was a clear trend of decreasing kurtosis with increases in feed and the number of passes. For example, surfaces O_8, O_9, O_17, O_18, O_26, and O_27 have kurtosis similar to the milled surface and upon checking its technological parameters, we found three and four passes, and higher feed levels of 0.14 mm and 0.2 mm feed, as common burnishing parameters. These show that applying four and three passes modified the topography to a great extent. Both methods changed the surface to leptokurtic, prone to higher friction, wear, and stress concentration.

4.2.2. **Functional parameters analysis study after milling and two burnishing methods**

The functional performance of the generated surfaces was evaluated through the parameters Sk (core roughness depth), Spk (reduced peak height), and Svk (reduced valley depth). These

parameters were analyzed for the initial milled condition and subsequently for the surfaces treated by the two burnishing methods. Unlike the arithmetic average (Sa), these three metrics provides a more nuanced characterization by deconstructing the surface profile into its core, peak, and valley components, which directly relate to functional behaviors like load capacity, wear resistance, and lubricant retention.

4.2.2.1. **Evaluation of core roughness depth (Sk)**

The change in burnishing parameters altered the core roughness depth. In all three force levels, Sk followed a similar trend, showing an insignificant contribution to the changes.

The combined feed of the new method in each number of passes level produced the lowest Sk value compared to its counterpart conventional method, as shown Figure 32 during the first force level (70 N) application. Both methods decreased the value significantly, except when the conventional method was applied with higher feeds of 3 and 4 passes. The milled initial surface had thick (Sk = 4.03 um) and was reduced to 1.12 um to 1.22 um by the new method and to 1.33 um to 3.73 um by the old method. Irrespective of changed feed combinations and number of passes, the new method stayed at a similar level, indicating reaching a saturation for the applied force. In the case of the old method, the same feed in different pass numbers (3 and 4) also showed no effect, increasing the Sk with their increase only.

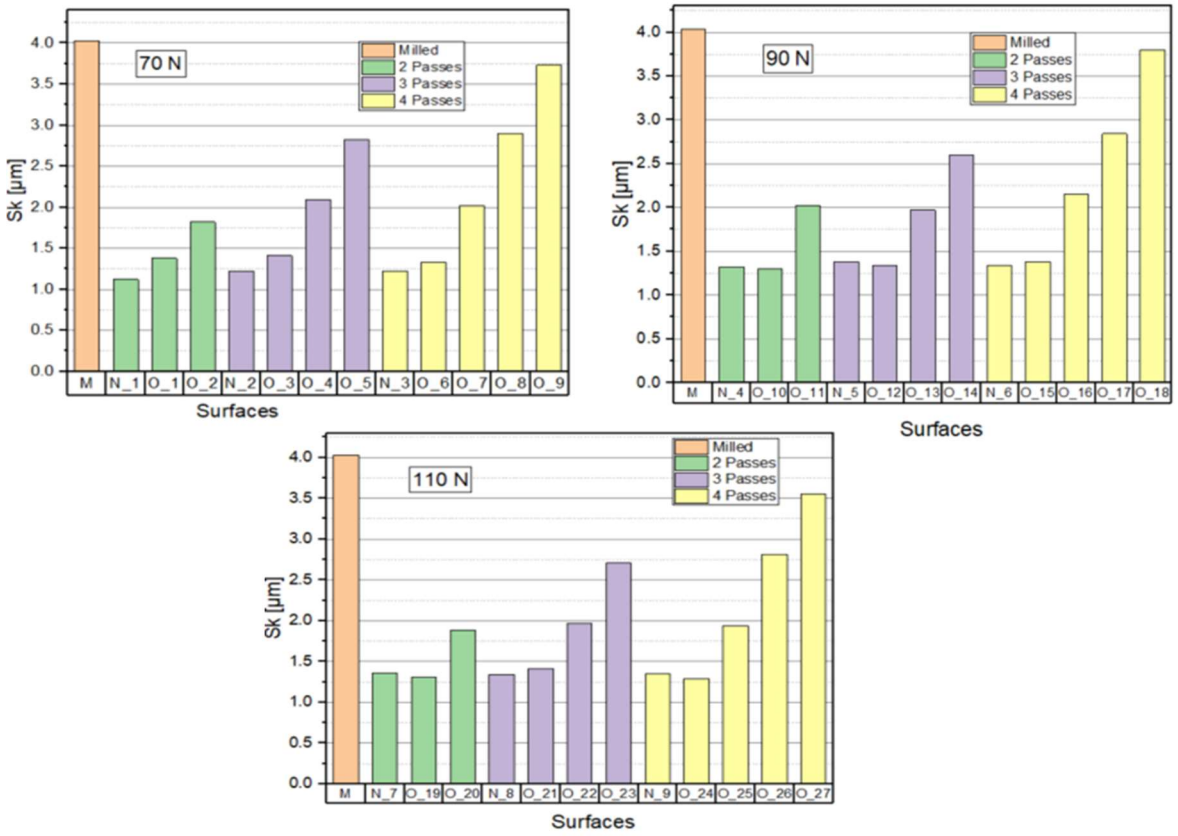

Figure 32. Core roughness depth (Sk) of milled and burnished surfaces (70 N), (90 N), and (110 N).

The application of a 90 N force only differs from 70 N in producing similar Sk surfaces by both methods when a 0.02 mm feed of the old method was used in all feed levels. The remaining feeds provided almost the same Sk values in pass number levels.

The last burnishing force (110 N) showed lower Sk by the old method when 0.02 mm feed was used with 2 and 4 passes, while keeping the same general trend as 90 N force. 4 passes of the old method also showed less value than in the other two forces. Generally, the new method managed to produce a lower Sk or similar value to the lowest achieved value by the old method. This indicates that the milled surface with tool marks, and as a result, a higher Sk was decreased by the two methods and showed a continuously increasing trend with the increase of the feed in the case of the old method. The core roughness depth was decreased by the processes as it destroyed the roughness and created a smoother surface with much reduced values. However, when the feed increased, it began to rise due to unattempted asperities, which is almost impossible to occur during burnishing with the new method.

4.2.2.2. **Evaluation of reduced peak height (Spk) of milled and burnished surfaces**

The systematically combined feed of the new method showed a comparative effect as the lowest achieved level by the conventional method. Figure 32 presents the Spk values of milled and burnished by the two methods, categorized by the applied force and number of passes. Unlike the Sk, the reduced peak height showed no regular trend, especially when 70 N and 110 N forces were applied. Upon the application of 70 N, the new method delivered the lowest Spk except in the 2-pass case. The lowest feed of the old method (0.02 mm) in all three passes showed higher values. In numerous cases (surface O_1, O_3, O_5, O_6, and O_8), the Spk was not reduced much compared to the milled surface (1.72 um).

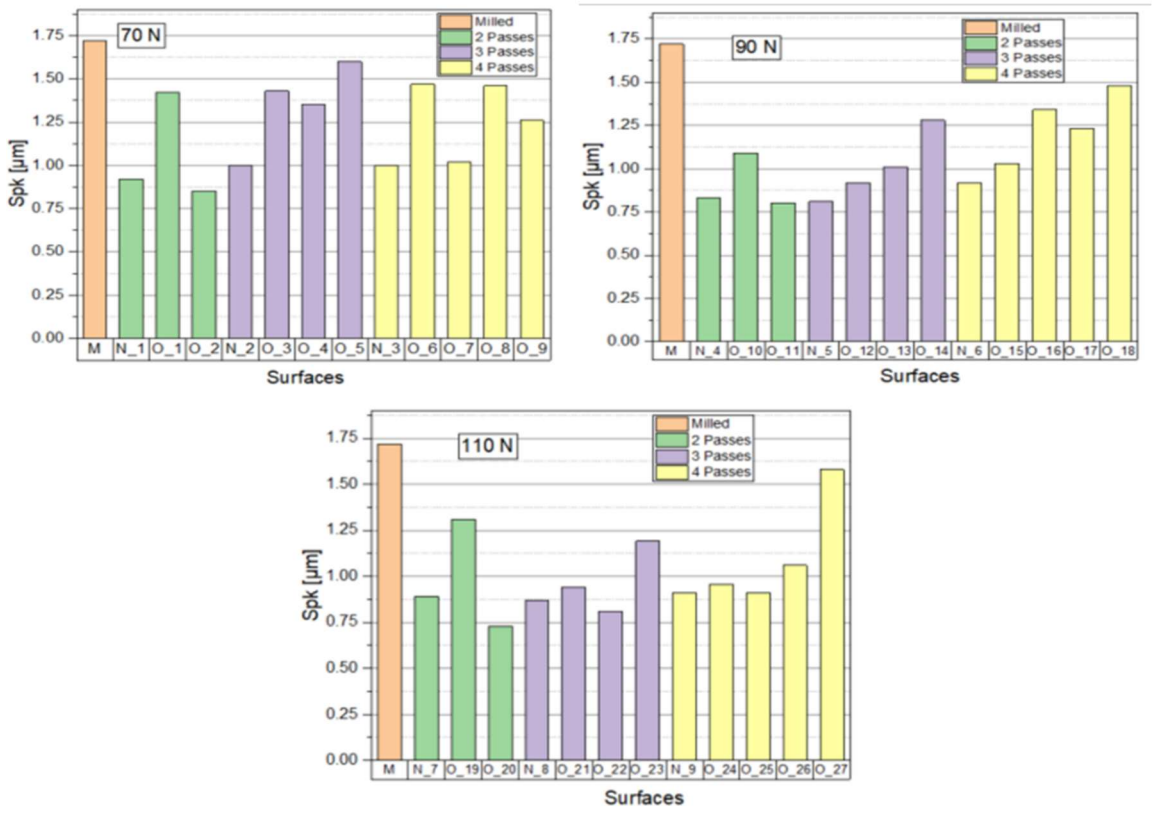

Figure 33. Reduced peak depth (Spk) of milled and two burnishing method surfaces (70 N), (90 N), and (110 N)

Increasing the force to 90 N made the new method to produce a little lower Spk values compared to 70 N and values shaped with the increase of feeds (during 3 and 4 passes) in the old method. The selected passes and feeds helped to tool to deform the peaks; however, when they are increased, the Spk also increases.

The final applied force (110 N) effect was much pronounced in the 3 and 4 passes of the old method, producing lower Spk compared to the two previous forces. Surfaces O_19, O_23, and O_27 have the highest values, and the last two share the highest feeds in their categories. In all three force levels, the lowest feed combined with 2 passes produced higher Spk, which is unexpected. This could be due to the fewer passes that are not enough to deform the asperities, or in some cases, material pileup formation. Generally, the 70 N force dominated feed and pass compared to the other two forces, which showed their effect by producing unstable results. This suggests that optimal force selection is crucial in conjunction with other burnishing parameters and material type. This in place, the proposed new burnishing method showed stable results which were insignificantly affected by the burnishing parameters.

4.2.2.3. **Reduced Valley depth (Svk) study of milled and burnished surfaces**

Reduced valley depth is another important indicator of the functional properties of the surface which can be measured as part of roughness parameters. Except in certain scenarios, Sk and Spk were affected by the changing burnishing parameters, unlike the insignificant Svk values changs shown in Figure 34. The applied burnishing methods either increased or kept in a close range the Svk in all force, feed, and number of passes cases. In the 70 N, the old method decreased when higher feed used. This was reflected on surfaces O_2, O_5, O_7, O_8, O_9, and surface O_14 burnished by 90 N. Raising the burnishing force to 90 N produced a surface with similar Svk in the majority of the feed and passes. Surfaces O_14 and O_16 are exceptions that differ from their feed and pass categories. Further increasing the force to 110 N produced no difference that can be considered a significant effect in all feed and pass levels. All tested combinations ended producing similar Svk values approximately equivalent to the milled Svk value. Both methods provided values in the range of 0.66 μm (surface: O_19) to 0.82 μm (surface: O_25). All results of Svk by the two burnishing methods indicate that the achieved Svk depth by the milling is shallow, in which further postprocessing creates no difference. Their average percentage change are 10.4% for the conventional and 7.1% for the new method. This indicates that the new method excels in a specific scenario only where the selected technological parameters are optimal.

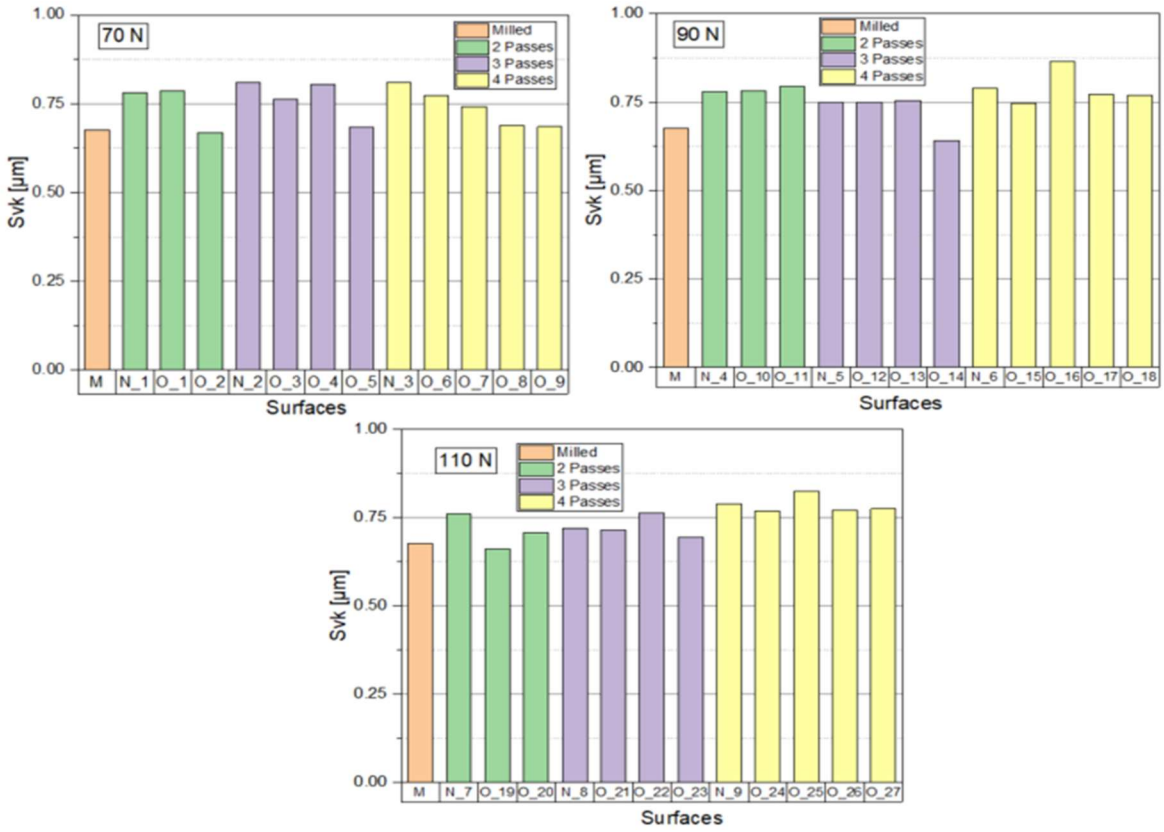

Figure 34. Reduced valley depth (Svk) of milled and burnished process by two methods (70 N), (90 N), and (110 N).

Functional parameters like the height parameters were affected by the two burnishing methods and the changes were more reflected on Sk and Spk than Svk. The findings aligned with the hypothesis, indicating that the predicted relationship of the roughness parameters with the new burnishing method was competitive with the results of the conventional burnishing method. The peak height and core roughness depth were reduced, translated as the creation of a smoother surface, which is required for critical component. Almost all selected feeds in the new method showed insignificant or no changes when the force and number of passes were changed, which can be an advantage, especially to select a few passes to finish the process, which can save time. This indicates reaching a saturation of plastic deformation before the surface starts to crack, material pileup, and other side effects due to work hardening, excess plastic strain caused by excessive burnishing. In the burnishing process, low feed and a higher number of passes produce a smoother surface with optimal burnishing force; however, it takes more time. The proposed method achieved lower or equivalent values to the lowest feed applied by the conventional method, considered as advantageous in the “lower is the best” scenario. As presented in Table 10 the average percentage change by the new method indicates that it was more effective to change the responses. For example, the average percentage change of kurtosis by the conventional method is 66.1% and by the new method 133.3%. Shortage of broad experimental data, for example, a full factorial experiment of the selected parameters or testing more burnishing technological parameters, were challenges of the experiment in general. So, I suggest further study to understand the new process in the full spectrum when the selected and other parameters are further changing.

4.3. **Improving Surface Roughness of 42CrMo4 Low Alloy Steel Shafts by Applying Varying Feed in the Multi-Pass Slide Burnishing Process**

Medium alloy 42CrMo4 cylindrical workpieces were turned before a comparative burnishing experiment was conducted to study the effectiveness of the proposed burnishing method. The focus of this subchapter is to apply the same burnishing tool that was employed on flat C45 to evaluate the impact of changing the feed in each pass across scenarios of harder material, different workpiece geometry (cylindrical), and different machine type (lathe). The distinguishable cutting tool marks in Figure 35 (a) indicates the transformation of the surface by the burnishing processes ((b) and (c)). Sa, Ssk, Sku, Sk, Spk, and Svk are the measured and analyzed roughness parameters in this section. To understand the effect of each burnishing method, the percentage change with reference to the turned initial status is compared. Table 11 presents the maximum and minimum achieved changes by the two methods as well as an average change. And each measured surface roughness parameter mentioned in this section is presented in Table 14.

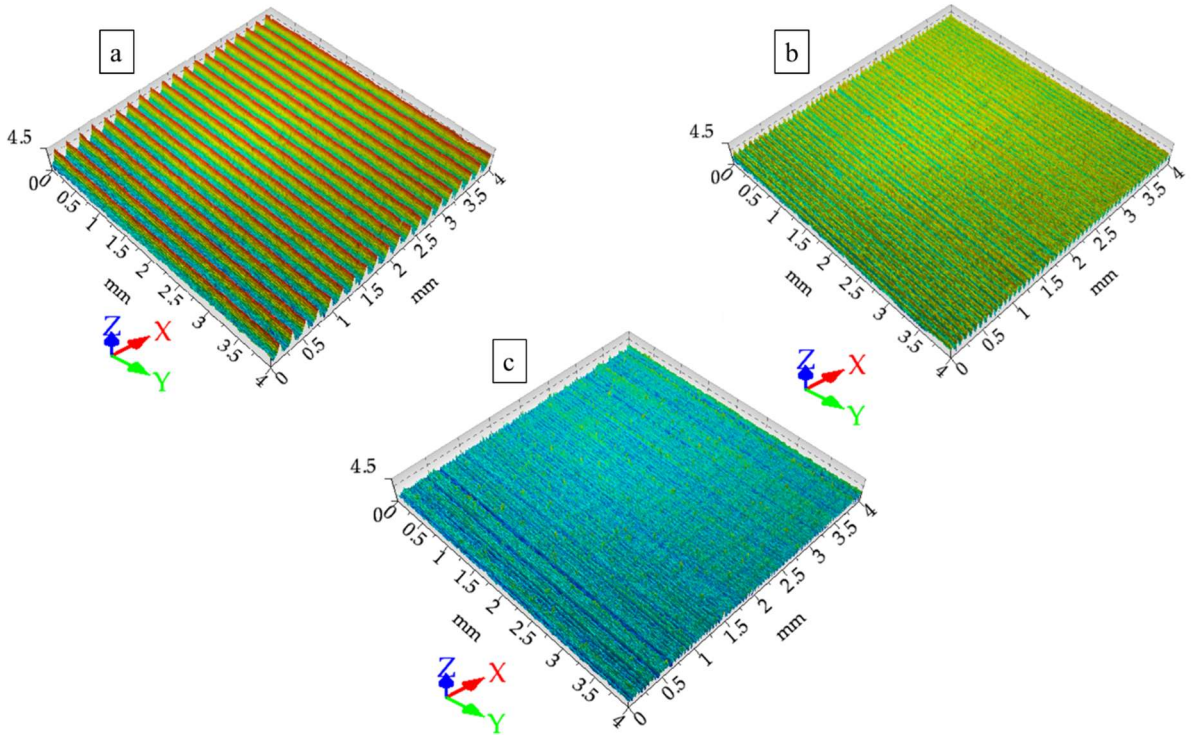

Figure 35. Turned (a), burnished by the old method ((b) O2 60 N, 0.08 mm/rev), and burnished by feed-varying method ((c) N1,60 N, 0.02, 0.08 mm/rev).

Table 11. Maximum and minimum percentage change of all measured responses after the two burnishing methods (Conventional and new).

Conventional Method						
	% Δ Sa	% Δ Ssk	% Δ Sku	% Δ Sk	% Δ Spk	% Δ Svk
Maximum	-14.6	70.0	66.4	23.6	-18.1	32.1
Minimum	-72.0	-242.5	-36.0	-65.4	-89.3	-82.1
Average	-40.2	-87.1	2.1	-17.9	-69.2	-48.5
New Method						
Maximum	-6.1	135.0	120.0	36.1	-20.8	-9.0
Minimum	-81.7	-270.0	-35.2	-76.4	-89.3	-84.6
Average	-56.7	-86.5	12.1	-41.6	-77.9	-61.6

4.3.1. **Study of amplitude parameter changes after successive turning and two burnishing methods**

The surfaces, in their initial turned state and after processing with two different burnishing methods, were analyzed using key 3D roughness parameters namely Sa, Ssk, and Sku. Together, these parameters provide a complete picture of surface smoothness. Sa gives the overall roughness, Ssk indicates whether peaks or valleys dominate the surface, and Sku describes the sharpness of the texture. By comparing these results, the study determines which burnishing technique achieved the most significant improvement in surface smoothness over the original turned surface.

4.3.1.1. **Arithmetic mean height (Sa) analysis**

All forces in a feed versus Sa line graph in the case of 2 and 3 passes, and as a bar graph when 4 passes were applied, are presented in Figure 36 and Figure 37. After comparatively stable decreased values when feeds v1 to v3 were applied, the new method results increased, indicating less improvement demonstrated in Figure 36. Almost all forces of the old method produced a rougher surface when the feed increased from 0.02 mm/rev to 0.14 mm/rev. Except for 150 N force, all surfaces burnished by the old method showed a roughness decrease when a 0.2 mm/rev feed was used. In terms of force magnitude, the new method showed smoother roughness when 120 N, 60 N, 90 N, and 150 N were used in the first three feeds consistently before 60 N shifted to a higher roughness zone in the last three feeds. In the case of the old method, no distinguishable distinction is observed when the forces are changed. When compared to each other, the new method performed better when feeds from v1 to v3 are used. In this 2 passes situation, the new method produced smoother roughness when feed combinations that include 0.02 mm/rev (v1 to v3) were involved. This helps the tool to burnish the surface with more overlapping paths than the other feeds. When 0.02 mm/rev feed was used, both methods provided close Sa values. Another important observation is that the selected

forces' unstable effect could be due to the selected gap (30 N) among them to produce a distinguishable difference.

Unlike in the 2 passes case, 3 passes of the new method with feeds that include 0.02 mm/rev produced a decreasing Sa value only when 60 N, 90 N and 150 N were applied, as shown in Figure 36b. After achieving its minimum Sa level, the 120 N force increased the roughness for the first two feeds (v8 and v9) and settled to a very close range but higher, similar to the other forces, when v10 and 0.2 mm/rev of the old feeds were used. The old method provided closer to the new method or better in some cases like 150 N Force vs v7 and v9, 60N force vs v10, and 120 N vs v7. 0.02 mm/rev and all force levels like in the 2 passes demonstrated values fell within a narrow range. This was repeated when 0.2 mm/rev was applied. These indicates the performance by the new method was better or proximate to the values achieved by the old method. Since the feed combinations could have different arrangements, for example, v8 could be applied before v7, the line trend can't define the property of the method. Sa, as in the two passes case, showed no strong favorite force, except hinting at 60 N and 90 N, showing a similar trend.

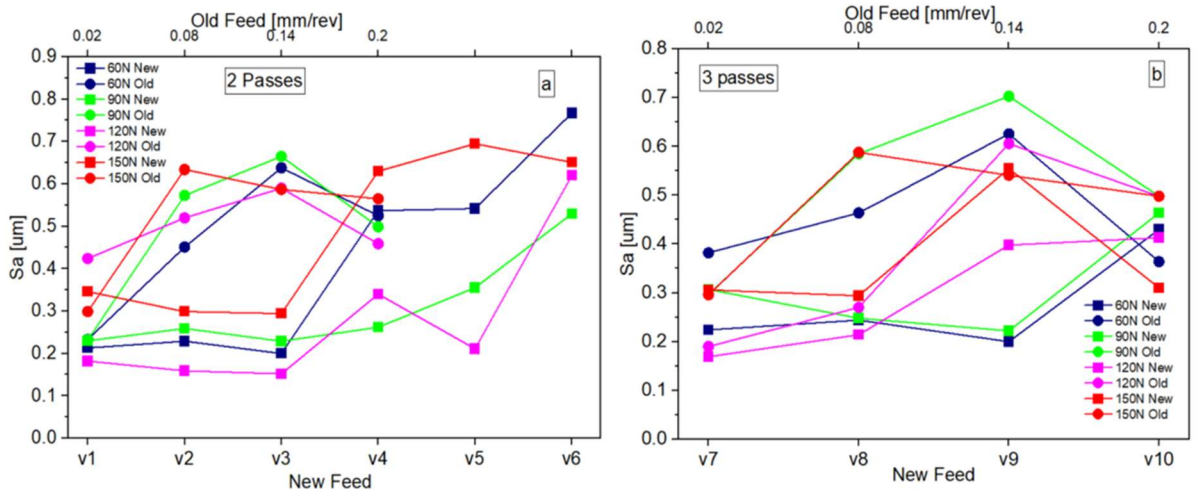

Figure 36. Feed varying and old method Sa of a, 2 and b, 3 passes.

The maximum applied number of passes in this experiment was 4, as demonstrated by the bar graph in Figure 37. Upon combining 4 feeds in the new method, one feed for each pass, each feed accepted 4 passes in the old method approach. Each first bar in all force levels is surface burnished by the new method, showing a lower Sa value except when the feed is 0.02 mm/rev. To the extent it scored lower than the surfaces burnished by the old method, and 120 N and 150 N in all feed levels, and closer values to the minimum roughness by the other two forces. In all force levels, the range of Sa value by the new method was 0.28 µm to 0.41 µm, indicating the force effect was minimum as it was the only factor changed. Changing the feed and force gave scattered results, except for a 0.02 mm/rev feed, which produced a smoother surface compared to the new method. Theoretically, passes are increased to enhance the surface integrity by giving the tool an extra passes to achieve the required quality. In this case, increasing the passes to four showed no marginal difference compared to the other passes. Except in the 150 N case, 2 and 3 passes showed smoother roughness in some runs. This indicates that the pass number strongly depends on the other selected burnishing parameters to produce the aimed property.

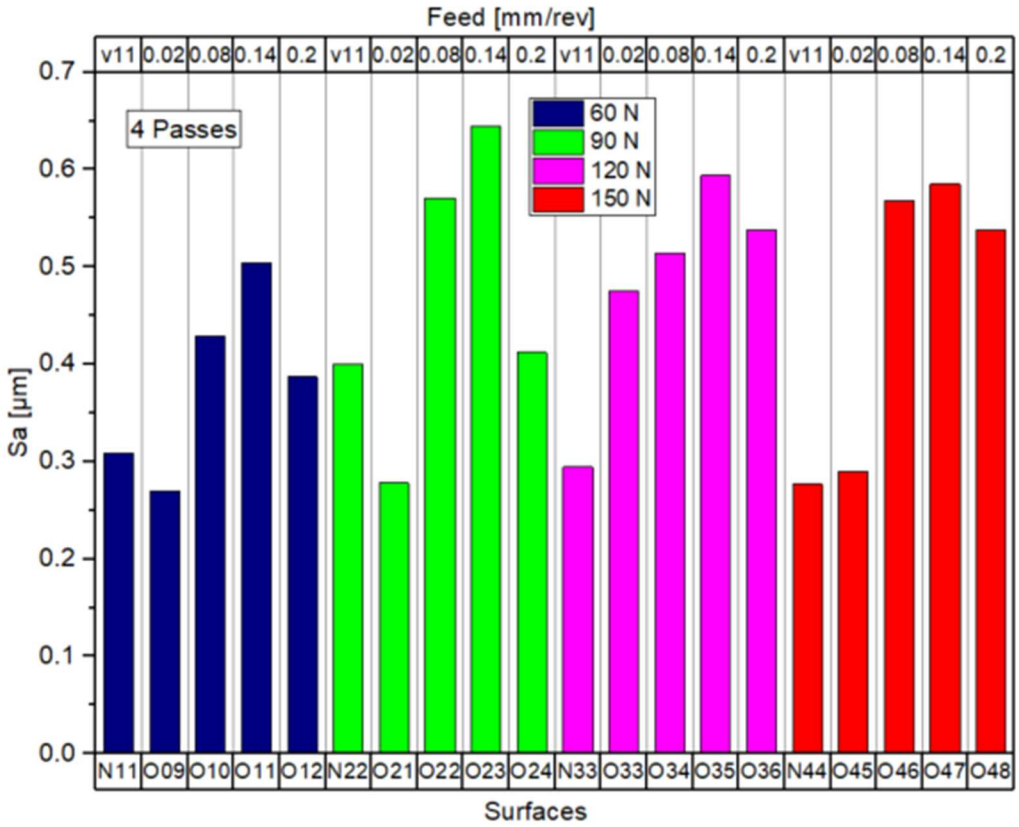

Figure 37. Feed varying and old method Sa of 4 passes.

4.3.1.2. **Analysis of the skewness (Ssk)**

Changing the tool path by applying different feeds in each pass so that a smoother surface can be produced is the aim of this study, and it is important to measure the created surface's peak and valley vertical distribution. Higher peaks and deeper after turning process (Ssk = 0.40) were reduced by both processes in all force, feed, and pass levels except in one case (60 N, v9, and 3 passes of new method).

The positively skewed initial surface was brought near symmetrical or negatively skewed level by both processes when two passes were applied (Figure 38, 2 passes). The skewness were modified from 0.40 to a range of 0.38 to -0.44 with the new burnishing method and to 0.36 to -0.20 by the ordinary burnishing method. The 3D view of scanned sample surfaces (Figure 35) also shows the transformation of the roughness from visible tool marks to partially destroyed by the old method and to much improved roughness. The combined effect of force and feed when 2 passes were used showed no linear relationship of skewness. 150 N force when v1-v3 was used and 120 N when v4 was applied were the lowest achieved skewness was achieved. The new method increased the skewness when v4, v5, and v6 feed combinations were used compared to when v1, v2, and v3 were used, except for 120 N when v4 was applied. Another important observation is the decrease in the skewness when the feed was changed from v5 to v6. But, generally, no clear relation between the old and new counterparts feed and force was observed apart from decreased values.

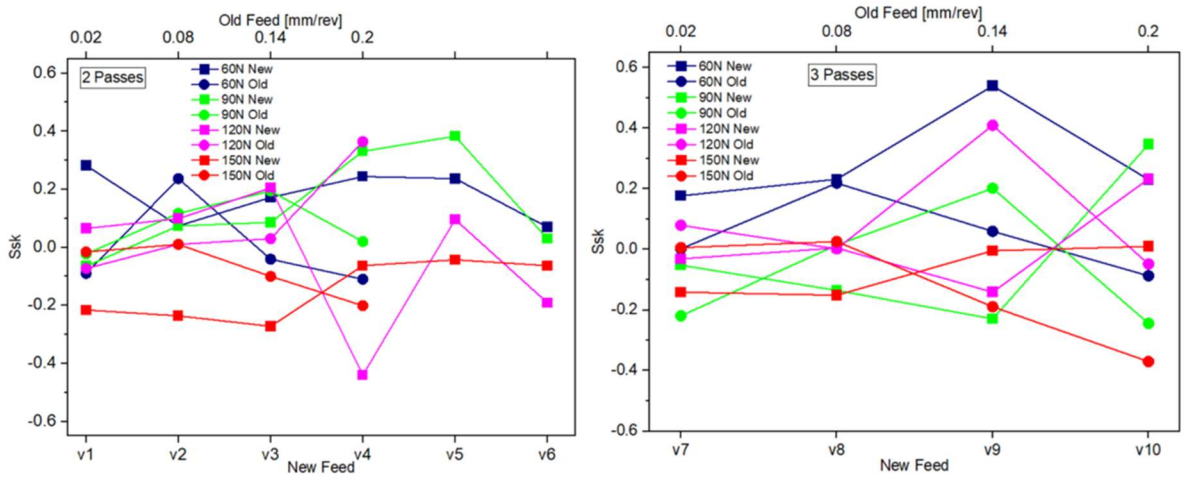

Figure 38. Ssk values of feed-varying and old methods with 2 passes and 3 passes.

The application of three passes (Figure 38) to both methods provided a decreased skewness except in two cases when a 60 N with a v9 feed and a 120 N with a 0.14 mm/rev feed and force pairs were used. For all force levels in both methods, v7 and v8 as well as 0.02 mm/rev and 0.08 mm/rev, provided close-range values that can be interpreted as unskewed surface roughness compared to the other two feed pairs. Under the new feed method (v7–v9), forces of 90 N and 150 N produced negatively skewed surfaces. In contrast, the old method generally maintained positive skewness at 60 N for all feeds. The old method also proved superior when using a 0.2 mm/rev feed across all force levels, consistently generating valley-dominated surfaces. The most extreme negative skew was observed with the old method at 150 N.

Four passes application (Figure 39) in the case the new method deformed the asperities until negatively skewed with a maximum value of -0.17 (v11 feed and surface N33). For the old method, only 60 N and 150 N forces achieved more negatively skewed roughness with exceptions (0.08 mm/rev and 0.14 mm/rev feeds). But it showed no clear trend with the change of feed and force. The valley-dominated surface roughness generated by the new method indicates better performance with oil and debris retention in a tribological sense.

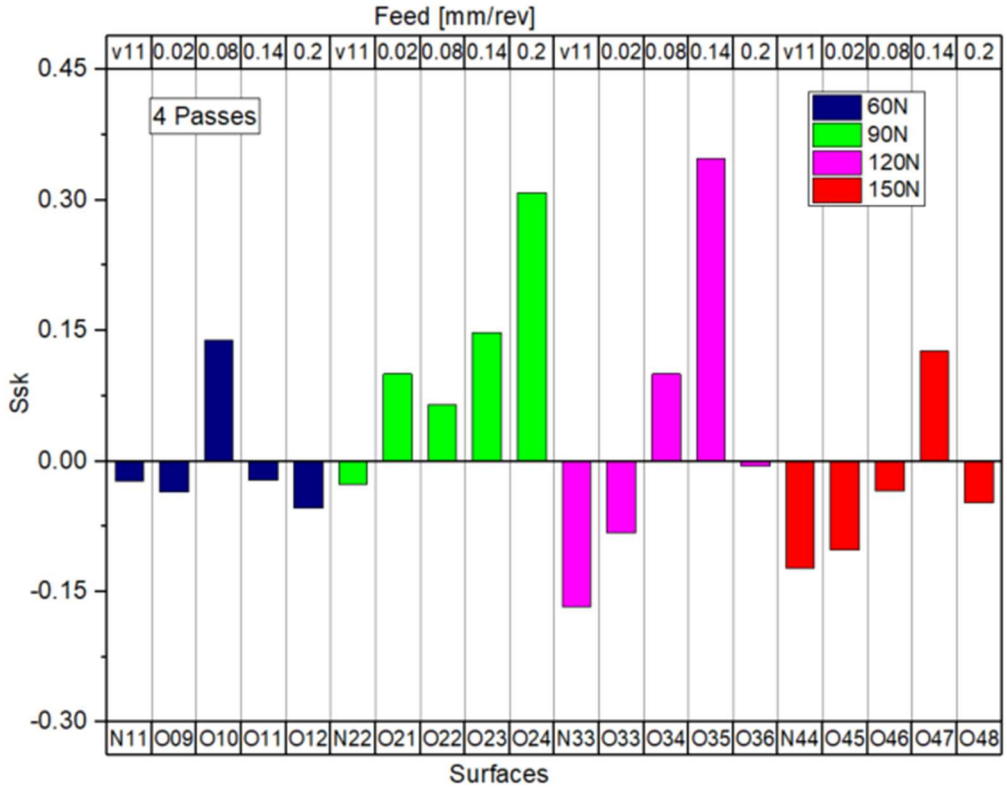

Figure 39. Skewness (Ssk) values comparison of the feed-varying and the old burnishing methods after 4 passes.

4.3.1.3. **Investigation of the Kurtosis (Sku)**

The initial turning process produced a surface with a kurtosis (Sku) of 2.50, indicating a balanced distribution of peaks and valleys from turning tool marks. Subsequent burnishing altered this topography, with both methods generally driving kurtosis closer to the Gaussian reference value of 3 or flattening it further, as predicted by the peak-deforming mechanism of the process. Performance, however, was highly parameter dependent. The new method, as shown in Figure 40 (2 passes) demonstrated superior control at higher forces, producing the flattest distributions at 150 N (Sku = 1.73 – 2.95) and maintaining a tight range at 90 N (Sku = 2.76 – 3.55). In contrast, the old method showed a propensity for higher kurtosis, particularly at 150 N (Sku = 2.02–4.02), indicating sharper peak distributions.

Specific trends revealed that a low force of 60 N allowed both methods to effectively reduce kurtosis across all feeds (New = 1.62 – 3.76; Old = 1.74 – 2.90). For intermediate feeds (0.08 mm/rev and 0.14 mm/rev), the old method performed better for loads of 60 N, 90 N, and 150 N. However, this advantage was counteracted by a significant drawback, when using a high feed of 0.2 mm/rev caused a consistent increase in kurtosis for the old method across all force levels, a trend mirrored in the new method when its equivalent v6 feed was applied. Furthermore, the new method (60 N, 150 N) and the old method (60 N) were particularly effective, experiencing decreasing kurtosis values for all selected feeds. In conclusion, while the old method excelled in specific intermediate feed and force combinations, the new method provided more consistent and flatter surface distributions, especially under higher burnishing forces.

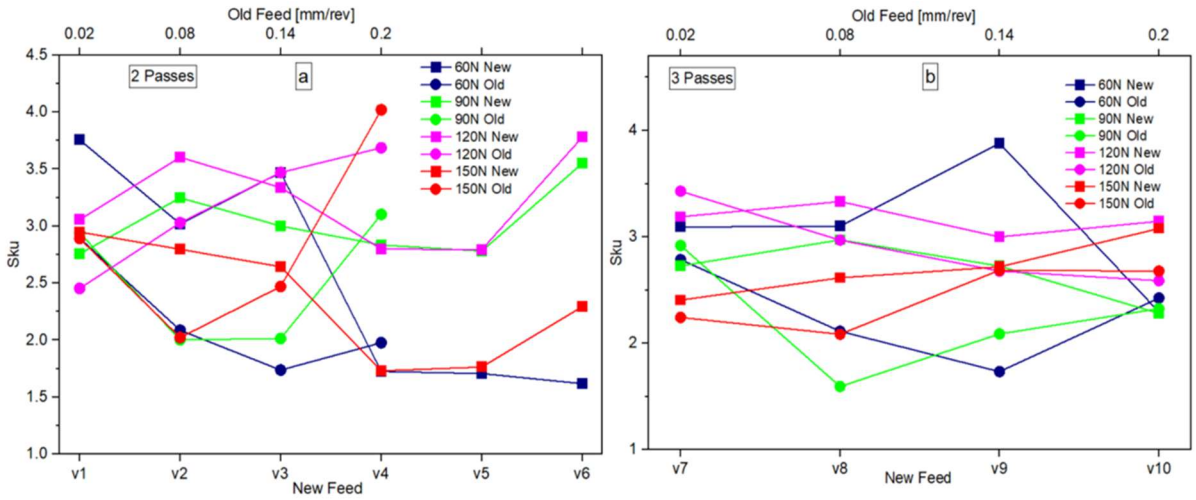

Figure 40. Kurtosis (Sku) change in feed-varying and old methods applying (a) 2 passes and (b) 3 passes.

The sudden changes of the values during two pass burnishing when force and feed are changing, are settled slightly when three passes are used. The kurtosis of the burnished surfaces attained a close range during the first and last feed (v7/0.02 mm/rev and v10/0.2 mm/rev). Applying the other intermediate feed also produced close values except for 60 N and 90 N when comparing the two methods. In addition, the old method provided lower kurtosis in almost all feed and force levels, which can be interpreted as a valley-dominated smoother surface. Moreover, higher forces (120 N and 150 N) and v9/0.14 mm/rev are shown providing almost identical values. Taking the turned surface as a reference, the new method increased the kurtosis to around 3 from 2.5, changing the property from valley-dominated to a flatter surface.

Further increasing the pass number produced no exaggerated differences as shown in Figure 41. The new method ranges from 2.69 (v11/90 N) to 2.79 (v11/120 N), telling the values are close to the Gaussian distribution. Ranging from 1.71 to 3.39, the old method also produced similar kurtosis. Except for 120 N force, the old method with 0.08 mm/rev and 0.14 mm/rev feeds yielded surfaces with kurtosis less than that of the initial turned surface. The combined 4 feeds (v11) produced identical kurtosis irrespective of the force magnitude, with little more variation for the old method, indicating reaching the saturation limit of the plastic deformation.

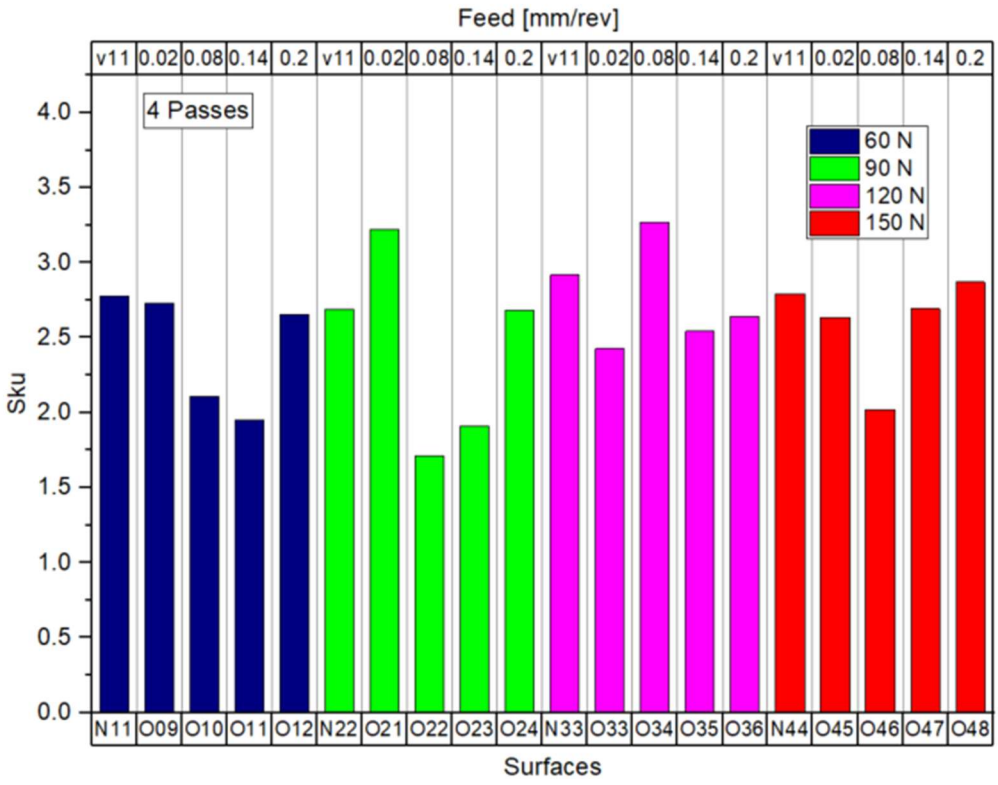

Figure 41. Feed-varying and old method Sku values comparison using 4 passes.

4.3.1.4. **Study of core roughness depth (Sk)**

Even though there are separate tests to study the tribological and other characteristics of a product, roughness parameters like core roughness depth can also provide good information on functional properties. Figure 42 shows the Abbott-Firestone curve measuring the vertical height to indicate the distribution of the peaks, valleys, and core roughness values. The roughness zone is truncated into three parts, namely reduced peak height, core roughness depth, and reduced valley depth, on moving from top to bottom. These surface texture parameters are critical for understanding tribological performance. They reveal initial contact characteristics and potential stress concentration points. After a run-in period, they further provide information on load-bearing peaks, lubrication retention, and valleys for debris entrapment. In this study, the core roughness depth (Sk), reduced peak height (Spk), and reduced valley depth (Svk) each underwent distinct changes in response to the different burnishing methods.

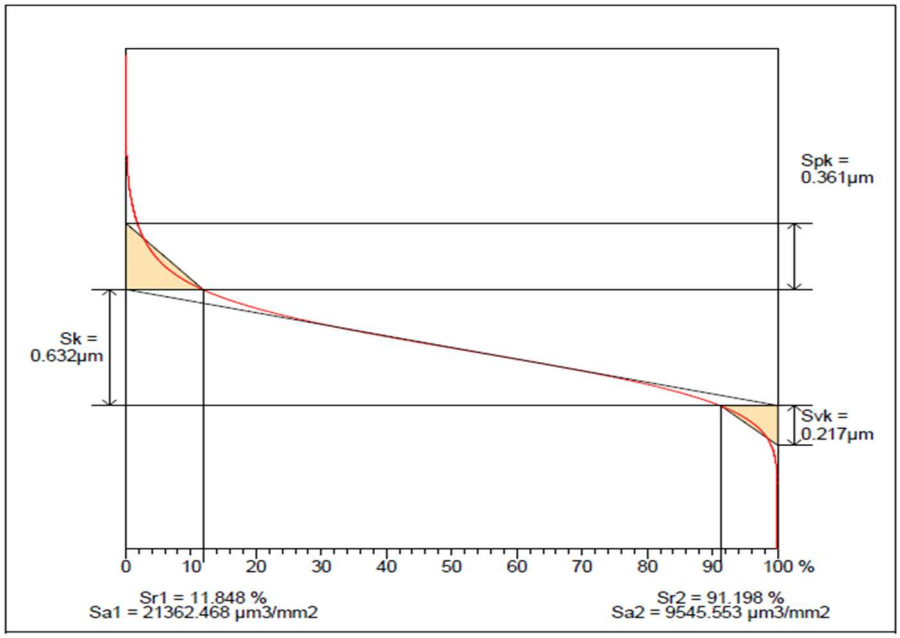

Figure 42. Abbott-Firestone curve (Bearing area curve) of burnished surface (N9) using the new method.

Like on the height roughness parameters, the varied burnishing technological parameters also reflected on the Sk responses. Its values were reduced when two passes were applied in combination with all forces as well as 0.02 mm/rev and v1 feed, as shown in Figure 43a. The core roughness depth (Sk) typically increased with higher feeds (v4, v5, and v6) when 60 and 150 N forces were applied compared to the level they attained during the first 3 feeds. A key exception was the new method using v1 to v3 feeds, which reduced Sk below the levels of the initial turned value of 1.91 µm. This signifies a reduction of extreme peaks and valleys, leading to a smoother core profile or low load-carrying roughness height. Overall, the new method produced lower Sk values, proving superior for generating smooth surfaces, though its performance is highly feed dependent. Optimal results for this method were achieved at moderate forces (90-120 N), whereas the old method showed no consistent response to changes in force. But the lowest applied feed (0.02 mm/rev) provided the lowest Sk value.

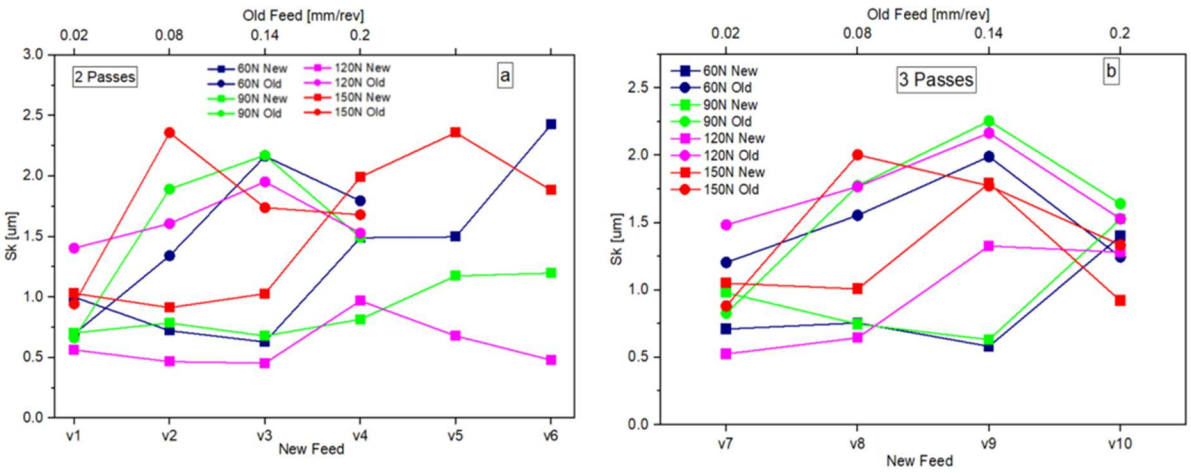

Figure 43. Core roughness depth (Sk) comparison after burnishing by feed-varying and old method process, (a) 2 passes and (b) 3 passes.

Increasing the number of passes to three showed in Figure 43b depicts the dominance of the new method in all ranges of feed and forces over the old method. They performed similarly when the feeds were v7/0.02 mm/rev and v10/0.2 mm/rev. Except for 60 N and 90 N of the new method, when the feed changed from v7 – v9 and its equivalent in the old method from 0.02 -0.14 mm/rev, the Sk values increased. In this specific case, the values decreased after they reached their maximum level when the feed was further changed to the final value. The entangled lines representing Sk vs feed of different forces explain that there are additional factors that affect apart from the employed technological parameters. The two applied burnishing methods reduced the core roughness depth during low feed or feed combinations in the case of the new method, which involves the low feed, and these low values were preserved for most cases. When interpreting this, it shows that the load-bearing capacity of the surface was decreased, which needs consideration based on the application of the surface. Increasing the feed in both methods increased Sk to an extent more than the turned Sk values from the achieved minimum level .

Consistent with the findings in other subsections, the new method yielded similar or superior surface finish metrics compared to the old method, which was optimized at a 0.02 mm/rev feed. This characteristic was also evident in the Sk parameter, as demonstrated in Figure 44 for four-pass operations. Under these conditions, the feed-varying method generated surfaces with reduced Sk values, distributed between 0.89 μm and 1.33 μm for all force levels. The improved performance is attributed to the increased number of passes, which provided more opportunities for the tool to plastically smooth surface asperities. Conversely, any deviation from the 0.02 mm/rev feed in the old method resulted in a noticeably rougher surface.

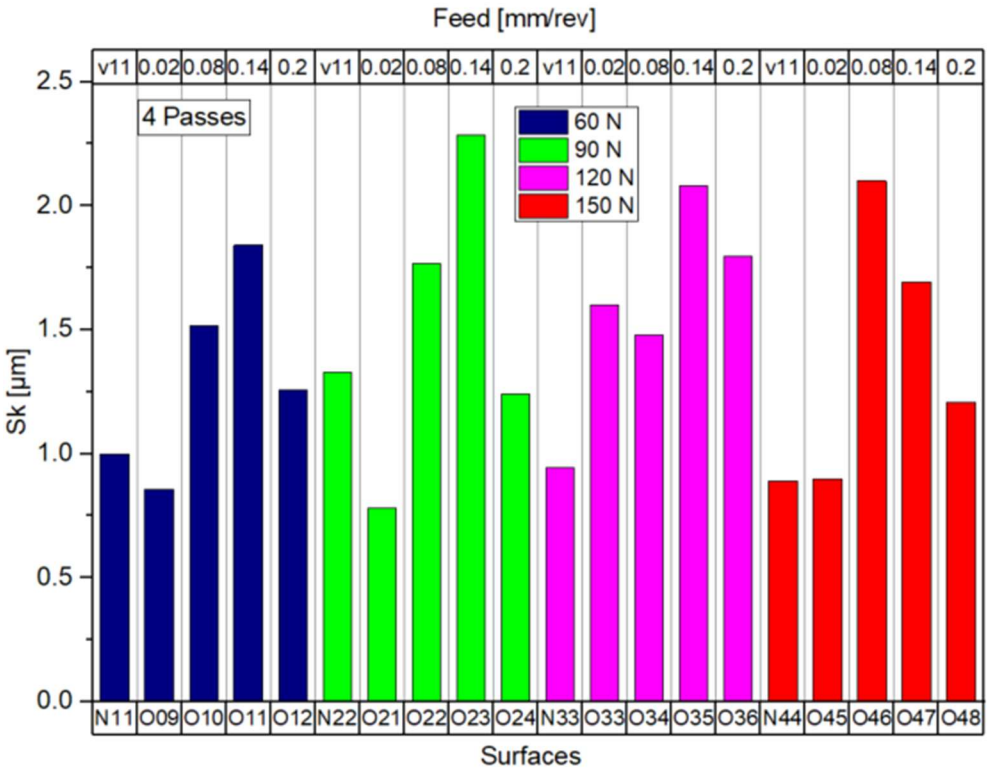

Figure 44. Core roughness depth (Sk) comparison after burnishing by feed-varying and old methods applying 4 passes.

4.3.1.5. **Analysis of reduced peak height (Spk)**

From the three roughness layers, the top one is called reduced peak height, representing the peak portion of the roughness. The generated peaks resulting from the different machining processes receive the initial contact and load between the fitting surfaces and are removed during the run-in. Further applying post-machining in this case, two burnishing methods naturally deal with these peaks, changing their characteristics through their plastic deformation. Both burnishing methods and under all applied technological parameters, Spk was reduced significantly from its initial 1.49 µm turned status. Applying two passes depicted in Figure 45a, produced surface with Spk (new method), ranging from 0.16 µm utilizing v3 feed and 150 N force to 0.48 µm utilizing v4 feed and 60 N force. In the case of the old burnishing method, 0.16 µm with 0.14 mm/rev feed and 60 N force to 0.76 µm with 0.2 mm/rev feed and 120 N force. Surfaces burnished by 120 N and 150 N of the new method showed much more reduced Spk values when compared with the other two forces and all the old method forces. When the specific forces of each method are compared with its counterpart, 90 N showed a slightly higher variation, while the old method increased when higher feeds were applied. Except for outliers, the reduced peak height was consistently approximately 0.3 µm across nearly all feed and force levels, indicating no significant correlation.

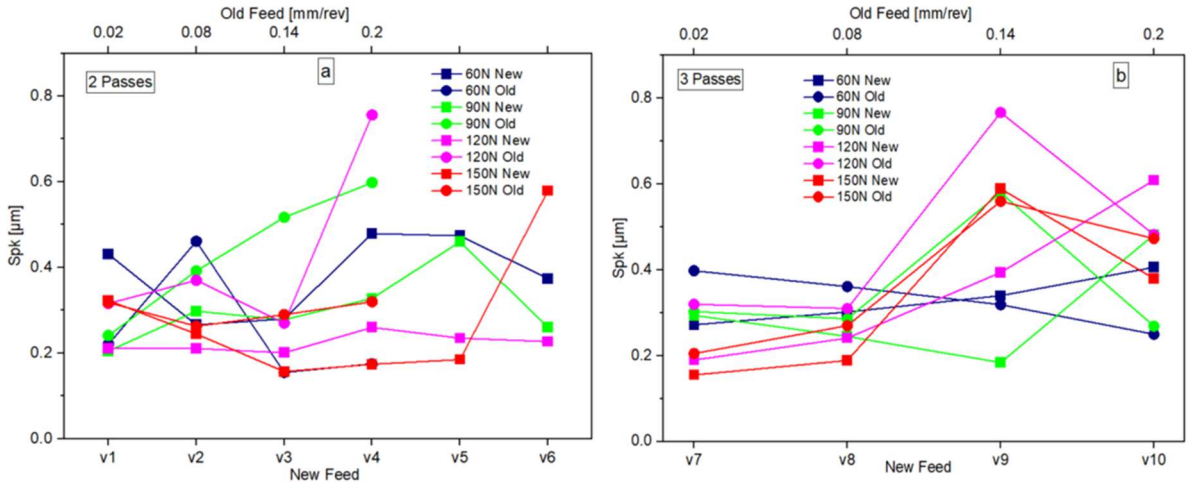

Figure 45. Feed-varying and old methods burnishing process Spk values applying (a) 2 passes and (b) 3 passes.

The experimental results after applying three passes detailed in Figure 45b, demonstrates a substantial improvement in surface finish during the initial stages. Specifically, the first two feeds in both methods produced a significant reduction in Spk values by a factor of three to nine across all applied force levels. Within this specific range of feeds and forces, the Spk values from both methods converged within a narrow comparable band. However, beyond this range, Spk began to increase, reaching a maximum during the application of the v9 and 0.14 mm/rev feeds. A subsequent decrease in Spk was observed upon the application of the final feeds, although this trend did not hold for the 60 N and 90 N force levels, which remained high. When compared to the two-pass process, the three-pass method generated Spk trends (both increasing and decreasing) that were more moderate and well defined, indicating a greater process stability. Furthermore, the new method consistently outperformed the old method, yielding lower Spk results in the majority of test cases.

Across all force categories in the four-pass experiments (Figure 46), the Spk values achieved by the new method were similar to those produced by the old method at feeds of 0.02 mm/rev and 0.08 mm/rev. Furthermore, all these surfaces showed only minor deviation from achieved minimum Spk, suggesting that the feed parameter had a negligible effect within this lower feed range. In contrast, the old method performed poorly with higher feeds (0.14 mm/rev and 0.2 mm/rev) creating a pronounced difference, characterized by a significant rise in Spk values that indicates the formation of higher peaks.

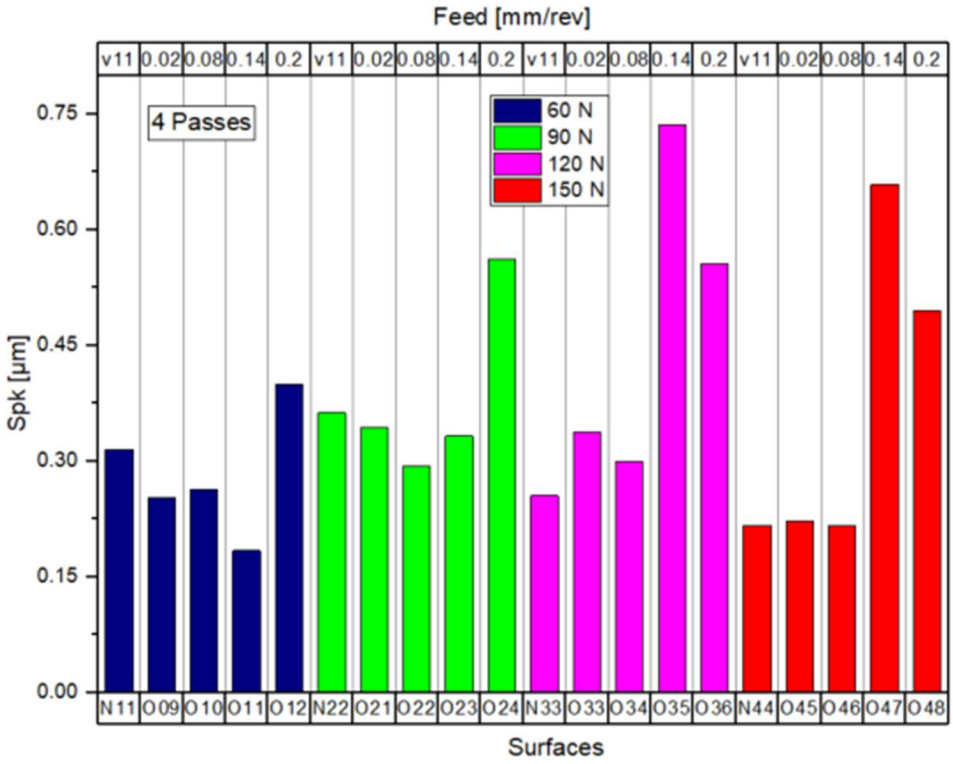

Figure 46. Feed-varying and old methods burnishing process Spk after 4 passes.

4.3.1.6. **Investigation of reduced valley depth (Svk)**

Another important roughness parameter from the Firestone-Abott curve is the reduced valley depth, which provides information about the vertical valley depth interpreted in relation to tribological characteristics. Like the other two parameters, Svk presented in Figure 47 and Figure 48 is studied when pass, feed, and force are changed. Two passes presented in Figure 47a shows similar performance by both burnishing methods, with lower values achieved when lower forces were applied. The surface roughness value (Svk) decreased from 0.78 µm (initial turned surface) to 0.12 µm by applying v5 and a 60 N force. Decreasing Svk means shallow valley depth with reduced lubricant and debris holding capacity. Generally, most results from the new method showed insignificant change. The only exceptions were the 120 N force (feeds v4, v5, v6) and the 150 N force (feed v6), which followed a sudden surge. Additionally, 60 N and 90 N of the new method showed a stable Spk value irrespective of the changes in feed and force. After reaching an average Svk of 0.3 µm, both methods almost stayed the same for all levels of feed and force, using the same 2 passes.

Increasing the number of passes to three consistently improved valley roughness by reducing Svk values, as provided in Figure 15b. This trend repeats the behavior observed with Spk values under the same machining conditions. For both the new and the conventional method, all force levels and the first two feed rates generated surfaces with decreased valley characteristics, achieving a reduced valley depth within a narrow range of 0.14 µm to 0.4 µm. However, beyond these initial feed rates, a divergence occurred. Any further increase in feed rates typically led to a increase of the valley surface, resulting in higher Svk values that indicate the formation of deeper valleys. The single exception to this behaviour was the 90 N force applied using the new method, which maintained a lower Svk despite the increased feed. This phenomenon can

be explained by the fundamental difference between the two methods. In the conventional method, increasing the feed simply creates a rougher surface with deeper valleys. In contrast, the strategic combination of parameters in the new method, specifically the availability of higher feed settings allows for a more controlled process that can, in the case of the 90 N force, maintain valley integrity. Finally, echoing the results of other response parameters analyzed, the specific level of applied force did not produce a clear or predictable trend on its own.

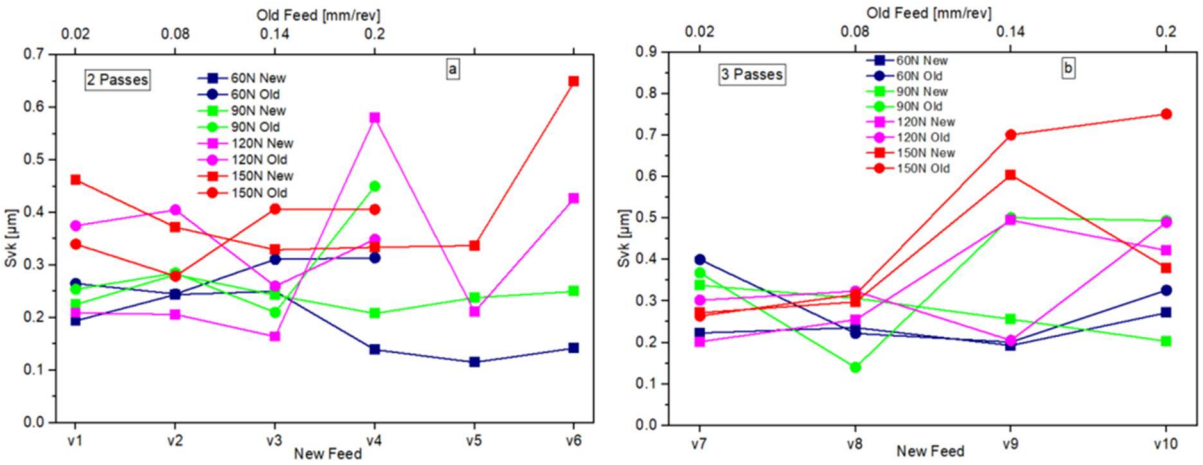

Figure 47. Feed-varying and old method burnishing process Svk value comparison, (a) 2 passes and (b) 3 passes.

Comparing the two burnishing methods after applying four passes presented in Figure 48 shows the achievement of lower Svk by the conventional burnishing method when 60 N, 90 N, and 150 N were used, except for a few higher feeds. Both methods reduced Svk when compared to the turned surface, with the highest and lowest values produced by the old method after 120 N with 0.2 mm/rev (Svk = 0.54 µm) and 90 N with 0.14 mm/rev (Svk = 0.16 µm) were applied.

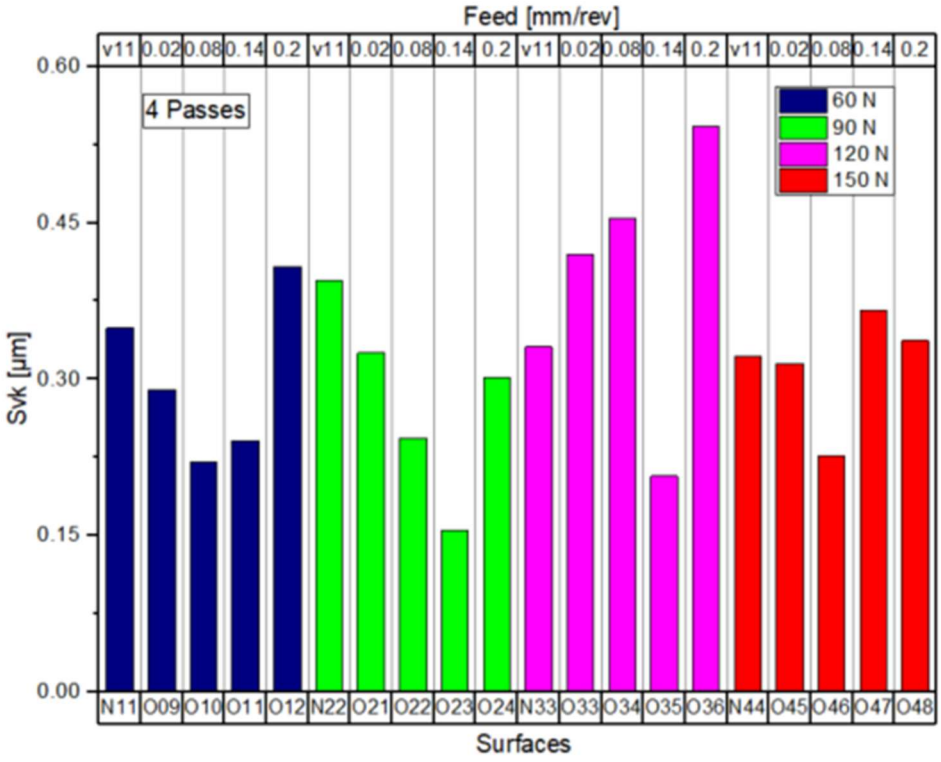

Figure 48. Feed-varying and old method burnishing process Svk value comparison after 4 passes.

The studied functional parameters in this experiment called core roughness depth (Sk), reduced peak height (Spk), and reduced valley depth (Svk), all exhibited a significant decrease, particularly when the 0.02 rev/min feed rate was applied. This improvement was consistent across all force levels and both burnishing methods. In many cases, these low roughness values were maintained across various parameter settings. However, a subsequent increase in the feed rate often caused the values to rise again from their achieved minimum, indicating an affected surface quality. These three parameters provide a comprehensive characterization of the manufactured surface. The core roughness depth (Sk) represents the core of the surface that bears the load. A higher Spk value signifies protruding peaks, which are undesirable as they concentrate stress at their tips and make the surface prone to wear and high friction. Conversely, a higher Svk value indicates deeper valleys, which are beneficial for retaining lubrication; this is preferred in applications where ease of movement between contacting surfaces is critical.

Amplitude parameters of the new method showed more effect if we compared the two methods with their average achieved changes, except for Ssk, which is similar. The average percentage changes of Sa, Ssk, and Sku are 40.2%, 87.1% reduction, and 2.1% increase for the conventional method, and 56.7%, 86.5% decrease, and 12.1% increase. The functional parameters also showed a similar dominant effect of the new method over the conventional method presented in Table 11.

Antal et al. [75] achieved Spk of a X5CrNi18-10 steel surface 0.35 µm from 1.13 µm (70.2% decrease) and 3.45 µm from 1.17 µm initial turned surface, which is -204% increase. They applied 3 passes, 0.05 mm/rev feed, and 10 N force. With the applied pass number and feed

range, the old method produced a 0.205 μm to 0.39 μm range that showed a much better result, but with consideration to the material type and utilized force, there is an experimental setup difference. There are no literature to compare with the employed new feed application mechanism and for that reason I conducted the counterpart conventional burnishing method.

This investigation reveals that both feed-varying and traditional slide burnishing techniques substantially decrease surface roughness parameters, including roughness height and core roughness, on 42CrMo4 steel. The new approach yields roughness values that are either lower or equivalent to those of the conventional method, particularly at a feed rate of 0.02 mm/rev. Compared to turning, both methods produce smoother surfaces, which may enhance fatigue life and other surface characteristics. The reduction in core roughness parameters indicates decreased friction-inducing peaks, lubrication retention, and load-bearing core roughness.

The effectiveness of the new method is likely due to its unique tool–workpiece interaction, where the tool path shifts relative to prior passes, allowing it to reshape surface asperities. This supports the hypothesis that feed variation enhances surface smoothing. The microscopic picture shown in Figure 49, taken using a Zeiss Stereo Discovery V8 microscope (Carl Zeiss Microscopy GmbH, Jena, Germany) at 80x magnification, illustrates distinct tool marks from turning and burnishing. Surfaces treated with the new method (see Figure 49c) show a notable reduction in roughness-inducing tool marks compared to those from turning.

Building on previous research on flat surfaces [23], this study introduces new burnishing as an innovative technique for 42CrMo4 steel, a material critical in high-strength applications. The new method achieves performance comparable to the conventional approach at 0.02 mm/rev while reducing processing time, offering potential efficiency gains for industries such as automotive and aerospace, where enhanced surface quality improves component durability. However, the study found no significant differences across various technological parameters, such as burnishing force, indicating a need for further exploration.

Future research should investigate additional materials, a broader range of burnishing parameters, and properties like surface hardness, residual stress, and wear resistance to expand the method’s applications. These findings highlight the promise of the new burnishing method for achieving smoother surfaces with reduced processing time compared to conventional methods, setting the stage for advancements in precision manufacturing.

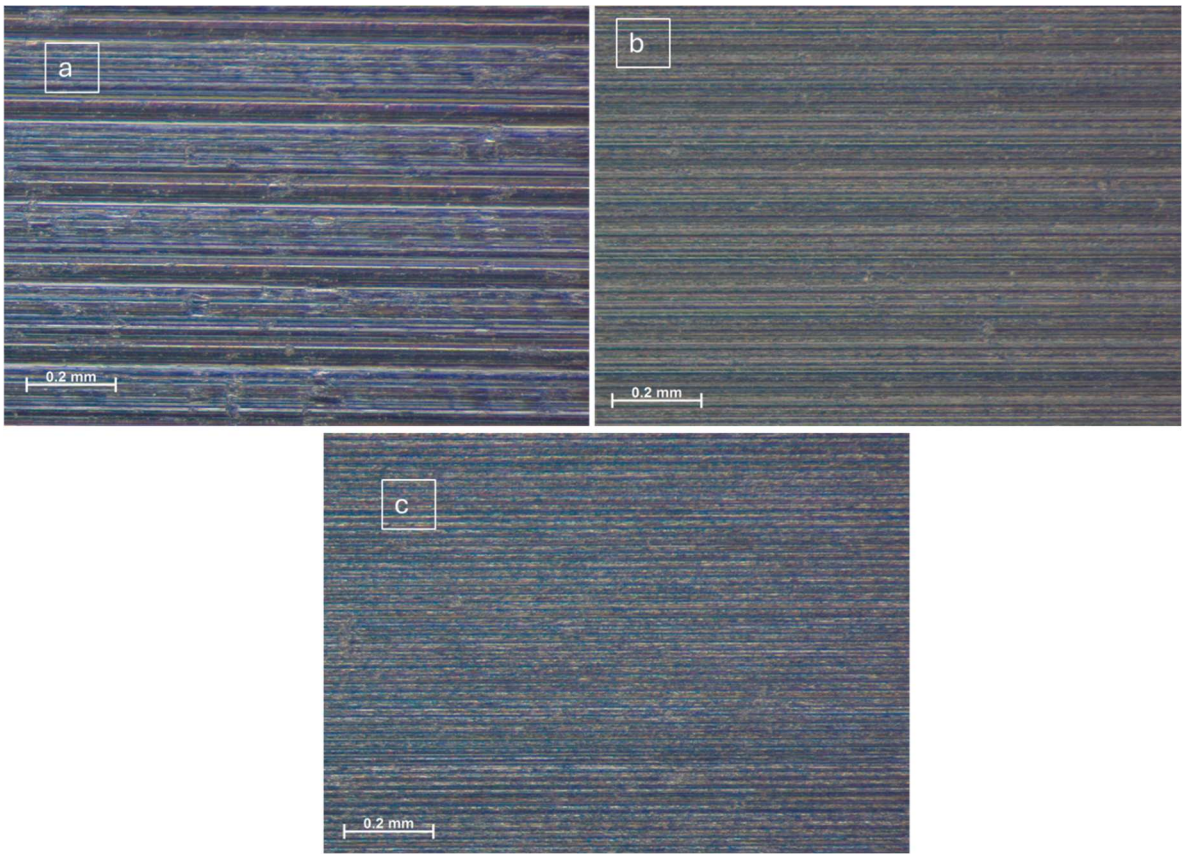

Figure 49. Microscopic picture of (a) turned surface, (b) O31 (burnished with 120 N, 0.14 rev/min, and 3 passes), and (c) N31 (burnished with 120 N, f9, and 3 passes).

4.3.2. **Comparison of burnishing time**

One of the main characteristics of the burnishing process is repeatedly attempting the process based on a preselected number of passes. For example, if the previous machining process left surface asperities to be removed by the burnishing process, the responsible person must decide how many passes are required to achieve the required smoothness. So, when the number of passes increases, the time required to finish the whole process is extended. We present elapsed time comparison calculations equation 1 and 2 for both methods.

$$t_{m,n} = 60 \cdot \frac{L_w}{n_w} \cdot \left[\frac{1}{f_1} + \frac{1}{f_2} + \frac{1}{f_3} + \frac{1}{f_4}\right], \quad (1)$$

$$t_{m,o} = 60 \cdot \frac{L_w}{n_w f_1} \cdot i. \quad (2)$$

where the machining time of the new ($t_{m,n}$) and the old ($t_{m,o}$) method are calculated based on the axial length of the burnished surface (L_w), the rotations of the workpiece (n_w), the applied feed in each pass (f_1,f_2,f_3, and f_4), and the number of passes (i).

The elapsed time calculation of the old burnishing method is simply calculating the time for a single pass and multiplying it by the number of passes factor (Equation (1)). On the other hand, the feed-varying method time is calculated independently for each pass, as they use different feeds and sum them up (Equation (2)).

Figure 50 demonstrates feed versus time graph comparison between the two methods. The lowest feed of the old method (0.02 mm/rev) and the first three feeds of the feed-varying method, which includes the slowest applied feed (0.02 mm/rev), have the longest elapsed time; see Figure 18a. Increasing the feeds, marked red on the top second x-axis and applying v4, v5, and f6 requires less time to finish. The same is true with three passes up, applying the smallest feed of 0.02 mm/rev (0.02 mm/rev and v7, v8, and v9); see Figure 50b. The v10 feed combination (0.08 mm/rev, 0.14 mm/rev, and 0.2 mm/rev) and 0.2 mm/rev finished the three passes at times close to each other, which also produced similar roughness results. In the case of four passes presented in Figure 50c, the proposed method finished the process faster when the old method applied a 0.02 mm/rev feed. Considering the time taken to complete the process, the feed-varying method is faster only when the old method uses the smallest feed; however, it produces a closer or smoother surface roughness, which can make it a competitive method. In this case, industries can select which method to use, balancing the trade-off between time and surface roughness level.

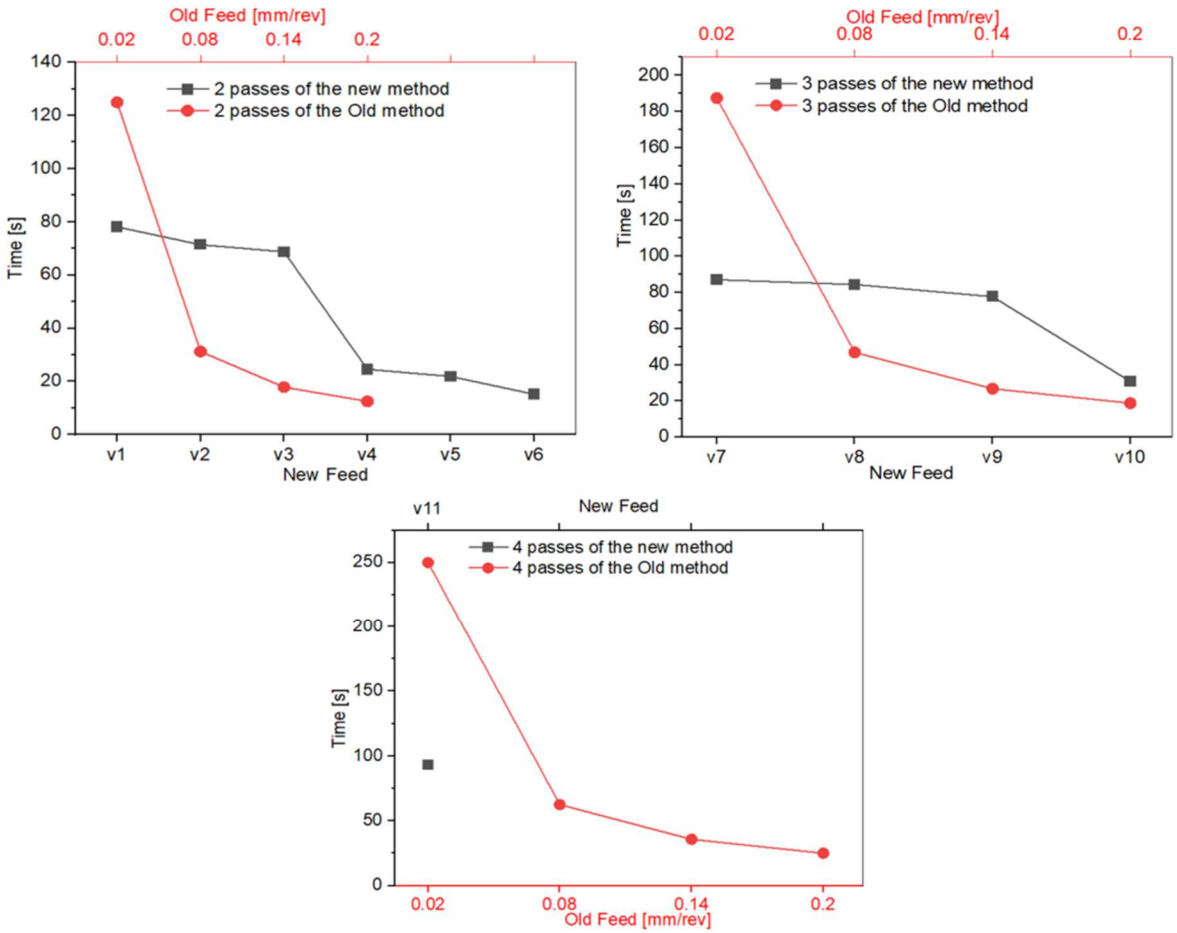

Figure 50. Elapsed time of the two methods when (a) 2 passes, (b) 3 passes, and (c) 4 passes are used.

5. THESES

Thesis 1

I developed and fabricated a custom-designed stepped shaft adapter that facilitates the seamless integration of a lathe-specific burnishing tool into a CNC milling machine, transformed it into an interchangeable tool, and validated it by applying it in all conducted experiments of the dissertation. This engineered solution directly addresses the limitation of tool incompatibility between machining platforms. By preserving the tool's native spring-force mechanism and enabling its use for planar surface finishing, the adapter eliminates the need for a dedicated burnishing tool for a milling machine. As a result, this research makes a significant contribution as it achieves significant cost reduction, enhances manufacturing process flexibility, and promotes resource efficiency, establishing a practical model for design for versatility in modern manufacturing. [FTK2, FTK3, FTK6, FTK9]

Thesis 2

I proved through experiments that successive grinding and slide diamond burnishing with an interchangeable burnishing tool enhances the poor surface integrity of MetcoAdd 17-4PH-A 3D-printed stainless steel, which restricts its use in high-performance applications. The approach reduced arithmetical mean height (Sa) by 57 %, inducing compressive surface residual stresses up to +346 % (transverse), increasing near-surface microhardness by 77 %, and generating beneficial compressive layers to 0.22 mm depth. By studying the successive processes for the first time on MetcoAdd 17-4PH-A, this research establishes a scalable, milling-compatible framework for precision surface finishing, offering significant potential to improve surface integrity in applications such as automotive, aerospace and biomedical industries. Selected parameter level range are, force (40 - 100 N), feed (0.02 – 0.17 mm), and pass (1 - 4). [FTK6]

Thesis 3

I introduced a novel burnishing strategy that modulates the inter-pass feed/feed rate to systematically shift the tool path, thereby overcoming the inherent inefficiency of conventional fixed-feed methods. A group of feeds is applied in a multi-pass burnishing process by changing the feed starting from larger to smaller in each pass. This ensures a more comprehensive plastic deformation of surface asperities by addressing peaks left unprocessed in previous cycles. Experimental results on C45 and 42CrMo4 steels confirm that this method yields a superior surface finish compared to conventional fixed-feed approaches. Its applicability across milling and lathe machines, along with its ease of use, makes it a convenient method for achieving an enhanced surface finish without requiring any capital investment or hardware modification. [FTK9, FTK10]

Thesis 4

I demonstrated through experiment that changing the feed after each pass in the multi-pass diamond slide burnishing process of flat C45 steel improves the amplitude and functional roughness parameters within the applied range, burnishing force (70 - 110 N,) feed (0.02 – 0.2 mm), and pass (2 – 4). It achieved equivalent or superior reductions in arithmetic mean roughness (average Sa = 67.4%) compared to the conventional method. Furthermore, it transforms topographies from platykurtic to leptokurtic with kurtosis (Sku) increasing up to

198.3%, outperforming the erratic trends in conventional methods that range from 196.1% rises to 10.9% declines. It yields core roughness depths (Sk) that are smaller or comparable to the optimal values from conventional methods, with reduced sensitivity to feed and pass variations and an average 72% reduction versus 46.9% in traditional techniques. These results establish the feed changing method as a superior, low-cost approach for controlled functional surface texturing in load-bearing tribological applications. [FTK9]

Thesis 5

Varying the feed in the multi-pass diamond slide burnishing applied on cylindrical 42CrMo4 low alloy steel significantly enhances amplitude roughness parameters compared to the conventional feed application method. I achieved average reductions of 56.7% in arithmetic mean height (Sa) and 86.5% in skewness (Ssk), alongside a 12.1% increase in kurtosis (Sku). The feed varying process outperformed the conventional method with 40.2% Sa reduction, 87.1% Ssk reduction, and 2.1% Sku increase, thereby demonstrating superior surface smoothness and topographic control for high-performance mechanical components. In the functional parameters, it achieved average reductions of 41.6% in core roughness depth (Sk), 77.9% in reduced peak height (Spk), and 61.6% in reduced valley depth (Svk). It enhances tribological performance by minimizing friction-inducing peaks and optimizing load-bearing capacity. Selected parameter level ranges are, force (60 - 150 N), feed (0.02 – 0.2 mm/rev), and pass (2 - 4). [FTK10]

Thesis 6

Applying the novel slide burnishing feed application method finishes the process faster than the conventional method when it incorporates the lowest selected feed (0.02 mm/rev) in the feed combination of cylindrical 42CrMo4 alloy burnishing. In the conducted experiment, a smoother surface by both methods was achieved when v1 and 0.02 mm/rev feeds were applied. In this case, the new method is faster by 1.6 times when 2 passes are applied, and 2.15 times as well as 2.7 times when 3 and 4 passes are used. This proves that the proposed method can produce an enhanced surface finish in substantially less time, offering a direct competitive advantage in manufacturing efficiency for precision-focused industries. [FTK10]

6. SUMMARY

The PhD. Study investigates the effect of diamond slide burnishing process of 3D printed and ground MetcoAdd 17-4PH-A stainless steel, milled C45 medium carbon steel and turned 42CrMo4 low alloy steel. A round sliding tool designed for a lathe machine was modified to fit in a milling machine to burnish flat surfaces (C45 and MetcoAdd 17-4PH-A). The tool followed a parallel path to perform the process.

Successive grinding and burnishing processes were applied to the 3D printed stainless steel to modify the surface integrity. Amplitude roughness parameters and functional parameters were measured and analyzed to understand the effect of the process on the surface. Additionally, surface, in-depth residual stress, and microhardness were studied.

A novel burnishing process was introduced and studied that changes the feed in each pass instead of applying a single feed for all selected passes. To test its functionality, it was applied to flat C45 steel and cylindrical 42CrMo4 workpieces. To compare with the conventional method, for each selected combined feeds of the new method, its conventional counterpart was tested. Amplitude functional roughness parameters were studied to evaluate the effectiveness. From the conducted experiments and evaluated results, the following conclusions were drawn.

MetcoAdd 17-4PH-A

1. Slide burnishing improved the surface of the printed stainless steel to a great extent. Sa was reduced by the successive grinding and burnishing from 11.3 μm to 0.46 μm (average). Burnishing reduced the roughness by 57.1% with reference to grinding. Lower feed medium force and intermediate passes from the applied technological burnishing parameters produced a lower Sa value.
2. The skewness and kurtosis results demonstrate that diamond sliding burnishing significantly alters surface texture without transforming their phase, making it more favorable for applications requiring improved lubrication retention (due to deeper valleys) but potentially increasing initial friction/wear due to higher kurtosis.
3. The core roughness depth was reduced by the grinding and burnishing (90.8% and 67.9%), which was further affected by the technological parameter change of the burnishing process. Lower burnishing force (40 N and 60 N) showed less effect than higher force (80 N and 100 N) in combination to feed with less effect on passes.
4. When higher force and fewer passes are combined, their effect produces a higher Spk value, indicating a peaky surface compared to the other forces and number of passes combined effect resulting on producing flatter surfaces.
5. Reduced valley depth was decreased when lower force was used except when higher feed was selected. Application of higher force on the contrary created deeper valleys when fewer feed and higher feed were selected.
6. An increased residual stress in transverse directions with an average increase of 346% was observed with a high burnishing force and a lower number of passes. The 130 MPa initial as-built surface was modified by grinding to −190 MPa and significantly increased in all the burnished surfaces.

7. Unlike the transverse residual stress, the longitudinal surfaces experienced an increasing trend when lower forces (40 N and 60 N) and fewer passes (one and two) were used. Another important observation was that the ground surface's stress direction was unchanged. Burnishing processes, like in the transverse direction, significantly increased the residual stress.
8. Both grinding and burnishing processes enhanced the microhardness of the printed surfaces. A 45.5% increase in grinding, an average increase of 22.3% after burnishing compared to grinding, and 78.6% compared to the initial state, were accomplished.
9. The in-depth residual stress study showed almost no change due to the grinding process, but after burnishing, the compressive stress distribution was up to 0.11 mm by 40 N and 60 N, and up to 0.22 mm by 80 N and 100 N. The feed variation in the burnishing process also showed a clear distinction when higher and lower force ranges were used.

C45 steel

10. The new method allows changing the feed so that the center of the tool is shifted to follow a different path that can help smooth the surface.
11. With burnishing force and number of passes limited effect, the proposed feed changing process after each pass performed similarly or better than the best achieved result (Sa) when a lower feed was applied by the conventional method.
12. With an increase in burnishing force from 70 N to 90 N and 110 N, the new method improved the skewness of the milled surface. With this parameter, the old method showed a changing trend with the change in burnishing parameters from an increase by 182.9% to a 78.9% reduction. In comparison, the new method showed more steady and predictable change than the old method with burnishing parameters change.
13. Kurtosis values of all of the surfaces burnished by the new method increased by up to 198.3%, indicating that the topographies were changed from platykurtic to leptokurtic. The old method showed a trend of decreasing with increasing passes from a 196.1% rise to a 10.9% decline, compared to the initial milled surface values. Additional study and adjustment of the introduced method are required to address the kurtosis behavior of the generated surface.
14. The core roughness depth of the new method was smaller or similar to the smallest value achieved by the conventional method. Feed and pass change are more reflected in the conventional method, with almost no effect for the new method. In the case of reduced peak height, burnishing parameters had no clear relation with the result. However, the result of the new method was competitive.
15. The reduced valley depth of both methods was not affected much by the selected burnishing technology parameters, reflected with very close results.
16. The functional parameters, especially core roughness depth and reduced peak height, were greatly affected by the burnishing process. Comparing the two methods using average percentage changes (Sk, Spk), the new method achieved 72% and 52.7% reduction while the conventional method achieved 46.9% and 32.1% reduction.

42CrMo4

17. Both methods decreased height roughness parameters, but the feed-varying method influenced more, especially when the number of passes were three and four. Sa, Ssk, and Sku of the new method showed 56.7%, 86.5% decrease, and 12.1% increase, and the conventional method showed 40.2%, 87.1% decrease, and 2.1% increase.
18. The functional parameters that study the peaks, core, and value heights decreased compared to the initial turning process, with the feed-varying method performing better or closer to the old method in achieving a lower height.
19. The smoothest surfaces were produced when 0.02 mm/rev feed in all force and pass levels was used in both methods.
20. The core roughness height (Sk) reached its minimum value when applying the lowest feed rates in both methods and exhibited a proportional increase with higher feed rates. Like in the amplitude parameters, functional parameters were influenced greatly by the new method. The average percentage change reflects this with 41.6%, 77.9%, and 61.6% (Sk, Spk, and Svk) decrease by the new method and 17.9%,68.2%, and 48.5% decrease by the conventional method.
21. The calculated time revealed that the feed-varying method generally requires more time than the conventional method, except when using the lowest feed rate of 0.02 mm/rev. Notably, the results obtained with 0.02 mm/rev in both the conventional method and feed-varying method (where 0.02 mm/rev was part of the combination) were closely comparable. This demonstrates that the feed-varying method can achieve similar performance while reducing processing time when both methods use the lowest feed.
22. Further study is required to understand the effect of burnishing technological parameters clearly, because in some scenarios, the relation between the responses and the burnishing parameters was not clear.

The experimental study shows promising results, opening the way to further research to capitalize on the advantages of using the proposed tool and novel burnishing method. As modern technology is demanding high surface integrity quality, a low-cost burnishing process with a different approach, like what I applied in this PhD. study could be a solution.

7. SUGGESTIONS FOR FUTURE RESEARCH

All performed burnishing experiments were conducted using one tool, and the same tool path strategy was used while burnishing a flat surface. I suggest testing different tool diameters with a variety of tool paths to optimize the adaptability of the tool for the milling machine.

Three burnishing technological parameters (force, feed, and pass) with limited levels were tested in this PhD. study. Some technological parameters effect were not clear, especially with the proposed new method. Further research that can explore the role of other technological parameters, increased scope of their levels, and test the method in different material types can help to understand the effectiveness of the new method.

Nowadays, there are lots of assisting technologies (mentioned in the introduction section) to enhance the burnishing process. Ultrasonic vibration-assisted burnishing and laser-assisted burnishing are among the popular techniques for enhancing burnishing processes. I suggest the application of those assisting technologies to enhance the response quality.

8. LIST OF PUBLICATIONS RELATED TO THE TOPIC OF THE RESEARCH FIELD

[FTK1]. Felhő, C., & Tesfom, F. Investigation of cutting force components and surface roughness in face milling with different cutting ratios. Mérnöki és Informatikai Megoldások, 3(2.), 52–65, 2022. DOI: https://doi.org/10.37775/EIS.2022.2.5

[FTK2]. Frezgi Tesfom, István Pásztor, Csaba Felhő. Flat diamond sliding burnishing surface roughness investigation. Vol. 12 No. 3 (2022): MultiScience - microCAD International Multidisciplinary Scientific Conference - Special Issue Part I. DOI: https://doi.org/10.35925/j.multi.2022.3.17

[FTK3]. Felhő, Csaba, Frezgi Tesfom, and Gyula Varga, ANOVA Analysis and L9 Taguchi Design for Examination of Flat Slide Burnishing of Unalloyed Structural Carbon Steel. Journal of Manufacturing and Materials Processing 7.4 (2023): 136. DOI: https://doi.org/10.3390/jmmp7040136, Scopus Indexed

[FTK4]. Frezgi Tesfom, Felhő, Csaba, Burnishing Process Technologies: Case Study of Sliding Burnishing. Miskolci Egyetem Gyártástudományi Intézet, pp 119-124 (2023), ISBN: 9789633583173

[FTK5]. Frezgi Tesfom, Felhő, Csaba, Examining the impact of slide burnishing parameters on the 3D surface features of medium carbon steel. Journal of production engineering 30-35 (2024): DOI: https://doi.org/10.24867/JPE-2024-01-030

[FTK6]. Kebede, Frezgi Tesfom, Jawad Zaghal, and Csaba Felho, Characterization of Surface Integrity of 3D-Printed Stainless Steel by Successive Grinding and Varied Burnishing Parameters. Machines 12.11 (2024): 790 DOI: https://doi.org/10.3390/machines12110790, Scopus Indexed

[FTK7]. Kebede, Frezgi Tesfom, and Csaba Felhő, 3D amplitude & spatial parameters study before and after successive grinding and burnishing processes on 3D printed stainless steel workpieces. Miskolci Egyetem Gyártástudományi Intézet, pp 189-196 (2024), ISBN: 9789633583524

[FTK8]. Kebede, Frezgi Tesfom, and Csaba Felhő. Analysis of topographic change by slide burnishing of C45 steel surface milled with variable number of inserts. DOI: https://doi.org/10.35925/j.multi.2024.3.4

[FTK9]. Kebede, Frezgi Tesfom, and Csaba Felho. Transforming Burnishing Techniques: A Novel Method to Enhance Efficiency and Surface Quality Through Tool Feed Variation. Journal of Manufacturing and Materials Processing 9.3 (2025): 71. DOI: https://doi.org/10.3390/jmmp9030071, Scopus Indexed

[FTK10]. Kebede, F. T., Felho, C., & Sztankovics, I. (2025). Improving Surface Roughness of 42CrMo4 Low Alloy Steel Shafts by Applying Varying Feed in the Multi-Pass Slide Burnishing Process. *Applied Sciences (2076-3417)*, *15*(16).

9. REFERENCES

[1] A. Travieso-Disotuar, R. Jerez-Mesa, M. Vilaseca, and J. A. Travieso-Rodriguez, "Surface integrity enhancement through vibration-assisted ball burnishing of maraging steel produced by selective laser melting," *Journal of Materials Research and Technology*, vol. 39, pp. 493–505, Nov. 2025, doi: 10.1016/J.JMRT.2025.09.078.

[2] J. Maximov and G. Duncheva, "Effects of diamond burnishing on surface integrity, fatigue, wear, and corrosion of metal components—review and perspectives," *International Journal of Advanced Manufacturing Technology*, vol. 139, no. 9, pp. 4233–4267, Aug. 2025, doi: 10.1007/S00170-025-16158-7/FIGURES/19.

[3] S. C. Cagan and K. Leksycki, "Analysis of Surface Roughness After Ball Burnishing of Pure Titanium Under Environmentally Friendly Conditions," *Applied Sciences 2025, Vol. 15, Page 1746*, vol. 15, no. 4, p. 1746, Feb. 2025, doi: 10.3390/APP15041746.

[4] J. Maximov and G. Duncheva, "The Correlation between Surface Integrity and Operating Behaviour of Slide Burnished Components—A Review and Prospects," *Applied Sciences 2023, Vol. 13, Page 3313*, vol. 13, no. 5, p. 3313, Mar. 2023, doi: 10.3390/APP13053313.

[5] W. Schütz, "The prediction of fatigue life in the crack initiation and propagation stages—a state of the art survey," *Eng Fract Mech*, vol. 11, no. 2, pp. 405–421, Jan. 1979, doi: 10.1016/0013-7944(79)90015-8.

[6] D.A. Wallace, "Burnishing apparatus," Pat. 2222270, 1940

[7] J. T. Maximov, G. V. Duncheva, A. P. Anchev, and M. D. Ichkova, "Slide burnishing—review and prospects," *International Journal of Advanced Manufacturing Technology*, vol. 104, no. 1–4, pp. 785–801, Sep. 2019, doi: 10.1007/S00170-019-03881-1/FIGURES/18.

[8] E. Becerra-Becerra, C. O. Aguilera Ojeda, A. Saldaña-Robles, J. F. Reveles-Arredondo, J. Barco-Burgos, and A. Vidal-Lesso, "A review of numerical simulation of ball burnishing process," *Finite Elements in Analysis and Design*, vol. 218, p. 103926, Jun. 2023, doi: 10.1016/J.FINEL.2023.103926.

[9] "Ecoroll Catalogue 'Tools and Solutions for Metal Surface Improvement,'" USA, 2006.

[10] W. Zielecki, M. Bucior, T. Trzepiecinski, and K. Ochał, "Effect of slide burnishing of shoulder fillets on the fatigue strength of X19NiCrMo4 steel shafts," *International Journal of Advanced Manufacturing Technology*, vol. 106, no. 5–6, pp. 2583–2593, Jan. 2020, doi: 10.1007/S00170-019-04815-7/FIGURES/16.

[11] E. Hull and A. Nerad, "Irregular surface diamond burnishing tool," 2966722A, Jan. 03, 1961 [Online]. Available: https://patents.google.com/patent/US2966722A/en

[12] T. Dyl, M. Wijata, and W. Kuśmierska-Matyszczak, "The slide broaching burnishing and the influence of deformation on roughness of 314L stainless steel sleeves," *Scientific Journal of Gdynia Maritime University*, no. 116, pp. 15–28, Dec. 2020, doi: 10.26408/116.02.

[13] R. Jerez-Mesa, J. A. Travieso-Rodriguez, G. Gomez-Gras, and J. Lluma-Fuentes, "Development, characterization and test of an ultrasonic vibration-assisted ball burnishing tool," *J Mater Process Technol*, vol. 257, pp. 203–212, Jul. 2018, doi: 10.1016/J.JMATPROTEC.2018.02.036.

[14] A. V. Kozlov, B. N. Mordyuk, and A. V. Chernyashevsky, "On the additivity of acoustoplastic and electroplastic effects," *Materials Science and Engineering: A*, vol. 190, no. 1–2, pp. 75–79, Jan. 1995, doi: 10.1016/0921-5093(94)09588-N.

[15] R. Ón Jerez-Mesa *et al.*, "Vibration-Assisted Ball Burnishing," *Encyclopedia 2021, Vol. 1, Pages 460-471*, vol. 1, no. 2, pp. 460–471, Jun. 2021, doi: 10.3390/ENCYCLOPEDIA1020038.

[16] R. Jerez-Mesa, J. A. Travieso-Rodríguez, Y. Landon, G. Dessein, J. Lluma-Fuentes, and V. Wagner, "Comprehensive analysis of surface integrity modification of ball-end milled Ti-6Al-

4V surfaces through vibration-assisted ball burnishing," *J Mater Process Technol*, vol. 267, pp. 230–240, May 2019, doi: 10.1016/J.JMATPROTEC.2018.12.022.

[17] N. Xu, X. Jiang, X. Shen, and H. Peng, "Improving the Surface Integrity and Tribological Behavior of a High-Temperature Friction Surface via the Synergy of Laser Cladding and Ultrasonic Burnishing," *Lubricants 2023, Vol. 11, Page 379*, vol. 11, no. 9, p. 379, Sep. 2023, doi: 10.3390/LUBRICANTS11090379.

[18] Y. Jeon and C. M. Lee, "Current research trend on laser assisted machining," *International Journal of Precision Engineering and Manufacturing*, vol. 13, no. 2, pp. 311–317, Feb. 2012, doi: 10.1007/S12541-012-0040-4.

[19] X. Chen, Y. Zhang, and A. Li, "Laser Processing and Multi-Energy Field Manufacturing of High-Performance Materials," *Materials*, vol. 16, no. 17, p. 5991, Aug. 2023, doi: 10.3390/MA16175991.

[20] Z. F. Kovács, Z. J. Viharos, and J. Kodácsy, "Improvements of surface tribological properties by magnetic assisted ball burnishing," *Surf Coat Technol*, vol. 437, p. 128317, May 2022, doi: 10.1016/J.SURFCOAT.2022.128317.

[21] Zsolt Kovács, Zsolt János Viharos, and János Kodácsy, "The effects of machining strategies of magnetic assisted roller burnishing on the resulted surface structure Optimization of Burnishing process by Taguchi method for surface enhancement of EN31 steel", doi: 10.1088/1757-899X/448/1/012002.

[22] D. F. Silva-Álvarez *et al.*, "Improving the surface integrity of the CoCrMo alloy by the ball burnishing technique," *Journal of Materials Research and Technology*, vol. 9, no. 4, pp. 7592–7601, Jul. 2020, doi: 10.1016/J.JMRT.2020.05.038.

[23] N. S. M. El-Tayeb, K. O. Low, and P. V. Brevern, "Influence of roller burnishing contact width and burnishing orientation on surface quality and tribological behaviour of Aluminium 6061," *J Mater Process Technol*, vol. 186, no. 1–3, pp. 272–278, May 2007, doi: 10.1016/J.JMATPROTEC.2006.12.044.

[24] A. Saldaña-Robles, J. Á. D. De La Peña, A. De Jesús Balvantín-García, E. Aguilera-Gómez, H. Plascencia-Mora, and N. Saldaña-Robles, "Ball burnishing process: State of the art of a technology in development," *Dyna (Spain)*, vol. 92, no. 1, pp. 28–33, Jan. 2017, doi: 10.6036/7916.

[25] F. J. Shiou and C. H. Chen, "Freeform surface finish of plastic injection mold by using ball-burnishing process," *J Mater Process Technol*, vol. 140, no. 1–3, pp. 248–254, Sep. 2003, doi: 10.1016/S0924-0136(03)00750-7.

[26] N. J. Varpe and R. Tajane, "Overview of Burnishing Process as a Surface Improvement Technique," *Manufacturing Strategies and Systems Technologies, Processes, and Machine Tools*, pp. 234–266, Jan. 2025, doi: 10.1201/9781032725086-16/OVERVIEW-BURNISHING-PROCESS-SURFACE-IMPROVEMENT-TECHNIQUE-NITIN-JALINDAR-VARPE-RAVINDRA-TAJANE.

[27] G. V. Duncheva *et al.*, "Improvement in surface integrity of CuAl8Fe3 bronze via diamond burnishing," *International Journal of Advanced Manufacturing Technology*, vol. 119, no. 9–10, pp. 5885–5902, Apr. 2022, doi: 10.1007/S00170-022-08664-9/FIGURES/14.

[28] B. Sachin, S. Narendranath, and D. Chakradhar, "Application of Desirability Approach to Optimize the Control Factors in Cryogenic Diamond Burnishing," *Arab J Sci Eng*, vol. 45, no. 2, pp. 1305–1317, Feb. 2020, doi: 10.1007/S13369-019-04326-3/FIGURES/13.

[29] J. T. Maximov, G. V. Duncheva, A. P. Anchev, and V. P. Dunchev, "Slide burnishing versus deep rolling—a comparative analysis," *International Journal of Advanced Manufacturing*

Technology, vol. 110, no. 7–8, pp. 1923–1939, Sep. 2020, doi: 10.1007/S00170-020-05950-2/FIGURES/15.

[30] T. Dyl, D. Rydz, A. Szarek, G. Stradomski, J. Fik, and M. Opydo, "The Influence of Slide Burnishing on the Technological Quality of X2CrNiMo17-12-2 Steel," *Materials 2024, Vol. 17, Page 3403*, vol. 17, no. 14, p. 3403, Jul. 2024, doi: 10.3390/MA17143403.

[31] K. Zaleski and A. Skoczylas, "EFFECT OF SLIDE BURNISHING ON THE SURFACE LAYER AND FATIGUE LIFE OF TITANIUM ALLOY PARTS," *ADVANCES IN MATERIALS SCIENCE*, vol. 19, no. 4, 2019, doi: 10.2478/adms-2019-0020.

[32] A. Rodríguez, L. N. López de Lacalle, A. Celaya, A. Lamikiz, and J. Albizuri, "Surface improvement of shafts by the deep ball-burnishing technique," *Surf Coat Technol*, vol. 206, no. 11–12, pp. 2817–2824, Feb. 2012, doi: 10.1016/J.SURFCOAT.2011.11.045.

[33] P. R. Babu, K. Ankamma, T. S. Prasad, A. V. S. Raju, and N. E. Prasad, "Optimization of burnishing parameters and determination of select surface characteristics in engineering materials," *Sadhana - Academy Proceedings in Engineering Sciences*, vol. 37, no. 4, pp. 503–520, Sep. 2012, doi: 10.1007/S12046-012-0092-2/TABLES/10.

[34] M. Keymanesh, H. Ji, X. Zhang, J. Wang, P. Feng, and J. Zhang, "Multi-roller taper burnishing of internal chamfers and its enhancement mechanism on 7050 aluminum alloy," *Int J Fatigue*, vol. 189, p. 108571, Dec. 2024, doi: 10.1016/J.IJFATIGUE.2024.108571.

[35] M. Okada, S. Suenobu, K. Watanabe, Y. Yamashita, and N. Asakawa, "Development and burnishing characteristics of roller burnishing method with rolling and sliding effects," *Mechatronics*, vol. 29, pp. 110–118, Aug. 2015, doi: 10.1016/J.MECHATRONICS.2014.11.002.

[36] T. Morimoto, "Examination of the burnishing process using a newly-designed tool," *Journal of Mechanical Working Technology*, vol. 13, no. 3, pp. 257–272, Oct. 1986, doi: 10.1016/0378-3804(86)90018-5.

[37] M. Okada, H. Nakagawa, M. Nikawa, and S. Kitagawa, "Texture Formation and Surface Characteristics in an Intermittent Burnishing Process Utilizing Plastic Flow of Surface Material," *Nanomanufacturing and Metrology*, vol. 8, no. 1, pp. 1–12, Dec. 2025, doi: 10.1007/S41871-025-00266-9/FIGURES/17.

[38] H. Basak and H. H. Goktas, "Burnishing process on al-alloy and optimization of surface roughness and surface hardness by fuzzy logic," *Mater Des*, vol. 30, no. 4, pp. 1275–1281, Apr. 2009, doi: 10.1016/J.MATDES.2008.06.063.

[39] A. M. Hassan and A. S. Al-Bsharat, "Improvements in some properties of non-ferrous metals by the application of the ball-burnishing process," *J Mater Process Technol*, vol. 59, no. 3, pp. 250–256, May 1996, doi: 10.1016/0924-0136(95)02149-3.

[40] A. Sagbas, "Analysis and optimization of surface roughness in the ball burnishing process using response surface methodology and desirabilty function," *Advances in Engineering Software*, vol. 42, no. 11, pp. 992–998, Nov. 2011, doi: 10.1016/J.ADVENGSOFT.2011.05.021.

[41] L. Hiegemann, C. Weddeling, N. Ben Khalifa, and A. E. Tekkaya, "Analytical Prediction of Roughness after Ball Burnishing of Thermally Coated Surfaces," *Procedia Eng*, vol. 81, pp. 1921–1926, Jan. 2014, doi: 10.1016/J.PROENG.2014.10.257.

[42] M. H. El-Axir, "An investigation into roller burnishing," *Int J Mach Tools Manuf*, vol. 40, no. 11, pp. 1603–1617, Sep. 2000, doi: 10.1016/S0890-6955(00)00019-5.

[43] A. M. Hassan and A. M. Maqableh, "The effects of initial burnishing parameters on non-ferrous components," *J Mater Process Technol*, vol. 102, no. 1–3, pp. 115–121, May 2000, doi: 10.1016/S0924-0136(00)00464-7.

[44] D. Grochała, S. Berczyński, and Z. Grzadziel, “Analysis of surface geometry changes after hybrid milling and burnishing by ceramic ball,” *Materials*, vol. 12, no. 7, 2019, doi: 10.3390/ma12071179.

[45] W. Zhang, H. Dong, Y. Li, C. Yang, and H. Xue, “Combining turning with slide burnishing to improve surface integrity and stress corrosion resistance,” *J Manuf Process*, vol. 107, pp. 16–33, Dec. 2023, doi: 10.1016/j.jmapro.2023.10.041.

[46] Y. Charfeddine, S. Youssef, S. Sghaier, and H. Hamdi, “Finite Element Residual Stress Computation for Combined Grinding/Burnishing Applied to 100Cr6 Steel,” *Lecture Notes in Mechanical Engineering*, vol. 1, pp. 131–137, 2021, doi: 10.1007/978-3-030-52071-7_19.

[47] D. J. . Whitehouse, *Surfaces and their measurement*, 1st ed., vol. 1. London, UK: Taylor & Francis, 2002.

[48] X. Tian, Y. Sun, W. Mu, L. Xia, and J. Han, “High-Speed and Low-Noise Gear Finishing by Gear Grinding and Honing: A Review,” *Chinese Journal of Mechanical Engineering (English Edition)*, vol. 37, no. 1, pp. 1–21, Dec. 2024, doi: 10.1186/S10033-024-01078-6/FIGURES/23.

[49] M. Uddin, R. Santifoller, C. Hall, and T. Schlaefer, “A Grinding-Burnishing Approach to Enhancing Surface Integrity, Tribological, and Corrosion Behavior of Laser-Cladded AISI 431 Alloys,” *Journal of Manufacturing Science and Engineering, Transactions of the ASME*, vol. 144, no. 7, Jul. 2022, doi: 10.1115/1.4052929/1123770.

[50] R. Karthick Raaj *et al.*, “Exploring grinding and burnishing as surface post-treatment options for electron beam additive manufactured Alloy 718,” *Surf Coat Technol*, vol. 397, p. 126063, Sep. 2020, doi: 10.1016/J.SURFCOAT.2020.126063.

[51] Y. Charfeddine, S. Youssef, S. Sghaier, J. Sghaier, and H. Hamdi, “Study of the simultaneous Grinding/Ball-burnishing of AISI 4140 based on finite element simulations and experiments,” *Int J Mech Sci*, vol. 192, p. 106097, Feb. 2021, doi: 10.1016/J.IJMECSCI.2020.106097.

[52] M. Arsalani, M. R. Razfar, A. Abdullah, and M. Khajehzadeh, “Fatigue behavior improvement of hardened parts using sequential hard turning, grinding, and ball burnishing operations,” *Proceedings of the Institution of Mechanical Engineers, Part L: Journal of Materials: Design and Applications*, vol. 235, no. 1, pp. 87–99, Jan. 2021, doi: 10.1177/1464420720951889;CTYPE:STRING:JOURNAL.

[53] H. Amdouni *et al.*, “Experimental study of a six new ball-burnishing strategies effects on the Al-alloy flat surfaces integrity enhancement,” *International Journal of Advanced Manufacturing Technology*, vol. 90, no. 5–8, pp. 2271–2282, May 2017, doi: 10.1007/S00170-016-9529-9/METRICS.

[54] L. N. López De Lacalle, A. Lamikiz, J. Muñoa, and J. A. Sánchez, “Quality improvement of ball-end milled sculptured surfaces by ball burnishing,” *Int J Mach Tools Manuf*, vol. 45, no. 15, pp. 1659–1668, Dec. 2005, doi: 10.1016/J.IJMACHTOOLS.2005.03.007.

[55] J. Kalisz, K. Żak, S. Wojciechowski, M. K. Gupta, and G. M. Krolczyk, “Technological and tribological aspects of milling-burnishing process of complex surfaces,” *Tribol Int*, vol. 155, p. 106770, Mar. 2021, doi: 10.1016/J.TRIBOINT.2020.106770.

[56] M. T. Le, A. Le Van, and T. T. Nguyen, “Performance optimization of multi-roller flat burnishing process in terms of surface properties,” *Journal of Machine Engineering*, vol. Vol. 23, No. 2, no. 2, pp. 159–173, 2023, doi: 10.36897/JME/161661.

[57] B. Sachin, S. Narendranath, and D. Chakradhar, “Application of Desirability Approach to Optimize the Control Factors in Cryogenic Diamond Burnishing,” *Arab J Sci Eng*, vol. 45, no. 2, pp. 1305–1317, Feb. 2020, doi: 10.1007/S13369-019-04326-3/FIGURES/13.

[58] J. Zaghal, V. Molnár, and M. Benke, “Improving surface integrity by optimizing slide diamond burnishing parameters after hard turning of 42CrMo4 steel,” *International Journal of Advanced*

Manufacturing Technology, vol. 128, no. 5–6, pp. 2087–2103, Sep. 2023, doi: 10.1007/S00170-023-12008-6/TABLES/11.

[59] J. T. Maximov, G. V. Duncheva, A. P. Anchev, N. Ganev, I. M. Amudjev, and V. P. Dunchev, "Effect of slide burnishing method on the surface integrity of AISI 316Ti chromium–nickel steel," *Journal of the Brazilian Society of Mechanical Sciences and Engineering*, vol. 40, no. 4, pp. 1–14, Apr. 2018, doi: 10.1007/S40430-018-1135-3/FIGURES/17.

[60] R. Kluz, K. Antosz, T. Trzepieciński, and M. Bucior, "Modelling the Influence of Slide Burnishing Parameters on the Surface Roughness of Shafts Made of 42CrMo4 Heat-Treatable Steel," *Materials 2021, Vol. 14, Page 1175*, vol. 14, no. 5, p. 1175, Mar. 2021, doi: 10.3390/MA14051175.

[61] J. T. Maximov, A. P. Anchev, G. V. Duncheva, N. Ganev, and K. F. Selimov, "Influence of the process parameters on the surface roughness, micro-hardness, and residual stresses in slide burnishing of high-strength aluminum alloys," *Journal of the Brazilian Society of Mechanical Sciences and Engineering*, vol. 39, no. 8, pp. 3067–3078, Aug. 2017, doi: 10.1007/S40430-016-0647-Y/FIGURES/13.

[62] C. Felhő, F. Tesfom, and G. Varga, "ANOVA Analysis and L9 Taguchi Design for Examination of Flat Slide Burnishing of Unalloyed Structural Carbon Steel," *Journal of Manufacturing and Materials Processing 2023, Vol. 7, Page 136*, vol. 7, no. 4, p. 136, Jul. 2023, doi: 10.3390/JMMP7040136.

[63] A. M. Hassan, H. F. Al-Jalu, and A. A. Ebied, "Burnishing force and number of ball passes for the optimum surface finish of brass components," *J Mater Process Technol*, vol. 83, no. 1–3, pp. 176–179, Nov. 1998, doi: 10.1016/S0924-0136(98)00058-2.

[64] M. Santhanakrishnan, P. S. Sivasakthivel, and R. Sudhakaran, "Modeling of geometrical and machining parameters on temperature rise while machining Al 6351 using response surface methodology and genetic algorithm," *Journal of the Brazilian Society of Mechanical Sciences and Engineering*, vol. 39, no. 2, pp. 487–496, Feb. 2017, doi: 10.1007/S40430-015-0378-5/FIGURES/7.

[65] M. Salahshoor and Y. B. Guo, "Process mechanics in ball burnishing biomedical magnesium-calcium alloy," *International Journal of Advanced Manufacturing Technology*, vol. 64, no. 1–4, pp. 133–144, Jan. 2013, doi: 10.1007/S00170-012-4024-4/METRICS.

[66] M. Posdzich, R. Stöckmann, M. Witt, and M. Putz, "Determination of surface shape deviation by using force-controlled burnishing," *Procedia CIRP*, vol. 93, pp. 1275–1280, Jan. 2020, doi: 10.1016/J.PROCIR.2020.04.095.

[67] Z. Zhen-yu, Z. Qiu-yang, D. Cong, Y. Ju-yu, P. Guang-jian, and P. Zhong-yu, "Research on the promotion mechanism of surface burnishing process by two-dimensional ultrasonic vibration," *Journal of Materials Research and Technology*, vol. 13, pp. 1068–1082, Jul. 2021, doi: 10.1016/J.JMRT.2021.05.038.

[68] C. Felhő and G. Varga, "2D FEM Investigation of Residual Stress in Diamond Burnishing," *Journal of Manufacturing and Materials Processing 2022, Vol. 6, Page 123*, vol. 6, no. 5, p. 123, Oct. 2022, doi: 10.3390/JMMP6050123.

[69] J. Caudill, B. Huang, C. Arvin, J. Schoop, K. Meyer, and I. S. Jawahir, "Enhancing the Surface Integrity of Ti-6Al-4V Alloy through Cryogenic Burnishing," *Procedia CIRP*, vol. 13, pp. 243–248, Jan. 2014, doi: 10.1016/J.PROCIR.2014.04.042.

[70] M. H. El-Axir, "An investigation into roller burnishing," *Int J Mach Tools Manuf*, vol. 40, no. 11, pp. 1603–1617, Sep. 2000, doi: 10.1016/S0890-6955(00)00019-5.

[71] H. Roohi, H. Baseri, and M. J. Mirnia, “Experimental Study of Slide Burnishing Process of the Pre-milled AA7075 Plate: Surface Topography and Hardening Aspects,” *Arab J Sci Eng*, pp. 1–21, Nov. 2024, doi: 10.1007/S13369-024-09784-Y/FIGURES/6.

[72] M. Okada, H. Kozuka, H. Tachiya, T. Iwasaki, and Y. Yamashita, “Burnishing Process Using Spherical 5-DOF Hybrid-Type Parallel Mechanism with Force Control,” *International Journal of Automation Technology*, vol. 8, no. 2, pp. 243–252, Mar. 2014, doi: 10.20965/IJAT.2014.P0243.

[73] P. Karolczak and M. Tomov, “Analysis of the Influence of the Number of Burnishing Passes on the Geometric Structure of Aluminium Composites Surface,” *Tehnički vjesnik*, vol. 30, no. 2, pp. 441–449, Feb. 2023, doi: 10.17559/TV-20220803122813.

[74] H. Roohi, H. Baseri, and M. J. Mirnia, “Evaluation of optimized surface characteristics in non-rotational sliding ball burnishing,” *Materials and Manufacturing Processes*, vol. 39, no. 16, pp. 2299–2308, Dec. 2024, doi: 10.1080/10426914.2024.2395010.

[75] A. Nagy and G. Varga, “ANALYZING THE EFFECT OF THE TOOL PASS NUMBER AND THE DIRECTION OF SLIDING BURNISHING ON SURFACE ROUGHNESS,” *Cutting & Tools in Technological System*, no. 97, pp. 70–82, Nov. 2022, doi: 10.20998/2078-7405.2022.97.06.

[76] R. Teimouri and S. Amini, “A comprehensive optimization of ultrasonic burnishing process regarding energy efficiency and workpiece quality,” *Surf Coat Technol*, vol. 375, pp. 229–242, Oct. 2019, doi: 10.1016/J.SURFCOAT.2019.07.038.

[77] G. Gomez–Gras, J. A. Travieso–Rodriguez, R. Jerez–Mesa, J. Lluma-Fuentes, and B. Gomis de la Calle, “Experimental study of lateral pass width in conventional and vibrations-assisted ball burnishing,” *International Journal of Advanced Manufacturing Technology*, vol. 87, no. 1–4, pp. 363–371, Oct. 2016, doi: 10.1007/S00170-016-8490-Y/METRICS.

[78] M. Bourebia, L. Laouar, H. Hamadache, and S. Dominiak, “Improvement of surface finish by ball burnishing: approach by fractal dimension,” *https://doi.org/10.1080/02670844.2016.1232778*, vol. 33, no. 4, pp. 255–262, Apr. 2017, doi: 10.1080/02670844.2016.1232778.

[79] S. Polanowski and W. Labuda, “Experimental study on the influence of burnish parameters on the surface roughness reduction index,” *Journal of KONES*, vol. Vol. 23, No. 3, 2016, doi: 10.5604/12314005.1216386.

[80] P. Kumara and G. K. Purohit, “Investigations on Effect of Different Ball Burnishing Conditions on Surface Roughness Using Response Surface Methodology,” *Journal of Modern Manufacturing Systems and Technology*, vol. 2, pp. 51–60, Mar. 2019, doi: 10.15282/JMMST.V2I1.1800.

[81] H. Amdouni, H. Bouzaiene, A. Montagne, M. Nasri, and A. Iost, “Modeling and optimization of a ball-burnished aluminum alloy flat surface with a crossed strategy based on response surface methodology,” *International Journal of Advanced Manufacturing Technology*, vol. 88, no. 1–4, pp. 801–814, Jan. 2017, doi: 10.1007/S00170-016-8817-8/METRICS.

[82] D. Herzog, V. Seyda, E. Wycisk, and C. Emmelmann, “Additive manufacturing of metals,” *Acta Mater*, vol. 117, pp. 371–392, Sep. 2016, doi: 10.1016/J.ACTAMAT.2016.07.019.

[83] D. M. Hajare and T. S. Gajbhiye, “Additive manufacturing (3D printing): Recent progress on advancement of materials and challenges”, doi: 10.1016/j.matpr.2022.02.391.

[84] S. Rathee, M. Srivastava, P. M. Pandey, A. Mahawar, and S. Shukla, “Metal additive manufacturing using friction stir engineering: A review on microstructural evolution, tooling and design strategies,” *CIRP J Manuf Sci Technol*, vol. 35, pp. 560–588, Nov. 2021, doi: 10.1016/J.CIRPJ.2021.08.003.

[85] S. Ghosh, J. Zollinger, M. Zaloznik, D. Banerjee, C. K. Newman, and R. Arroyave, “Modeling of hierarchical solidification microstructures in metal additive manufacturing: Challenges and opportunities,” *Addit Manuf*, vol. 78, p. 103845, Sep. 2023, doi: 10.1016/J.ADDMA.2023.103845.

[86] B. Qi *et al.*, “Surface integrity improvement of the ground surface of Inconel 718 fabricated by forging and additive manufacturing using a robotic rotational burnishing method,” *J Manuf Process*, vol. 125, pp. 566–579, Sep. 2024, doi: 10.1016/J.JMAPRO.2024.07.083.

[87] R. Deltombe, K. J. Kubiak, and M. Bigerelle, “How to select the most relevant 3D roughness parameters of a surface,” *Scanning*, vol. 36, no. 1, pp. 150–160, Jan. 2014, doi: 10.1002/SCA.21113;PAGEGROUP:STRING:PUBLICATION.

[88] E. S. Gadelmawla, M. M. Koura, T. M. A. Maksoud, I. M. Elewa, and H. H. Soliman, “Roughness parameters,” *J Mater Process Technol*, vol. 123, no. 1, pp. 133–145, Apr. 2002, doi: 10.1016/S0924-0136(02)00060-2.

[89] C. Sahay and G. Suhash, “Understanding Surface Quality: Beyond Average Roughness (Ra),” *American Society for Engineering Education*, vol. 1, 2018.

[90] J. Maximov, G. Duncheva, A. Anchev, V. Dunchev, K. Anastasov, and P. Daskalova, “Effect of Roller Burnishing and Slide Roller Burnishing on Surface Integrity of AISI 316 Steel: Theoretical and Experimental Comparative Analysis,” *Machines 2024, Vol. 12, Page 51*, vol. 12, no. 1, p. 51, Jan. 2024, doi: 10.3390/MACHINES12010051.

[91] A. Skoczylas, K. Zaleski, J. Matuszak, K. Ciecieląg, R. Zaleski, and M. Gorgol, “Influence of Slide Burnishing Parameters on the Surface Layer Properties of Stainless Steel and Mean Positron Lifetime,” *Materials 2022, Vol. 15, Page 8131*, vol. 15, no. 22, p. 8131, Nov. 2022, doi: 10.3390/MA15228131.

[92] M. Korzynski and T. Zarski, “Slide diamond burnishing influence on of surface stereometric structure of an AZ91 alloy,” *Surf Coat Technol*, vol. 307, no. Part A, pp. 590–595, Dec. 2016, doi: 10.1016/J.SURFCOAT.2016.09.045.

[93] J. Kalisz, K. Żak, S. Wojciechowski, M. K. Gupta, and G. M. Krolczyk, “Technological and tribological aspects of milling-burnishing process of complex surfaces,” *Tribol Int*, vol. 155, p. 106770, Mar. 2021, doi: 10.1016/J.TRIBOINT.2020.106770.

[94] R. Teimouri, M. Grabowski, M. Kowalczyk, and S. Skoczypiec, “Simulation of surface roughness alternation in milling-burnishing sequence,” *Measurement*, vol. 218, p. 113160, Aug. 2023, doi: 10.1016/J.MEASUREMENT.2023.113160.

[95] Oerlikon metco, “Order METCOADD 17-4PH-A Additive Manufacturing Powder Online at myMetco.” Accessed: Dec. 07, 2023. [Online]. Available: https://mymetco-europe.oerlikon.com/en-us/product/metcoadd174pha?isRegionSelection

[96] J. Villegas-Tovar *et al.*, “Electrochemical Corrosion Behavior of Passivated Precipitation Hardening Stainless Steels for Aerospace Applications,” *Metals 2023, Vol. 13, Page 835*, vol. 13, no. 5, p. 835, Apr. 2023, doi: 10.3390/MET13050835.

[97] R. Stöckmann, M. Posdzich, P. Klimant, and M. Putz, “Influence of the stiffness of burnishing tools on process force and surface quality of EN AW-2007 and C45 workpieces,” *Procedia Manuf*, vol. 43, pp. 635–641, Jan. 2020, doi: 10.1016/J.PROMFG.2020.02.142.

[98] A. Skoczylas and K. Zaleski, “Studies on the selected properties of C45 steel elements surface layer after laser cutting, finishing milling and burnishing,” *Advances in Science and Technology. Research Journal*, vol. Vol. 10, no. nr 32, pp. 118–123, Dec. 2016, doi: 10.12913/22998624/65127.

[99] A. Vazdirvanidis, G. Pantazopoulos, and A. Louvaris, “Failure analysis of a hardened and tempered structural steel (42CrMo4) bar for automotive applications,” *Eng Fail Anal*, vol. 16, no. 4, pp. 1033–1038, Jun. 2009, doi: 10.1016/J.ENGFAILANAL.2008.05.006.

[100] P. Singh, U. Batra, and S. Sangal, “Fracture Toughness Behavior of 38MnSiVS5 Microalloyed Steel After Isothermal Transformation and Thermomechanical Processing,” *Mater Today Proc*, vol. 4, no. 8, pp. 8528–8537, Jan. 2017, doi: 10.1016/J.MATPR.2017.07.199.

[101] “42CrMo4 Alloy Steel, BS EN 10250 Engineering Steel.” Accessed: Sep. 09, 2025. [Online]. Available: https://www.astmsteel.com/product/42crmo4-alloy-steel/

[102] V. Barahate, A. R. Govande, G. Tiwari, B. R. Sunil, and R. Dumpala, “Parameter optimization during single roller burnishing of AA6061-T6 alloy by design of experiments,” *Mater Today Proc*, vol. 50, pp. 1967–1970, Jan. 2022, doi: 10.1016/J.MATPR.2021.09.328.

[103] H. P. Pathade *et al.*, “A Review on Surface Integrity of Ball Burnishing Process,” *International Journal of Research Publication and Reviews*, pp. 137–151, Oct. 2022, doi: 10.55248/gengpi.2022.3.10.3.

[104] M. Raza, Z. Alam, and A. D. Udai, “ISO Standardized Form Removal and Filtering of Surface Texture for Areal Surface Roughness Measurement Using Zygo Mx,” *Mapan - Journal of Metrology Society of India*, pp. 1–6, Aug. 2025, doi: 10.1007/S12647-025-00844-8/TABLES/1.

[105] G. Varga, G. Dezső, and F. Szigeti, “Surface Roughness Improvement by Sliding Friction Burnishing of Parts Produced by Selective Laser Melting of Ti6Al4V Titanium Alloy,” *Machines 2022, Vol. 10, Page 400*, vol. 10, no. 5, p. 400, May 2022, doi: 10.3390/MACHINES10050400.

[106] G. Gomez–Gras, J. A. Travieso–Rodriguez, R. Jerez–Mesa, J. Lluma-Fuentes, and B. Gomis de la Calle, “Experimental study of lateral pass width in conventional and vibrations-assisted ball burnishing,” *International Journal of Advanced Manufacturing Technology*, vol. 87, no. 1–4, pp. 363–371, Oct. 2016, doi: 10.1007/S00170-016-8490-Y/METRICS.

[107] T. T. Nguyen and L. H. Cao, “Optimization of the Burnishing Process for Energy Responses and Surface Properties,” *International Journal of Precision Engineering and Manufacturing*, vol. 21, no. 6, pp. 1143–1152, Jun. 2020, doi: 10.1007/S12541-020-00326-8/TABLES/6.

[108] E. Velázquez-Corral, A. Travieso-Disotuar, R. Jerez-Mesa, M. Vilaseca, C. Keller, and G. Dessein, “Roughness and microstructure characterization of AISI 316L laser-powder bed fusion specimens after applying a vibration-assisted ball burnishing process,” *Journal of Materials and Manufacturing*, vol. 3, no. 2, pp. 32–40, Dec. 2024, doi: 10.5281/ZENODO.14274784.

[109] S. Swirad, “Changes in Areal Surface Textures Due to Ball Burnishing,” *Materials 2023, Vol. 16, Page 5904*, vol. 16, no. 17, p. 5904, Aug. 2023, doi: 10.3390/MA16175904.

[110] D. Lesyk *et al.*, “Enhancing the Surface Integrity of a Laser Powder Bed Fusion Inconel 718 Alloy by Tailoring the Microstructure and Microrelief Using Various Finishing Methods,” *Coatings 2025, Vol. 15, Page 425*, vol. 15, no. 4, p. 425, Apr. 2025, doi: 10.3390/COATINGS15040425.

[111] C. Li, Z. Y. Liu, X. Y. Fang, and Y. B. Guo, “Residual Stress in Metal Additive Manufacturing,” *Procedia CIRP*, vol. 71, pp. 348–353, Jan. 2018, doi: 10.1016/J.PROCIR.2018.05.039.

[112] R. Teimouri, S. Amini, and A. B. Bami, “Evaluation of optimized surface properties and residual stress in ultrasonic assisted ball burnishing of AA6061-T6,” *Measurement*, vol. 116, pp. 129–139, Feb. 2018, doi: 10.1016/J.MEASUREMENT.2017.11.001.

10. APPENDIX

Table 12. Measured roughness parameters and mechanical properties of 3D printed MetcoAdd 17-4PH-A.

Surf. No.	Sa [µm]	Ssk	Sku	Sk [µm]	Spk [µm]	Svk [µm]	σ-Trans [MPa]	σ-Long [MPa]	HV 0.2
1	0.37	-1.72	9.37	0.90	0.36	1.04	-784	-581	444
2	0.32	-1.75	11.10	0.81	0.34	0.82	-842	-581	433
3	0.34	-1.67	10.50	0.89	0.89	0.81	-890	-567	371
4	0.42	-2.00	12.60	0.86	0.34	1.10	-750	-578	423
5	0.38	-0.08	5.91	0.61	0.29	0.35	-847	-551	438
6	0.50	-1.76	9.56	1.07	0.52	1.32	-994	-609	451
7	0.32	-0.04	5.57	0.79	0.48	0.47	-680	-527	443
8	0.33	-0.93	8.21	0.34	0.48	0.66	-649	-560	457
9	0.22	-0.39	5.69	0.66	0.48	0.31	-802	-436	440
10	0.53	-0.62	5.61	1.23	0.57	0.57	-881	-500	425
11	0.65	-1.36	8.81	1.63	0.82	1.74	-933	-494	411
12	0.66	-1.20	8.51	1.74	0.80	1.54	-805	-532	420
13	0.61	-0.43	5.11	1.03	0.59	0.66	-984	-502	442
14	0.56	-0.54	5.04	1.22	0.56	0.72	-906	-561	424
15	0.54	-0.54	6.37	1.32	0.65	0.77	-896	-566	420
16	0.66	-0.94	7.34	1.78	0.86	1.46	-918	-498	445
Printed	11.30	-0.45	3.19	35.70	8.91	16.90	130	44	241
Ground	1.08	-0.21	3.82	3.29	1.37	1.64	-190	99	351

Table 13. Measured and calculated percentage change of milled and burnished C45 surfaces

Conventional Method												
Sur.No.	**Sa** [µm]	**% Δ Sa**	**Ssk**	**% Δ Ssk**	**Sku**	**% Δ Sku**	**Sk** [µm]	**% Δ Sk**	**Spk** [µm]	**% Δ Spk**	**Svk** [µm]	**% Δ Svk**
Milled	1.42		0.27		1.97		4.03		1.72		0.67	
O_1	0.55	-61.3	0.96	183.2	5.95	159.8	1.38	-65.8	1.42	-17.4	0.79	16.4
O_2	0.61	-57.4	0.33	-2.7	3.41	48.9	1.82	-54.8	0.85	-50.5	0.67	-1.0
O_3	0.54	-61.7	1.1	224.5	6.78	196.1	1.41	-65.0	1.43	-16.9	0.76	12.7
O_4	0.69	-51.3	0.58	71.1	4.53	97.8	2.09	-48.1	1.35	-21.5	0.81	19.1
O_5	1.05	-26.1	0.46	35.7	2.44	6.6	2.82	-30.0	1.60	-7.0	0.68	1.0
O_6	0.54	-62.0	1.05	209.7	6.37	178.2	1.33	-67.0	1.47	-14.5	0.77	14.3
O_7	0.64	-55.0	0.33	-2.7	3.81	66.4	2.02	-49.9	1.02	-40.7	0.74	9.8
O_8	1.04	-26.8	0.38	12.1	2.37	3.5	2.9	-28.0	1.46	-15.1	0.69	2.1
O_9	1.26	-11.3	0.22	-35.1	2.04	-10.9	3.73	-7.4	1.26	-26.7	0.69	1.3
O_10	0.49	-65.8	0.57	68.1	5.93	159.0	1.3	-67.7	1.09	-36.6	0.78	15.5
O_11	0.62	-56.1	0.07	-79.4	3.43	49.8	2.02	-49.9	0.80	-53.4	0.80	17.6
O_12	0.49	-65.8	0.33	-2.7	5.13	124.0	1.34	-66.7	0.92	-46.7	0.75	10.9
O_13	0.65	-54.6	0.36	6.2	3.67	60.3	1.97	-51.1	1.01	-41.3	0.75	11.5
O_14	0.98	-31.0	0.37	9.1	2.2	-3.9	2.6	-35.5	1.28	-25.6	0.64	-5.2
O_15	0.50	-65.1	0.49	44.5	5.1	122.7	1.38	-65.8	1.03	-40.1	0.75	10.5

O_16	0.73	-48.7	0.59	74.0	4.3	87.8	2.15	-46.7	1.34	-22.1	0.86	27.8
O_17	1.03	-27.5	0.29	-14.5	2.3	0.4	2.84	-29.5	1.23	-28.5	0.77	14.2
O_18	1.33	-6.3	0.29	-14.5	2.1	-8.3	3.8	-5.7	1.48	-14.0	0.77	13.9
O_19	0.49	-65.7	0.65	91.7	5	118.3	1.31	-67.5	1.31	-23.8	0.66	-2.1
O_20	0.61	-56.8	0.12	-64.6	3	31.0	1.88	-53.3	0.73	-57.6	0.71	4.7
O_21	0.50	-64.9	0.38	12.1	4.7	105.2	1.41	-65.0	0.94	-45.2	0.72	5.8
O_22	0.65	-54.4	0.17	-49.9	3.1	35.4	1.97	-51.1	0.81	-53.0	0.76	13.0
O_23	0.99	-30.4	0.31	-8.6	2.21	-3.5	2.71	-32.8	1.19	-30.8	0.70	2.8
O_24	0.48	-66.3	0.33	-2.7	4.91	114.4	1.29	-68.0	0.96	-44.4	0.77	13.8
O_25	0.66	-53.7	0.22	-35.1	3.54	54.6	1.94	-51.9	0.91	-47.0	0.83	22.0
O_26	0.98	-30.7	0.24	-29.2	2.24	-2.2	2.81	-30.3	1.06	-38.4	0.77	14.2
O_27	1.29	-9.2	0.32	-5.6	2.15	-6.1	3.55	-11.9	1.58	-8.1	0.78	14.6
Max.	1.33	-6.3	1.10	224.5	6.78	196.1	3.8	-5.7	1.60	-7.0	0.86	27.8
Min.	0.48	-66.3	0.07	-79.4	2.04	-10.9	1.29	-68.0	0.73	-57.6	0.64	-5.2
Ave.	0.75	-46.9	0.43	25.8	3.80	66.1	2.14	-46.9	1.17	-32.1	0.75	10.4
New Method												
N_1	0.42	-70.2	0.35	3.2	6.83	198.3	1.12	-72.2	0.92	-46.7	0.78	15.8
N_2	0.45	-68.2	0.36	7.1	5.68	148.0	1.22	-69.7	1.00	-41.9	0.81	19.7
N_3	0.49	-65.6	0.35	2.4	5.75	151.1	1.22	-69.7	1.00	-42.0	0.81	20.1
N_4	0.46	-68.0	0.10	-69.3	4.99	117.9	1.32	-67.2	0.83	-52.0	0.78	14.8
N_5	0.47	-66.9	0.15	-55.5	4.58	100.0	1.38	-65.8	0.81	-52.7	0.75	10.7
N_6	0.47	-66.8	0.29	-15.3	5.32	132.3	1.34	-66.7	0.92	-46.8	0.79	17.0
N_7	0.47	-66.6	0.15	-56.3	4.95	116.2	1.36	-66.3	0.89	-48.4	0.76	11.8
N_8	0.46	-67.3	0.23	-31.3	4.90	114.0	1.34	-66.7	0.87	-49.4	0.72	7.1
N_9	0.47	-66.8	0.19	-43.1	5.09	122.3	1.35	-66.5	0.91	-46.9	0.79	16.1
Max.	0.49	-65.6	0.36	7.1	6.83	198.3	1.38	-65.8	1.00	-41.9	0.81	20.1
Min.	0.46	-67.4	0.24	-28.7	5.34	133.3	1.29	-67.9	0.90	-47.4	0.78	14.8
Ave.	0.42	-70.2	0.10	-69.3	4.58	100.0	1.12	-72.2	0.81	-52.7	0.72	7.1

Table 14. Measured and calculated percentage change data of turned and burnished 42CrMo4 surfaces

Conventional Method												
Sur.No.	**Sa** [µm]	**% Δ Sa**	**Ssk**	**% Δ Ssk**	**Sku**	**% Δ Sku**	**Sk** [µm]	**% Δ Sk**	**Spk** [µm]	**% Δ Spk**	**Svk** [µm]	**% Δ Svk**
Turned	0.82		0.40		2.50		1.91		1.49		0.78	
O01	0.23	-72.0	-0.09	-122.5	2.9	16	0.7	-63.4	0.22	-85.2	0.27	-65.4
O02	0.45	-45.1	0.24	-40	2.09	-16.4	1.34	-29.8	0.46	-69.1	0.25	-67.9
O03	0.64	-22.0	-0.04	-110	1.74	-30.4	2.17	13.6	0.16	-89.3	0.31	-60.3
O04	0.53	-35.4	-0.11	-127.5	1.98	-20.8	1.8	-5.8	0.18	-87.9	0.31	-60.3
O05	0.38	-53.7	0	-100	2.79	11.6	1.2	-37.2	0.4	-73.2	0.4	-48.7
O06	0.46	-43.9	0.22	-45	2.11	-15.6	1.55	-18.8	0.36	-75.8	0.22	-71.8
O07	0.63	-23.2	0.06	-85	1.74	-30.4	1.99	4.2	0.32	-78.5	0.2	-74.4
O08	0.36	-56.1	-0.09	-122.5	2.43	-2.8	1.25	-34.6	0.25	-83.2	0.33	-57.7
O09	0.27	-67.1	-0.04	-110	2.73	9.2	0.86	-55.0	0.25	-83.2	0.29	-62.8
O10	0.43	-47.6	0.14	-65	2.11	-15.6	1.52	-20.4	0.26	-82.6	0.22	-71.8

O11	0.5	-39.0	-0.02	-105	1.95	-22	1.84	-3.7	0.18	-87.9	0.24	-69.2
O12	0.39	-52.4	-0.05	-112.5	2.66	6.4	1.26	-34.0	0.4	-73.2	0.41	-47.4
O13	0.23	-72.0	-0.02	-105	2.94	17.6	0.66	-65.4	0.24	-83.9	0.25	-67.9
O14	0.57	-30.5	0.12	-70	2	-20	1.89	-1.0	0.39	-73.8	0.29	-62.8
O15	0.67	-18.3	0.19	-52.5	2.01	-19.6	2.17	13.6	0.52	-65.1	0.21	-73.1
O16	0.5	-39.0	0.02	-95	3.1	24	1.49	-22.0	0.6	-59.7	0.69	-11.5
O17	0.3	-63.4	-0.22	-155	2.92	16.8	0.83	-56.5	0.3	-79.9	0.37	-52.6
O18	0.59	-28.0	0.02	-95	1.6	-36	1.77	-7.3	0.29	-80.5	0.14	-82.1
O19	0.7	-14.6	0.2	-50	2.09	-16.4	2.25	17.8	0.58	-61.1	0.5	-35.9
O20	0.5	-39.0	-0.24	-160	2.33	-6.8	1.64	-14.1	0.27	-81.9	0.49	-37.2
O21	0.28	-65.9	-0.03	-107.5	3.22	28.8	0.78	-59.2	0.34	-77.2	0.33	-57.7
O22	0.57	-30.5	0.07	-82.5	1.71	-31.6	1.77	-7.3	0.29	-80.5	0.24	-69.2
O23	0.64	-22.0	0.15	-62.5	1.91	-23.6	2.29	19.9	0.33	-77.9	0.16	-79.5
O24	0.41	-50.0	0.31	-22.5	2.68	7.2	1.24	-35.1	0.56	-62.4	0.3	-61.5
O25	0.42	-48.8	-0.07	-117.5	2.45	-2	1.41	-26.2	0.32	-78.5	0.38	-51.3
O26	0.52	-36.6	0.65	62.5	3.44	37.6	1.61	-15.7	1.08	-27.5	0.5	-35.9
O27	0.59	-28.0	0.64	60	3.51	40.4	1.95	2.1	1.02	-31.5	0.26	-66.7
O28	0.46	-43.9	0.36	-10	3.69	47.6	1.53	-19.9	0.76	-49.0	0.35	-55.1
O29	0.53	-35.4	0.68	70	4.16	66.4	1.48	-22.5	1.22	-18.1	0.75	-3.8
O30	0.56	-31.7	-0.01	-102.5	2.49	-0.4	1.77	-7.3	0.52	-65.1	0.56	-28.2
O31	0.61	-25.6	0.41	2.5	2.68	7.2	2.17	13.6	0.77	-48.3	0.21	-73.1
O32	0.5	-39.0	-0.05	-112.5	2.59	3.6	1.53	-19.9	0.48	-67.8	0.49	-37.2
O33	0.48	-41.5	-0.08	-120	2.43	-2.8	1.6	-16.2	0.34	-77.2	0.42	-46.2
O34	0.51	-37.8	0.61	52.5	3.76	50.4	1.48	-22.5	1.1	-26.2	0.45	-42.3
O35	0.59	-28.0	0.35	-12.5	2.54	1.6	2.08	8.9	0.74	-50.3	0.21	-73.1
O36	0.54	-34.1	-0.01	-102.5	2.64	5.6	1.8	-5.8	0.56	-62.4	0.54	-30.8
O37	0.3	-63.4	-0.02	-105	2.89	15.6	0.94	-50.8	0.32	-78.5	0.34	-56.4
O38	0.63	-23.2	0.01	-97.5	2.02	-19.2	2.36	23.6	0.26	-82.6	0.28	-64.1
O39	0.59	-28.0	-0.07	-117.5	2.61	4.4	1.74	-8.9	0.64	-57.0	0.76	-2.6
O40	0.57	-30.5	-0.2	-150	2.96	18.4	1.68	-12.0	0.61	-59.1	0.86	10.3
O41	0.3	-63.4	0.01	-97.5	2.24	-10.4	0.88	-53.9	0.21	-85.9	0.26	-66.7
O42	0.59	-28.0	0.03	-92.5	2.09	-16.4	2	4.7	0.27	-81.9	0.32	-59.0
O43	0.54	-34.1	-0.19	-147.5	2.69	7.6	1.77	-7.3	0.56	-62.4	0.7	-10.3
O44	0.5	-39.0	-0.37	-192.5	2.68	7.2	1.33	-30.4	0.47	-68.5	0.75	-3.8
O45	0.29	-64.6	-0.1	-125	2.64	5.6	0.9	-52.9	0.22	-85.2	0.32	-59.0
O46	0.57	-30.5	-0.03	-107.5	2.02	-19.2	2.1	9.9	0.22	-85.2	0.23	-70.5
O47	0.59	-28.0	-0.29	-172.5	2.69	7.6	1.69	-11.5	0.66	-55.7	0.88	12.8
O48	0.54	-34.1	-0.57	-242.5	2.87	14.8	1.21	-36.6	0.5	-66.4	1.03	32.1
Max.	0.7	-14.6	0.68	70	4.16	66.4	2.36	23.6	1.22	-18.1	1.03	32.1
Min.	0.23	-72.0	-0.57	-242.5	1.6	-36	0.66	-65.4	0.16	-89.3	0.14	-82.1
Ave.	0.49	-40.2	0.05	-87.08	2.55	2.10	1.57	-17.9	0.46	-69.2	0.40	-48.5
New Method												
Sur.No.	**Sa**	**% Δ Sa**	**Ssk**	**% Δ Ssk**	**Sku**	**% Δ Sku**	**Sk**	**% Δ Sk**	**Spk**	**% Δ Spk**	**Svk**	**% Δ Svk**
N01	0.21	-74.4	0.28	-30	3.76	50.4	1	-47.6	0.43	-71.1	0.19	-75.6
N02	0.23	-72.0	0.07	-82.5	3.02	20.8	0.72	-62.3	0.27	-81.9	0.24	-69.2

N03	0.18	-78.0	0.22	-45	3.66	46.4	0.54	-71.7	0.23	-84.6	0.22	-71.8
N04	0.54	-34.1	0.24	-40	1.73	-30.8	1.49	-22.0	0.48	-67.8	0.14	-82.1
N05	0.54	-34.1	0.24	-40	1.71	-31.6	1.5	-21.5	0.47	-68.5	0.12	-84.6
N06	0.77	-6.1	0.07	-82.5	1.62	-35.2	2.43	27.2	0.37	-75.2	0.14	-82.1
N07	0.22	-73.2	0.18	-55	3.09	23.6	0.71	-62.8	0.27	-81.9	0.22	-71.8
N08	0.24	-70.7	0.23	-42.5	3.1	24	0.76	-60.2	0.3	-79.9	0.24	-69.2
N09	0.21	-74.4	0.94	135	5.5	120	0.58	-69.6	0.4	-73.2	0.19	-75.6
N10	0.43	-47.6	0.23	-42.5	2.3	-8	1.4	-26.7	0.41	-72.5	0.27	-65.4
N11	0.31	-62.2	-0.02	-105	2.78	11.2	1	-47.6	0.32	-78.5	0.35	-55.1
N12	0.23	-72.0	-0.07	-117.5	2.76	10.4	0.7	-63.4	0.21	-85.9	0.23	-70.5
N13	0.26	-68.3	0.07	-82.5	3.25	30	0.79	-58.6	0.3	-79.9	0.28	-64.1
N14	0.23	-72.0	0.09	-77.5	3	20	0.68	-64.4	0.28	-81.2	0.24	-69.2
N15	0.26	-68.3	0.33	-17.5	2.84	13.6	0.82	-57.1	0.33	-77.9	0.21	-73.1
N16	0.36	-56.1	0.38	-5	2.78	11.2	1.18	-38.2	0.46	-69.1	0.24	-69.2
N17	0.54	-34.1	0.85	112.5	2.85	14	1.2	-37.2	1.18	-20.8	0.21	-73.1
N18	0.31	-62.2	-0.05	-112.5	2.73	9.2	0.98	-48.7	0.29	-80.5	0.34	-56.4
N19	0.25	-69.5	-0.14	-135	2.97	18.8	0.75	-60.7	0.25	-83.2	0.31	-60.3
N20	0.22	-73.2	-0.23	-157.5	2.73	9.2	0.63	-67.0	0.18	-87.9	0.26	-66.7
N21	0.46	-43.9	0.35	-12.5	2.28	-8.8	1.53	-19.9	0.48	-67.8	0.2	-74.4
N22	0.4	-51.2	-0.03	-107.5	2.69	7.6	1.33	-30.4	0.36	-75.8	0.4	-48.7
N23	0.18	-78.0	0.07	-82.5	3.06	22.4	0.56	-70.7	0.21	-85.9	0.21	-73.1
N24	0.16	-80.5	0.1	-75	3.6	44	0.47	-75.4	0.21	-85.9	0.21	-73.1
N25	0.15	-81.7	0.21	-47.5	3.34	33.6	0.45	-76.4	0.2	-86.6	0.16	-79.5
N26	0.35	-57.3	-0.68	-270	3.2	28	0.96	-49.7	0.25	-83.2	0.71	-9.0
N27	0.21	-74.4	0.1	-75	2.79	11.6	0.68	-64.4	0.24	-83.9	0.21	-73.1
N28	0.62	-24.4	-0.19	-147.5	1.87	-25.2	1.97	3.1	0.23	-84.6	0.43	-44.9
N29	0.17	-79.3	-0.03	-107.5	3.19	27.6	0.53	-72.3	0.19	-87.2	0.2	-74.4
N30	0.21	-74.4	0.01	-97.5	3.33	33.2	0.65	-66.0	0.24	-83.9	0.26	-66.7
N31	0.4	-51.2	-0.14	-135	3	20	1.33	-30.4	0.39	-73.8	0.5	-35.9
N32	0.41	-50.0	0.23	-42.5	3.15	26	1.28	-33.0	0.61	-59.1	0.42	-46.2
N33	0.29	-64.6	-0.17	-142.5	2.92	16.8	0.94	-50.8	0.26	-82.6	0.33	-57.7
N34	0.35	-57.3	-0.22	-155	2.95	18	1.03	-46.1	0.32	-78.5	0.46	-41.0
N35	0.3	-63.4	-0.24	-160	2.8	12	0.91	-52.4	0.25	-83.2	0.37	-52.6
N36	0.29	-64.6	-0.27	-167.5	2.64	5.6	1.03	-46.1	0.16	-89.3	0.33	-57.7
N37	0.63	-23.2	-0.06	-115	1.73	-30.8	1.99	4.2	0.17	-88.6	0.33	-57.7
N38	0.7	-14.6	-0.04	-110	1.76	-29.6	2.36	23.6	0.19	-87.2	0.34	-56.4
N39	0.65	-20.7	-0.06	-115	2.29	-8.4	1.88	-1.6	0.58	-61.1	0.65	-16.7
N40	0.31	-62.2	-0.14	-135	2.41	-3.6	1.05	-45.0	0.16	-89.3	0.27	-65.4
N41	0.29	-64.6	-0.15	-137.5	2.62	4.8	1.01	-47.1	0.19	-87.2	0.3	-61.5
N42	0.56	-31.7	0.03	-100	2.72	8.8	1.79	-6.3	0.59	-60.4	0.6	-23.1
N43	0.71	-13.4	-0.06	-115	2.05	-18	2.6	36.1	0.36	-75.8	0.34	-56.4
N44	0.28	-65.9	-0.12	-130	2.79	11.6	0.89	-53.4	0.22	-85.2	0.32	-59.0
Max.	0.77	-6.1	0.94	135	5.5	120	2.6	36.1	1.18	-20.8	0.71	-9.0
Min.	0.15	-81.7	-0.68	-270	1.62	-35.2	0.45	-76.4	0.16	-89.3	0.12	-84.6
Ave.	0.36	-56.7	0.05	-86.48	2.80	12.15	1.12	-41.6	0.33	-77.9	0.30	-61.6